SCUOLA DI DOTTORATO

UNIVERSITÀ DEGLI STUDI DI MILANO-BICOCCA

Department of Medicine and Surgery

PhD Program in Translational and

Molecular Medicine XXXIII Cycle

# Shwachman-Diamond Syndrome: an autosomal recessive inherited bone marrow failure disorder with defective angiogenesis and lymphoid lineage impairment

Dr. Gloria Bedini

registration number: 835519

Tutor: Prof. Andrea Biondi

Co-tutor: Dr. Giovanna D'Amico

Coordinator: Prof. Andrea Biondi

**ACADEMIC YEAR**

2019/2020

*Yeah, I know you're struggling right now*
*We all are, in different ways*
*It's like a new world that we don't even know*
*It's hard to sleep, even harder to dream*
*But look,*
*you've got 7 billion brothers and sisters all in the same boat*
*So, don't panic*
*Life has a way of surviving and going on and on*
*We're not fragile, and we sure don't break easy!*

Alice Cooper – Don’t give up

# Table of Contents

# Chapter 1 - Introduction

## Shwachman-Diamond Syndrome and bone marrow angiogenesis

## 1.1 A general introduction of SDS clinical and molecular pathophysiology

Shwachman-Diamond Syndrome (SDS) [1] (OMIM # 260400) is a rare recessive bone marrow (BM) failure disorder characterised by a highly variable phenotype. The diagnosis of SDS is based on institutional clinical criteria, which include exocrine pancreatic dysfunctions and haematological abnormalities [2-6]. Similar to other BM failure disorders, SDS patients show also an increased risk of transformation to myelodysplastic syndrome (MDS) and acute myeloid leukaemia (AML) [5-8].

In Italy, SDS affects 1/168,000 new-borns with a mean of 3.0 new cases/year [9]. No racial predilection is known, and the ratio males to females is 1.7:1 [6].

SDS is most commonly associated with biallelic mutation in Shwachman-Bodian-Diamond Syndrome (*SBDS*) gene [10]. However, 5-10% of patients clinically diagnosed with SDS are negative for this variant. The molecular pathology of SDS has indeed now been expanded to include biallelic mutations in 60S ribosome assembly factor *DNAJC21* (yeast *JJJ1*) [11,12] or elongation factor-like GTPase 1 (*EFL1*) genes, or to the presence of a heterozygous pathogenic variant in signal recognition particle 54 (*SRP54*) gene [8].

## 1.2 SDS clinical presentation

The multi-organ involvement and clinical heterogeneity of SDS was clear since 1980, when the first extensive study of phenotypic and histopathological features of SDS patients was published (**Table 1.1**) [12]. Whereas pancreatic dysfunction tends to normalize with age, skeletal and haematological changes are progressive [7].

*Diagnostic Criteria*

Biallelic SBDS mutations known or predicted to be pathogenic, or mutations in other SDS-associated genes DNAJC21, ELF1, SRP54 (autosomal dominant)

Clinical Diagnosis

Hematologic features (present on at least two occasions)

- Neutropenia (absolute neutrophil count <1500)
- Anemia or macrocytosis (unexplained by other causes, such as iron/$B_{12}$ deficiency)
- Thrombocytopenia (platelet count <150,000) on at least two occasions
- Bone marrow findings
  - Hypocellularity for age
  - Myelodysplasia
  - Leukemia
  - Cytogenetic abnormalities

Pancreatic features

- Reduced levels of pancreatic enzyme relevant to age
  - Trypsinogen <3 years
  - Isoamylase >3 years
- Low levels of fecal elastase
- Supportive features
  - Abnormal pancreatic imaging with lipomatosis
  - Elevated fecal fat excretion >72 hours

Additional supportive features

- Skeletal abnormalities including thoracic dystrophy
- Neurocognitive/behavioral problems
- Unexplained height less than third percentile
- First-degree family member with SDS

**Table 1.1**: *SDS current diagnostic criteria*

*Abbreviations*: *DNAJC21*, 60S ribosome assembly factor *DNAJC21* (yeast *JJJ1*) gene; *ELF1*, elongation factor-like GTPase 1 gene; *SBSD*, Shwachman-Bodian-Diamond Syndrome gene; SDS, Shwachman-Diamond Syndrome; *SRP54*, signal recognition particle 54 gene [adapted from Nelson A.S., Myers K.C. "Diagnosis, Treatment, and Molecular Pathology of Shwachman-Diamond Syndrome". Hematol Oncol Clin North Am. 2018 Aug;32(4):687-700]

### 1.2.1 Exocrine pancreatic insufficiency and hepatic involvement

Depletion of pancreatic acinar cells is one of the hallmarks of the exocrine pancreatic dysfunction observed in SDS patients [5,7]. Symptoms of pancreatic insufficiency are typically seen within the first 6 to 12 months of life, although the varied clinical spectrum. Histological specimens of the pancreas demonstrate an extensive fatty replacement of pancreatic acini with preserved islets of Langerhans and ductal architecture [7]. SDS is the second most common cause of inherited/congenital pancreatic insufficiency after cystic fibrosis. However, many patients with SDS and exocrine pancreatic dysfunction spontaneously improve over time, with almost half of patients no longer requiring supplemental pancreatic enzyme therapy, despite persistent native secretory enzyme deficiency [7]. From a diagnostic point of view, ductular electrolyte and fluid secretion have been shown to remain normal, but the secretion of proteolytic enzymes is severely decreased leading to steatorrhea [5-8]. In SDS, faecal elastase-1 test has been used to rule out pancreatic insufficiency. However, abnormal test data should be interpreted with caution since malabsorption could be related to other reasons. Serum trypsinogen and isoamylase levels, indeed, have been shown to be more useful markers for SDS pancreatic dysfunction [5-8;14].

The endocrine component of the pancreas is generally unaffected in SDS. However, both children and adults with type-

1 and -2 diabetes mellitus have occasionally been reported [15,16].

Other gastrointestinal alterations associated with SDS include abnormalities of the liver. Elevation of transaminases and hepatomegaly of unclear causes are often present in early life. However, liver enzymes and liver enlargement appear to normalize over time [5-8].

### 1.2.2 Haematological alterations and immune dysfunctions

SDS is the third most common inherited blood dyscrasia after Fanconi and Diamond-Blackfan Anemia [7,8]. The most frequent SDS haematological deficiencies is neutropenia, defined as the absolute neutrophil count (ANC) less than 1500/μL. Neutropenia can occur in 88-100% of SDS patients, and it is typical of the first year of life, although it can present in the adulthood or may be absent in a small number of patients. Neutropenia is of unpredictable severity and may be also intermittent or persistent. Therefore, this specific haematological feature underlines the importance of repeated blood counts when results are normal [5,7].

Other cytopenias are also frequently present in SDS patients. For example, normochromic anaemia with low reticulocyte count is encountered in 80% of these patients, whereas thrombocytopenia (defined as platelets < 150 x $10^9$ cells/L) is variably seen. Cytopenia affecting all three cell lines is the lifelong risk of SDS patients. This haematological alteration is described in 10-65% of affected patients, and

occasionally results in severe BM aplasia [5-8]. The different degrees of marrow hypoplasia include the reduced numbers of BM progenitors, such as granulocyte-monocyte colony-forming units (CFU-GM) and erythrocyte burst-forming units (BFU-E), as well as fat infiltration [17]. Not surprisingly, BM aspirates of SDS patients have a significantly low number of $CD34^+$ cells. Particularly, these cells showed a markedly impaired colony production potential tested by *in vitro* clonogenic assays. Indeed, the ability of marrow stromal cells from SDS patients to support normal $CD34^+$ is diminished. SDS patients also have a generalized marrow dysfunction with abnormal BM stroma in terms of its ability to maintain and support haematopoiesis [18]. The molecular mechanism of this specific BM failure appears to be mediated by the increased expression of Fas antigen on marrow cells, and due to the hyperactivation of Fas signalling pathway [19,20].

MDS and AML can be found in approximately one third of SDS patients. Clonal changes, most often monosomy 7, 7q deletion, isochromosome 7q (i [7] [q10]), trisomy 8, and 20q deletion (del [20] [q11]), may fluctuate and sometimes even become undetectable over time [6,21]. Particularly, isochromosome 7q abnormalities and 20q deletion do not seem to be associated with malignant SDS BM transformation. However, the presence of one or more independent clones with other chromosome abnormalities could be linked to a higher risk [21,22]. For example, trisomy 8 and chromosome 7 alterations other than those involving isochromosome 7q may

contribute to leukemic progression in SDS patients [6,21]. Recently, novel cytogenetic abnormalities with or without 20q deletion and isochromosome 7q anomalies were reported in a cohort of 91 Italian SDS patients, including unbalanced structural anomalies of chromosome 7 and complex rearrangements of 20q deletion [22]. Some of these SDS patients did progress to MDS or AML, both with isochromosome 7q or 20q deletion and without. Although significance of infrequent acquired chromosomal changes in SDS remains unclear, additional acquired cytogenetic abnormalities may pre-empt the development of MDS or AML [22]. From sex ratio, males are extremely over-represented among SDS patients with leukemic transformation: 92% of reported SDS subjects with leukaemia are males [6]. SDS-related leukaemia has a poor prognosis; indeed, these patients usually fail to respond to chemotherapy, and appear to have pronounced susceptibility to complications and organ toxicity in conjunction with stem cell transplantation. It has been reported that 83% of these patients had succumbed from therapy-related complications [17].

The implication of the immune system in SDS is not yet clear. Particularly at early age, SDS patients are at risk of different types of infections (including bacterial, viral, and fungal) generally believed to be beyond that expected in patients with neutropenia [5,7]. However, it has also been demonstrated that even if a large number of patients suffer from recurrent infections at early age, the severity and the frequency of infections do not correlate with the degree of neutropenia.

Moreover, the risk of both infections and neutropenia tends to decrease over time [13].

Several other defects in humoral (decreased B cell numbers, low IgG levels) and cellular (decreased T cell proliferation) immunity have been also described in SDS patients [17].

### 1.2.3 Skeletal abnormalities

A number of skeletal abnormalities have been reported in this syndrome, and are considered an important clinical feature in supporting the diagnosis. Classical skeletal manifestations of SDS include short stature, progressive metaphyseal dysplasia/thickening of the long bones and costochondral junctions, thoracic abnormalities (one third to one half of children with SDS have ribcage abnormalities, including short ribs with flared ends and a narrow rib cage). Other typical skeletal alteration comprises the developmental delay of normally shaped epiphyses and Wormian appearance of skull bones [5,7]. All these abnormalities may evolve over time.

The pathogenesis of skeletal abnormalities is not clear, even if poor vascularisation or avascular necrosis has been hypothesised. Skeletal abnormalities would seem to be inherent in the syndrome rather than secondary to malnutrition. Even though the trend of these features seems to represent stability of the condition rather than deterioration, surgical intervention may occasionally be necessary to correct some anomalies [5,7].

SDS is also associated with a low-turnover osteoporosis, and abnormalities of bone health, including low z score and vertebral compression fractures. Other markers of bone health are abnormal, including vitamin D and K deficiency, and associated secondary hyperparathyroidism. However, no improvement was observed in the bone abnormalities with intensive vitamin D therapy [23].

No phenotype-genotype correlation was observed, and the severity of the skeletal findings varied even in patients with identical *SBDS* mutations [24].

### 1.2.4 Cognitive impairment and additional clinical features

Since 1964, either adequate development or slight retardation were found in SDS patients [1]. Subsequently, learning disabilities (including delayed development and low IQ), limiting independence and socialization were reported. With regard to aetiology, cognitive impairment is clearly characterized as primary, being independent of the family environment, malnutrition or suffering from a chronic illness [7;25-27].

Magnetic resonance imaging (MRI) studies revealed that SDS patients are characterised by small size of posterior fossa, cerebellar vermis, corpus callosum, and brainstem compared to age- and gender-matched controls [28]. Moreover, the volumes of corpus callosum, brainstem, cerebellum, and thalamus seem to be correlated to a dysregulation of the dopaminergic system [29]. More recently, the combined assessment of cognitive

abilities and MRI neuroimaging demonstrated that cognitive impairment is associated with diffuse changes in grey and white matter [25]. However, whether these changes signify a static change, a delay in neurocognitive development, or will continue to advance is still unknown.

Fatal neonatal cardiac manifestations have been associated with both SDS and pancreatic lipomatosis in several early reports, and in most of these cases histopathology has shown myocardial necrosis or fibrosis [7]. Patients with SDS have high prevalence of oral diseases. Extensive caries of both primary and permanent teeth, and delayed dental maturation are common; up to 72% of these patients have tooth enamel defects ranging from hypo-maturation to hypoplasia. Periodontal disorders, such as recurrent oral ulcerations and gingival bleeding are commonly seen in SDS patients [7,8]. Skin involvement, ranging from slight scaling of the skin to severe ichthyosis, has also been observed in about 50% of them [7,8]. Skin lesions are frequently reported at early age, but tend to improve and resolve after the first year of life [7,8].

## 1.3 SDS treatment and follow-up

There is no cure or treatment for SDS. Therefore, comprehensive screening for known disease complications should be pursued at diagnosis and at regular intervals thereafter.

Pancreatic insufficiency is usually treated with pancreatic enzyme substitution with meals, snacks, and supplements for fat-soluble vitamins A, D and E. With clinically improved pancreatic function over time, some of the patients may no longer require pancreatic enzyme substitution [7].

Monitoring blood cell count and BM evaluation are vital to assess malignant transformation. Leuko-filtered red blood cell and thrombocyte transfusions have been used in cases of severe anaemia or thrombocytopenia; leuko-filtration reduces the risks of developing graft rejection after possible BM transplant. Neutropenic patients with SDS and fever should be evaluated without delay and promptly treated with antibiotics, bearing in mind the risks of serious, potentially life-threatening infections. Persistent severe neutropenia with severe or recurrent bacterial or fungal infections is an indication for granulocyte colony-stimulating factor (G-CSF) therapy. Most SDS patients have adequate response with low-dose G-CSF but may range from intermittent to continuous daily dosing. Bone marrow evaluation, including cytogenetics and fluorescence *in situ* hybridization studies, is recommended before starting G-CSF whenever feasible, to avoid potentially

promoting abnormal clone growth. In MDS and AML secondary to SDS, standard chemotherapy regimens are not indicated. Due to a high risk of persistent aplasia an attempt should be made to provide haematopoietic stem cell transplantation (HSCT). Unfortunately, outcomes are poor with high treatment-related mortality using standard myeloablative preparative regimens [7,17].

Bone deformities may require orthopaedic consultation and skeletal survey is recommended. Intake of vitamin D and calcium should be supplemented if necessary [23]. Endocrine functionality should be screened, to exclude problems, such as hypothyroidism, that may contribute to osteopenia. In addition, dental problems are commonly seen in children with SDS and could be minimized with a regular dental care, and appropriate advice from early age. Annual reviews are generally recommended [7].

Because the multiple organ involvement, multidisciplinary approach to SDS clinical care is expected to improve the treatment and quality of life of the patients.

## 1.4 SDS genetics and molecular biology

SDS is caused by pathogenic variants in *SBDS*, *DNAJC21*, *EFL1*, or *SRP54* genes (**Table 1.2**). The majority of SDS cases are associated with *SBDS* gene, which encodes SBDS, a protein involved in ribosome biogenesis. Interestingly, all genes recently found to be associated with SDS phenotype play a role in ribosome biogenesis and function [7,8].

| Gene [1, 2] | Proportion of SDS Attributed to Pathogenic Variants in This Gene |
|---|---|
| *EFL1* | <1% |
| *DNAJC21* | <1% |
| *SBDS* | ~92% |
| *SRP54* | <1% |
| Unknown | <10% |

**Table 1.2**: *Molecular genetics of Shwachman-Diamond Syndrome*

[1]genes are listed in alphabetical order; [2]see the text for details and abbreviation [adapted from Nelson A., Myers K. "Shwachman-Diamond Syndrome". 2008 Jul 17 [Updated 2018 Oct 18]. In: Adam M.P., et al., editors. GeneReviews® [Internet]. Seattle (WA): University of Washington, Seattle; 1993-2020]

### 1.4.1 Genetics

***SBDS* gene**. In 2003, biallelic mutations in the highly conserved *SBDS* gene was found in the majority of SDS patients [30]. *SBDS* maps on chromosome 7 near the centromere (in the interval of 1.9 cM at [7] [q11]), and encodes for a predicted

protein of 28.8 kDa. The gene is composed of 5 exons and has a 1.6 kb mRNA transcript [17]. Pathogenic mutations arise as a consequence of gene conversion due to recombination between *SBDS* and an un-processed pseudogene (*pSBDS*) located in a distal paralogous duplicon. More than 90% of affected individuals carry one of three common pathogenic *SBDS* variants on one allele of exon 2: (I) 183_184 TA > CT, (II) 258+2 T > C, or the combined (III) 183_18 TA > CT + 258+2 T > C [8]. The mutation 258+2 T > C disrupts the donor splice site of intron 2, while the dinucleotide alteration, 183_184 TA > CT, introduces an in-frame stop codon (K62X). Although most parents of SDS affected children are carriers, about 10% of *SBDS* mutations arise *de novo* [8]. Nearly 100 novel sequence variants identified in the 5 exons of *SBDS* are consistent with loss-of-function alterations [8,30], seven of which have been found in multiple, apparently unrelated families. However, no individuals have been identified as homozygous for the in-frame stop codon dinucleotide variant (183_184 TA > CT), suggesting that the complete absence of functional SBDS protein is incompatible with life [30].

***DNAJC21* gene**. *DNAJC21* is a ubiquitously expressed gene, located on the short arm of chromosome 5 ([5] [p13.2]). It contains at least 12 exons and spans more than 25.6 kb [8,31]. The *DNAJC21* mutations reported so far include two homozygous nonsense variants (c.517 C > T, p.R173*; c.793G > T, p.E265*), a splice variant (c.983+1 G > T), a missense mutation (c.94C > G,p.P32A), two nonsense mutations

(p.Q174*; p.V148Kfs*30), and a missense variant (c.100 A > G, p.K34E) [31].

***EFL1* gene**. *EFL1* has 13 exons and it is located on the long arm of chromosome 13 ([13] [q14.11]). Recently, six patients with pancytopenia, exocrine pancreatic insufficiency and skeletal abnormalities belonging to three unrelated families, were identified as carriers of homozygous nonsense variants c.3284 G > A and c.2645 T > A in the *EFL1* GTPase [32].

***SRP54* gene**. *SRP54* is located on chromosome 14 ([14] [q13.2]), and contains 14 exons. *De novo* pathogenic variants c.343 A > G(p.T115A), c.349_351del(p.T117del), and c.677 G > A (p.G226E) have been described in patients with SDS-like phenotype [33].

### 1.4.2 Molecular pathogenesis

*SBDS* encodes a highly conserved protein of 250 amino acids, presents in all animals, plants, and archaea [30]. Structural analysis of archaeal ortholog indicated that SBDS protein contains a three-domain architecture: (I) N-terminal domain (or FYSH) with a mixed α/β-fold, (II) central three-helical bundle, and (III) C-terminal ferredoxin-like domain with striking structural similarity to domain V of elongation factor 2 (and EFL1). Particularly, N-terminal domain is the most frequent target for disease mutations [31]. Overall, SBDS protein is similar in size and shape to tRNA and to ribosome recycling factor.

SBDS protein is widely expressed throughout human tissues, and its prominent localization within sub-regions of nucleus corresponds to the nucleolus, shuttling-in and -out depending on the cell cycle phase. One explanation of this localization is that SBDS could act in the nucleolus, a primary site of rRNA processing. Not surprisingly, *SBDS* gene has been implicated in multiple biologic processes including ribosome biogenesis, mitochondrial function, stabilization of the mitotic spindle, and cell motility [7]. However, the functional defect considered the cause of SDS phenotype has not yet been clear.

Genetic studies of the yeast homolog support a role in 60S ribosomal subunit biogenesis and translational activation, whereas other studies, examining the interaction between SBDS and ELF1 GTPase, endorse a model in which SBDS initiates the joining of 40S and 60S subunits for active translation through the creation of the active 80S ribosome [8]. Particularly, premature joining of the ribosomal subunits is prevented by a protein called eukaryotic translation initiation factor 6 (eIF6), which binds the 60S ribosomal subunit. After nuclear export of 60S subunit, SBDS cooperates with EFL1 to cause the release of eIF6 from the 60S to form the mature ribosome (**Figure 1.1**) [31;34,35]. Other functional studies, instead, demonstrated that the reduced expression of *SBDS* decreases mitochondrial membrane potential and increases the production of reactive oxygen species, which may contribute to SDS pathophysiology [34].

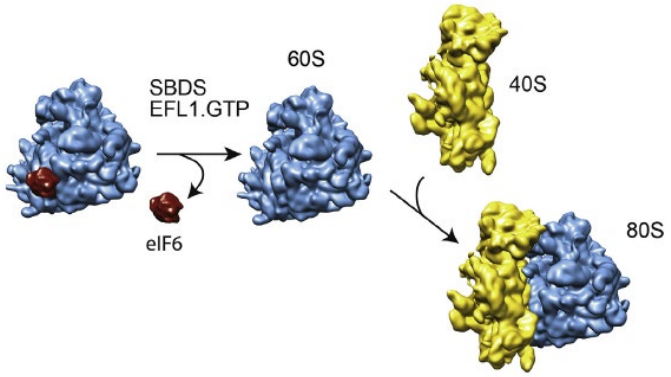


**Figure 1.1**: *eIF6 release by SBDS and EFL1*

SBDS stimulates 60S-dependent GTP hydrolysis by EFL1, generating EFL1.GDP.Pi. Following release of inorganic Pi, EFL1 adopts its GDP-bound conformation, and domain I of SBDS is rotated relative to domains II and III, directly or indirectly disrupting the inter-subunit bridge B6. Binding of eIF6 is destabilized, release of eIF6 is triggered and EFL1.GDP and SBDS dissociate from the ribosome. Release of eIF6 allows the formation of actively translating 80S ribosomes.

*Abbreviations*: eIF6, eukaryotic translation initiation factor 6; EFL1.GTP, elongation factor-like GTPase 1; SBDS, Shwachman-Bodian-Diamond Syndrome protein [adapted from Warren A.J. "Molecular basis of the human ribosomopathy Shwachman-Diamond syndrome". Adv Biol Regul. 2018 Jan;67:109-27]

SBDS protein colocalized also within the mitotic spindle, promoting its stability and chromosome segregation during cell division process. Indeed, fibroblasts and lymphocytes from SDS patients have an increased number of multipolar spindles, leading to an elevated genomic instability which can be rescued by purified SBDS protein. Interestingly, the addition of microtubule stabilizing agents has also been demonstrated to improve primary BM haematopoietic progenitor colony formation. Colocalization of SBDS within centromeres as well

as mitotic spindle and organizing centre of the microtubules during interphase has been confirmed in neutrophils [7]. Even though *SBDS* was found not to be necessary for neutrophil maturation, SDS-derived neutrophils show an impaired ability to migrate in response to chemoattractant molecules. In particular, SBDS protein seems to be involved in the regulation of F-actin cytoskeleton and its polymerization. Nevertheless, in murine myeloid cell line 32Dcl3, which has the potential to differentiate into mature neutrophils, SBDS acts to maintain survival of granulocyte precursor cells [36,37]. Moreover, decreased expression of *SBDS* in stromal cells may alter the haematopoietic microenvironment and favour the development of BM failure and/or malignant transformation [38].

Loss of *SBDS* expression is also associated with hyper-activation of mTOR-STAT3 pathway [39]. Indeed, it has been demonstrated that mammalian target of rapamycin (mTOR) and signal transducer and activator of transcription-3 (STAT3) are constitutively up-regulated in lymphoblastoid cell lines and primary leukocytes derived from SDS patients [39]. Particularly, both mTOR and STAT3 are highly hyper-activated upon interleukin-6 (IL6) stimulation. Moreover, SDS-derived cells also reported a constitutive activation of MAPK ERK1/2 signalling, which strongly decreased in the presence of ERK1/2 endogenous inhibitor both in un-stimulated and IL6 stimulated condition, thus resulting in a significant reduction of IL6-dependent mTOR activation [39]. Recently, we demonstrated that mTOR-STAT3 pathway is markedly up-regulated also in

SDS lymphoid compartment [40], providing some new important clues on the understanding of the molecular mechanism behind AML development in SDS patients (see ***Chapter 3***).

DNAJC21 is a ubiquitously expressed 531 amino acid protein which contains a highly conserved N-terminal J domain and two zinc finger (C2H2 type) domains. Specifically, J proteins comprise a highly conserved ~70 amino acid J domain, including four α-helices with a conserved His, Pro, Asp (HPD) tripeptide which lies within a helical hairpin between helices II and IV. The HPD motif lies at the interaction interface with the Hsp70 client protein, and it is critical for stimulating Hsp70 ATPase activity [31]. The yeast DNAJC21 homologue (*Jjj1*) is a cytosolic J protein which, together with cytoplasmic zinc-finger protein Rei1, stimulates the ATPase activity of Hsp70 chaperone protein Ssa (human heat shock 70 kDa protein 8) (HSPA8), thus promoting the release and recycling of nuclear export factor Arx1 (human proliferation-associated protein 2G4) (PA2G4) and IRES specific cellular transacting factor 45. It has been demonstrated that the deletion of the yeast *DNAJC21* homolog *Jjj1* leads to the reduction of mature ribosomes, and to a dysfunctional 60S ribosome subunit biogenesis [8]. Moreover, the missense variant p.P32A alters the fold of J domain HPD motif, disrupting the interaction with HSPA8 and its ATPase stimulatory activities. The p.K34E missense variant, instead, reverses the surface charge of a key amino acid adjacent to the HPD motif and also disrupts the interaction with HSPA8. Interestingly, individuals lacking functional *DNAJC21* are viable,

whereas biallelic *SBDS* null mutations do not appear to be compatible with life [31].

In eukaryotes, EFL1 is a cytoplasmic GTPase homologous to prokaryotic elongation factor G (EF-G) and ribosomal translocase EF-2. Like EF-G, EFL1 has a five-domain architecture [41] but it is distinguished from EF-G by an insertion loop of variable length within domain II. Interestingly, while *EF-2* orthologues *SBDS* and *eIF6* are found in archaea, *EFL1* is absent, suggesting that *EF-2* has dual roles in biogenesis (i.e. eIF6 release) and translation. Therefore, hypo-morphic *EFL1* mutations might be predicted to phenocopy SDS clinically, as EFL1 and SBDS functionally cooperate to catalyse eIF6 release during the final cytoplasmic step in 60S ribosomal subunit maturation [31]. Notably, increased phosphorylation of mTOR was also observed in affecting 60S maturation, and the binding of SBDS and EIF6 probably modulate defective ribosome biogenesis through the increase of cytoplasmic calcium concentration to drive nuclear import of EIF6 [7].

SRP54 is a 504 amino acids protein belongs to the GTP-binding SRP family. SRP54 protein is characterized by two domains: (I) G-domain which binds GTP, and (II) M-domain which leads to the binding of signal sequence. As previously reported, novel mutations in *SRP54* lead to SDS-like phenotype. Particularly, a trio of patients with this characteristic were found to have *de novo* missense variants in *SRP54*, resulting in neutropenia and other SDS features. GTPase

activity of the mutated proteins was impaired, and BM level of *SRP54* mRNA was 3.6-fold lower in patients with *SRP54* mutations compared to healthy-control subjects. The SDS phenotype with neutropenia was also observed in a zebrafish *srp54* knock-down model, suggesting that this variant could be a novel mutation to search in previously *SBDS*-negative affected patients [7].

## 1.5 SDS bone marrow niche

Mesenchymal stromal cells (MSCs) are key component of the bone marrow stroma with peculiar anti-inflammatory and immune-regulatory activities [42]. However, it is still unclear whether these cells have tumour-suppressing or tumour-promoting effects in haematological malignancies (**Figure 1.2**) [43].

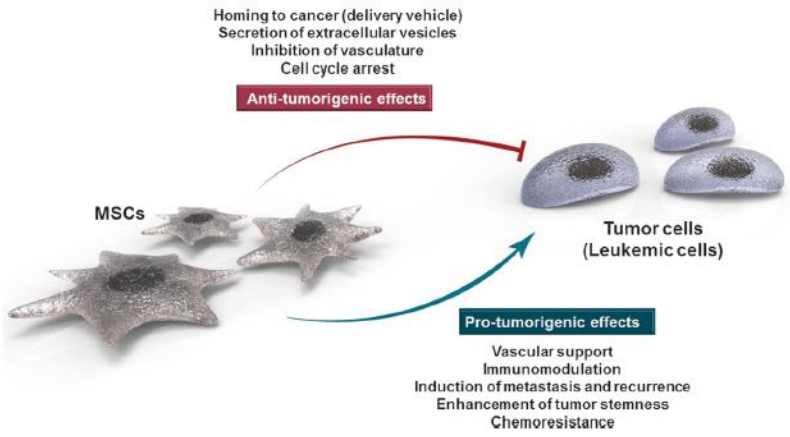


**Figure 1.2**: *Dual role of MSCs in haematologic malignancy*

*Abbreviations*: MSCs, mesenchymal stromal cells [adapted from Lee M.W., et al. "Mesenchymal stem cells in suppression or progression of hematologic malignancy: current status and challenges". Leukemia. 2019 Mar;33(3):597-611]

### 1.5.1 Mesenchymal stomal cells in haematological disorders and SDS

Nowadays, MSCs are not just only considered an inert and structural element of the BM niche. Indeed, it has been shown their involvement in supporting, driving and maintaining several haematopoietic disorders, such as myelodysplasia and aplastic anaemia [43]. Particularly, Raaijmakers and colleagues demonstrated that *Dicer1* deletion in mesenchymal osteoprogenitor cells can induce the development of MDS [44]. Specifically, by the generation of Osx-GFP-Cre$^{+}$: Dicer$^{fl/+}$ (OCD$^{fl/+}$control) and Osx-GFP-Cre$^{+}$Dicer$^{fl/fl}$ (OCD$^{fl/fl}$ mutant) mice, Raaijmakers showed that only OCD$^{fl/fl}$ animals has reduced B cells and B cell progenitors with a concomitant increased frequency of myeloid cells in the bone marrow as observed in human MDS [44]. Interestingly, gene expression profiling of primary OCD$^{fl/+}$ and OCD$^{fl/fl}$ osteolineage cells (GFP$^{+}$CD45$^{-}$lin$^{-}$CD31$^{-}$) also reported a differential expression of 656 genes. Notably, in differentially expressed genes and pathways included stress response and cytokines, a significant down-regulation of *Sbds* was found. Indeed, the intercrossing between Osterix-Cre mice and mice containing conditional *Sbds* alleles leads to alteration of cortical bone, leukopenia and lymphopenia (but not neutropenia), dysplastic features of neutrophils in the peripheral blood, and micro-megakaryocytes with increased vascularity of the bone marrow, as well as other important similarities with OCD$^{fl/fl}$ mice included the decreased frequency of B cells and B cell progenitors, and intramedullary

apoptosis of haematopoietic progenitor cells. Collectively, these data were the first striking evidence of the connection between genetic disruption of crucial elements of the bone marrow niche and malignant transformation to MDS [44]. Subsequently, it has also been demonstrated that human MDS-MSCs are characterised by a significantly reduction of *SBDS* expression [45].

Concerning SDS, using long-term cultures of marrow stromal cells, it was shown that SDS bone marrow is characterised by a reduced ability to support and maintain haematopoiesis as well as by impairment in cytokine production [18]. However, our research group demonstrated that SDS-MSCs are similar to normal HD-derived cells in terms of morphology and growth kinetics. Indeed, SDS- share the same immunophenotype to HD-MSCs, and can differentiate into adipocytes and osteoblast [46]. Moreover, SDS-MSCs do not evidence any differences in the ability to support neutrophils growth, even if an increased tendency of IL6 production in cell culture supernatants was found [46]. Nevertheless, our unpublished results also demonstrated that several genes involved in haematopoietic cell development, lymphopoiesis and neoplastic progression are differently expressed between SDS- and HD-MSCs, suggesting that these alterations could underlying a possible functional defect of SDS-MSCs.

### 1.5.2 SDS altered bone marrow microenvironment

In 2018, our research demonstrated that implanted cartilaginous pellets (CPs) derived from SDS-MSCs display a marked impairment in their angiogenic potential, resulting in the formation of a dysfunctional BM niche [47]. Specifically, even if we succeeded in obtaining correct *in vitro* chondrogenic differentiation of both SDS- and HD-MSCs, only implanted CPs derived from HD-MSCs were able to recreate a well-defined BM niche. Indeed, harvested HD-CPs were characterised by bone intra-trabecular spaces, murine marrow cells, marrow sinusoids and adipose tissue, whereas SDS implants were only an undifferentiated mesengetic tissue, apparently due to a stop at the chondrogenic differentiation phase. More in detail, from a total of 150 SDS-CPs derived from 19 different patients, only 24 pellets (16%) were harvested, none of which displayed vascularization or BM niche formation. Notably, inflammatory elements, such as infiltrating macrophages, mesengetic undifferentiated and chondrogenic tissue, as well as fibrotic capsules were the main histological features found in SDS-CPs (**Figure 1.3**). Since vascularization is one critical step for bone marrow niche formation, we analysed the *in vitro* angiogenic capability of SDS-MSCs. Accordingly, we further demonstrated that the ability of SDS-MSCs to form correct tube-networks under specific angiogenic *stimuli* was severely affected compared to HD-MSCs. Moreover, we also showed that SDS-MSCs defective *in vitro* angiogenic capability is associated to a specific decreased in the expression of vascular endothelial

growth factor A (*VEGFα*), one of the main player in the angiogenesis cascade. Altogether, these results suggest that the *in vitro* defects of SDS-MSCs could be at the basis of the altered CP-marrow biopsies [47]. Moreover, our data point out on the possible role of functional altered MSCs in vascular, haematological and non-haematological defects typical of SDS.

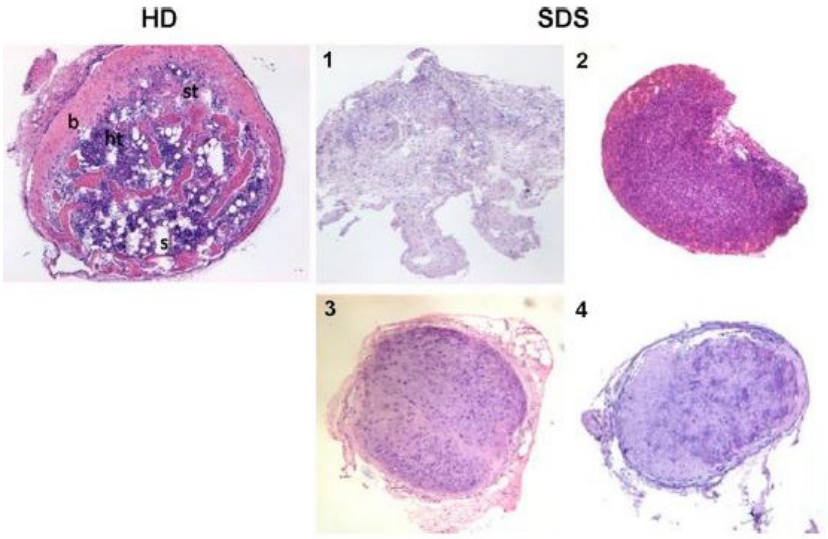


**Figure 1.3**: *SDS- and HD-CPs bone marrow niche (magnification 4X)*

Left: representative HD-CPs stained with haematoxylin and eosin (H&E), showing the complete formation of BM cavity (b: bone; ht: haematopoietic tissue; st: stroma; s: sinusoids). Right: histology of SDS-CPs harvested at 8 weeks post-transplant. The differentiation process seems to have stopped at the mesengetic (2) or chondrogenic phase (3 and 4). Occasionally, inflammatory elements (1) or fibrotic capsule (4) could be detected [adapted from Bardelli D., et al. “Mesenchymal stromal cells from Shwachman-Diamond syndrome patients fail to recreate a bone marrow niche *in vivo* and exhibit impaired angiogenesis”. Br J Haematol. 2018 Jul;182(1):114-24]

### 1.5.3 SDS and angiogenesis

The evaluation of microvascular density (MVD) represents a useful tool to estimate the overall angiogenic capacity of haematological malignancies (i.e. MDS and AML). Indeed, it is also considered an effective disease progression marker [48]. Assumed the high propensity to malignant transformation and the functional abnormalities of bone marrow stroma [18], the evaluation of bone marrow angiogenesis in SDS patients could reveal some important insides in pathophysiology of MDS and/or AML secondary to SDS. In 2006, indeed, it has been demonstrated that BM biopsies of SDS patients are characterized by an increased number of microvessels compared to healthy bone marrow aspirates of the same age [49]. Particularly, blood vessels of SDS-BM biopsies seem to be more tortuous and collapsed or even characterised by constricted lumens *vs* the open and organized vascular architecture of control specimens. However, in this report the increased MVD did not correlate with severe aplastic anaemia, MDS or leukaemia, probably because SDS patients who develop MDS and/or AML accumulate multiple molecular and cellular aberrations until transformation becomes clear.

### 1.5.4 Congenital neutropenia and SDS bone marrow microenvironment

Neutrophil granulocytopoiesis is the process of proliferation, differentiation and expansion of BM haematopoietic progenitor and precursor cells into functional

mature neutrophils. Although *in vivo* mechanisms able to promote and regulate the multi-step process of normal granulocytopoiesis remain still largely speculative, local regulatory events including haematopoietic-to-stromal cell interactions, activation of colony-stimulating factors and their cognate receptors, up-regulation of specific transcriptional factors that rescue myeloid cells from apoptosis and direct myeloid development to neutrophil differentiation, have been suggested [50]. A regulatory negative feedback effect of peripheral blood neutrophils on BM granulocytopoiesis has also been proposed. While the exact mechanisms that govern normal granulocytic development are still not well understood, there have been remarkable advances in the identification of cellular, genetic and molecular mechanisms implicated in the pathophysiology of chronic neutropenia syndromes associated with BM failure. These neutropenia states include distinct congenital and acquired haematologic disorders with varying degree of neutropenia due to decreased or ineffective BM neutrophil production. The most severe cases comprise patients with congenital disorders of granulocytopoiesis, while acquired idiopathic cases may display neutorpenia of varying severity [50].

Congenital neutropenias are rare haematological diseases usually characterized by extremely low levels of circulating neutrophils predisposing patients to recurrent severe infections, oropharyngeal ulcers, gingivitis, malaise, and fever. They may occur both sporadically and as autosomal inherited

disorders, and comprise distinct disease entities such as cyclic neutropenia [51], severe congenital neutropenia [52], SDS [6], and myelokathexis [53]. All these syndromes are commonly characterized by impaired formation and reduced delivery of neutrophils from the BM to the periphery but display distinctive BM morphological features. However, a series of studies have shown that neutropenia syndromes display overlapping pathophysiologic features and there is strong evidence suggesting that accelerated apoptosis of BM granulocytic progenitor cells is the central mechanism responsible for the underlying faulty granulocytopoiesis [50]. Longitudinal studies have also shown that patients with BM failure-associated neutropenia syndromes display increased risk of developing myelodysplasia or AML. Such evolution occurs mainly in patients with SDS, where the over-expression of P53 protein has been reported to precede the clonal evolution [54].

Neutropenia is the main SDS haematologic manifestation, but the cellular and molecular mechanisms underlying this specific disease phenotype remain poorly understood. As previously mentioned, SDS bone marrow failure is associated with an intrinsic haematopoietic progenitor cell abnormality and a faulty marrow microenvironment [6;18,19]. Specifically, it has been shown low frequency and decreased clonogenic potential of SDS BM $CD34^{+}$ cells due to accelerated apoptotic cell death. Experimental evidence has demonstrated that the increased propensity of haematopoietic progenitor cells to apoptosis is mainly due to Fas antigen over-expression and

Fas signalling hyperactivation in patient $CD34^+$ cells. Interestingly, Fas up-regulation is evident in all stages of granulocytic differentiation, from the early progenitors to the mature neutrophils, and thus seems likely to be largely involved in patients' neutropenia [19]. However, it remains unclear whether this abnormality is a sequel of the underlying genetic defect or is the consequence of a consistent inhibitory effect of patients' BM microenvironment. Indeed, data from SDS long-term cultures of marrow stromal cells have demonstrated impaired capacity of patient stromal layers to sustain not only the autologous but also the normal haematopoiesis, suggesting a primary BM microenvironment defect in addition to the haematopoietic progenitor cell abnormality in SDS [18]. Previous investigations have also shown that stromal-derived inhibitory cytokines such as tumour necrosis factor-α (TNFα) and interferon-ɣ (IFNɣ) may induce Fas-mediated haematopoietic progenitor cell apoptosis in BM failure associated with aplastic anemia and autoimmune systemic diseases [50].

## 1.6 Bone marrow niche angiogenesis

Angiogenesis, vasculogenesis, and arteriogenesis are the three the major processes by which blood vessels are formed and remodelled. Angiogenesis, the budding of new capillary branches from existing blood vessels, is mandatory for tissue survival in both normal and pathological conditions. For example, in the BM niche, this biological process becomes vital for the maintenance and migration of HSCs, their progeny and supportive cells [55]. On the other hand, increased angiogenesis is correlated with leukaemia progression and resistance to treatment. Vasculogenesis, instead, denotes *de novo* blood vessel formation during embryogenesis, in which angiogenic progenitor cells migrate to sites of vascularization, differentiate into endothelial cells (ECs), and coalesce to form the initial vascular plexus. Finally, arteriogenesis refers to the remodelling of an existing artery to growth its luminal diameter in response to increased blood flow [55].

### 1.6.1 Bone marrow niche and vessel formation

There are two types of BM niches: endosteal and non-endosteal (vascular/sinusoidal) [56,57]. These structures are complex, encompassing a broad range of BM cells including bone lining cells (osteoblasts and osteoclasts), MSCs, sinusoidal endothelium and perivascular stromal cells, immune cells, and several other elements which play different roles in HSC regulation [56].

The endosteal niche is localized in the internal bone shell surface, and it is considered the major HSC niche. The endosteum is the inner surface of the BM cavity, made up of both cortical and trabecular bone types, where haematopoiesis occurs actively. This surface is lined by bone cells such as osteoblasts (OBs) and osteoclasts (OCs). OBs are progenitor bone-forming cells that work in tandem with OCs in osteogenesis process [57]. OBs are transient cells that actively provide mineralization during bone development and replace lost bone tissues in adults. Several studies have shown direct associations between OBs and HSCs. For instance, it has been demonstrated that the knocking down of *osterix*, an osteoblast-specific transcription factor essential for endochondral ossification, leads to the impairment of the bone formation, the absence of the HSC niche, as well as the decrease of HSCs. Other OB and HSC surface molecules are involved in the fine-tune regulation of endosteal HSCs' fate. Indeed, it has been proved that HSCs able to adhere to OBs on the bone surface express angiopoietin receptor-2 (TIE2) and, in the adult BM, the lining cells produce angiopoietin-1 (ANG1) [57]. The *in vitro* activation of TIE2 by ANG1 induces the adhesion of these two types of cells and consequently favours the immature HSCs phenotype. Moreover, ANG1 promotes quiescence, enhances HSCs survival, and protects them from various cellular stresses. HSC quiescence and retention in the BM niche is also facilitated by the interaction between NOTCH1 and JAG1 or δ-like ligand 4 (Dll4) expressed by niche cells. Not surprisingly, a

specific relationship exists between NOTCH and stromal cell derived factor-1 (SDF-1 or CXCL12), a small chemokine belonging to the CXC subfamily with a strong chemoattractant property, and its receptor, C-X-C chemokine receptor type 4 (CXCR4). Indeed, in MSCs migration and function are regulated by the Notch/Dll4 pathway, as well as the expression of CXCR4 in ECs. Moreover, immature OBs in the endosteal niche express higher levels of CXCL12 and support the HSCs maintenance [58]. CXCL12 is also constitutively produced by BM stromal cells [59] to regulates HSC mobilization in the BM as well as cell adhesion, survival, and cell-cycle status [60]. Finally, CXCL12 expression is negatively modulated by G-CSF treatment and CXCR4 on HSCs may be inactivated during G-CSF treatment [61].

OCs are bone-resorbing cells coordinated with OBs in the bone formation process [62]. OCs are less well characterized than OBs in the context of HSC niche formation and maintenance. Nevertheless, new findings are beginning to emerge on the role of OCs in the haematopoiesis process. Specifically, it has been demonstrated that an OCs impairment reduce the OBs differentiation and HSCs localization in the *oc*/*oc* mouse model [63].

Although in the endosteal niche the regulatory signals released from neighbouring cells in the form of bound or secreted molecules and physical signals (i.e. oxygen tension) are crucial in the control of HSCs quiescence and activation, the soluble factors and signalling pathways present in the

vascular niche are important in HSCs self-renewal and maintenance.

The sinusoidal niche is composed by BM sinusoids. These vascular structures are thin walled vessels that serve as the medium for communication between the marrow cavity and blood circulation. BM sinusoids are lined by a single layer of endothelium and directly continue from arterioles to venules. A broad range of cells, including adventitial reticular cells, perivascular stromal cells, MSCs, and neurons, associate with sinusoids to form a niche able to sustain and regulate HSCs [51].

BM, in addition to its crucial role in the haematopoietic process, is also involved in both vasculogenesis and angiogenesis processes. Particularly, BM-derived endothelial cells (BM-DECs) indirectly promote vascular growth through the expression of angiogenic factors at the site where the neovascularization occurs [64,65]. BM-DECs express highly CXCR4 which is involved in their mobilization and homing [66,67]. Moreover, CXCL12 expression is directly regulated by VEGF [68]. Another mechanism proposed for the release of BM-DECs from BM involves the matrix metalloproteinase-9 (MMP9). Indeed, in hypoxic conditions, VEGF and CXCL12 are up-regulated and induce the release of activated MMP9 within the BM cell niches, which in turn activates soluble kit-ligand, resulting in the release of BM-DECs into the peripheral blood [69].

New vessels formed through angiogenesis during endochondral ossification are a source of perivascular osteoprogenitor cells and OCs, important for modelling and remodelling processes that ensure correct skeletal development and growth [70]. Bone cells secrete pro-angiogenic factors such as VEGF, which interacts with vascular endothelial growth factor receptor (VEGFR)-expressing cells including ECs, chondrocytes, OBs, and OCs. ECs release factors that regulate chondrocytes and cells of the osteoblast lineage [71]. During angiogenesis, which occurs in endochondral ossification, ECs of the advancing capillaries directly and indirectly influence the matrix resorption by producing proteases and regulatory molecules and by recruiting osteoclast precursors from the circulation. Also, osteocytes contribute to angiogenesis. It is thought that during bone damage the osteocytes that undergo apoptosis express VEGF [72].

Notch/Dll4 signalling is also involved in angiogenesis of adult long bones. Arteries express Dll4 and JAG1, the latter also in perivascular osteoprogenitor cells. The role of the Notch/Dll4 system is to stimulate vessel growth and ECs proliferation by regulating VEGFR expression. Moreover, mice with an impaired Notch/Dll4 pathway showed a reduction in long bone development, and an increased number of immature OBs [73].

### 1.6.2 Mesenchymal stromal cells and angiogenesis

Mesenchymal stromal cells (MSCs) can promote angiogenesis through several different mechanisms, including: (1) secretion of specific trophic and chemo-attractive factors; (2) organization of pericytes and endothelial supporting cells during neovascularization; (3) stimulation of endogenous endothelial progenitor cells (EPCs); (4) regulation of the immune microenvironment to enhance cell survival and, therefore, angiogenesis [74,75] (**Figure 1.4**).

MSCs express both direct and indirect pro-angiogenic factors considered essential biological mediators of vascular network remodelling [75]. One of the most important direct pro-angiogenic factors is VEGFA, which not only actively participate to this process but has also an autocrine ability to promote the synthesis of other multiple angiogenic molecules [76]. Among the indirect pro-angiogenic factors, instead, transforming growth factor beta-1 (TGFβ1) is considered a key player in the physiopathology of tissue repair and plays a crucial role in malignant transformation of epithelial cells. However, it has also been demonstrated that TGFβ1 induces the expression of many pro-angiogenic factors [77,78]. Moreover, TGFβ1 mediates both *in vitro* and *in vivo* angiogenesis through the autocrine or paracrine activation of vascular endothelial growth factor receptor-2 (VEGFR2) by VEGFA [78,79].

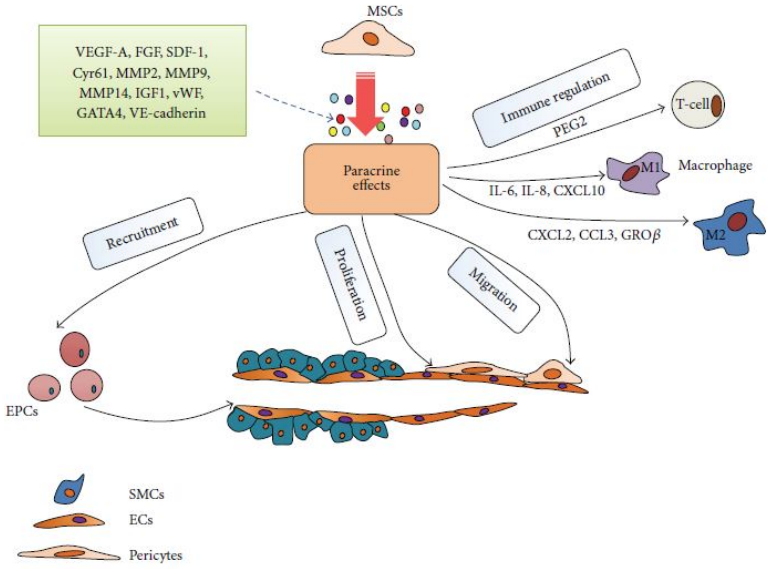


**Figure 1.4**: *Pro-angiogenic roles of MSCs*

The pro-angiogenic *stimuli* of MSCs are widely believed to be mediated by paracrine pathways particularly through the actions of VEGFA, FGF, and SDF-1α. Capillary growth requires degradation of the surrounding extracellular matrix (ECM) to allow ECs sprouting. Matrix metalloproteinases including MMP2, MMP9, and MMP14 are secreted by MSCs and target the ECM through distinct proteolytic actions thereby modulating the microenvironment and promoting appropriate interactions between MSCs and ECs. MSCs also secrete a rich mixture of cytokines and immune-modulating factors that enhance angiogenesis directly and indirectly.

*Abbreviations*: CCL3, macrophage inflammatory protein 1-alpha (MCP-1α); CXCL2/GROβ, chemokine (C-X-C motif) ligand 2; CXCL10, chemokine (C-X-C motif) ligand 10; Cyr61, cysteine-rich angiogenic inducer 61; ECs, endothelial cells; EPCs, endothelial progenitor cells; FGF, fibroblast growth factor; GATA4, GATA binding protein 4; IGF1, insulin-like growth factor-1; IL-6, interleukin-6; IL-8, interleukin-8; MMP2, matrix metalloproteinase-2; MMP9, matrix metalloproteinase-9; MMP14, matrix metalloproteinase-14; MSCs, mesenchymal stroma cells; PEG2, prostaglandin E2; SMCs, smooth muscle cells; VE-cadherin, vascular endothelial cadherin; VEGFA, vascular endothelial growth factor A [adapted from Xia X., et al. “Growth Hormone-Releasing Hormone and Its Analogues: Significance for MSCs-Mediated Angiogenesis”. Stem Cells Int. 2016;8737589]

### 1.6.3 Vascular endothelial growth factor family and related pro-angiogenic molecules

Vascular endothelial growth factor (VEGF) is the most well-known direct pro-angiogenic factor involved in EC migration, mitogenesis, sprouting, and tube formation. It is regulated by intrinsic and extrinsic factors as well as genetic alterations [75,80]. This heparin-binding molecule exists in several isoforms resulting from alternative splice variants from a single gene product. The soluble or membrane bound form binds to transmembrane receptor tyrosine kinases, VEGFR-1 (Flt-1) and VEGFR-2 (KDR/Flk-1) [81,82]. A third transmembrane receptor neuropilin-1 (NRP1), binding the VEGFA splice variant of $VEGF_{165}$, is involved in capillary morphogenesis, and appears to be required for EC filopodial tip directionality during angiogenesis [83]. Even though isolated MSCs are negative for VEGFRs expression, it has been demonstrated that VEGFA can induce MSCs to migrate and proliferate by binding and activating platelet-derived growth factor receptors (PDGFRs) [84,85]. Thus, VEGFA-induced PDGFR signalling is an important determinant in dictating the functionality of MSCs during postnatal physiological and pathological neovascularization. Moreover, it is tempting to speculate that the autocrine VEGFA production derived from MSCs may act trough this specific signalling. VEGFA is also one of the major growth factors used to induce endothelial differentiation of MSCs [86,87]. However, some researchers have raised doubts about this process, since it has been demonstrated that only very few MSCs exposed to the

exogenous administration of VEGFA (about less than 0.01%) are able to differentiate into endothelial marker-expressing cells [88]. More interesting, instead, is the paracrine activity exerted by VEGFA released from MSCs. VEGFA is able to promote the synthesis of several other angiogenic molecules [74], including TGFβ1, basic fibroblast growth factor (bFGF), platelet-derived growth factor (PDGF), and IL6. MSCs are able to exert their paracrine activity on ECs by synthesizing and secreting all these multiple factors, and promoting therefore angiogenesis. Indeed, it has been demonstrated that VEGFA produced and released by MSCs stimulates both the *in vitro* growth of human umbilical vein endothelial cells (HUVECs), and growth of tumour vessel density in a murine model of pancreatic β cell-derived tumours [88].

**Platelet-derived growth factor (PDGF)**. During angiogenesis, PDGF is thought to be mainly involved in the recruitment and proliferation of pericytes. However, it has been demonstrated that PDGF is also a mitogen and chemoattractant molecule for fibroblasts, smooth muscle cells (SMCs), and MSCs. There are four mammalian PDGF polypeptide chains (PDGFA, PDGFB, PDGFC and PDGFD), containing a motif of eight similarly spaced cysteine residues, resembling the structural pattern within VEGF ligands. PDGF ligands interact with, and activate, two distinct class III receptor tyrosine kinases, PDGF receptor-alpha (PDGFRα) and PDGF receptor-beta (PDGFRβ) [89-91]. PDGF induces angiogenesis by up-regulating VEGF production and modulating the proliferation and recruitment of perivascular

cells [80]. The angiogenic activity of PDGF might not only be based on the increased VEGFA production, because PDGFB stimulation induces also an augmented ECs lineage commitment and restricted differentiation of hematopoietic precursors [80]. Adult BM-MSCs express high levels of both PDGFRα and PDGFRβ on their cell surface, and isolated MSCs are defined by abundant cell surface PDGFRα and a high PDGFRα:PDGFRβ ratio [84]. Particularly, during MSC differentiation towards endothelial or smooth muscle cells (SMCs), PDGF signalling not only regulates individual transcription factors to induce gene expression, but also controls MSC fate by suppressing specific target transcripts. For example, during MSC commitment to SMCs, PDGFRα signalling activated RhoA, resulting in enhanced SM α-actin transcription and filament polymerization [92]. PDGFRα phosphorylation activates RhoA which, through Rho-associated kinase (ROCK)-dependent cofilin phosphorylation and myosin light chain kinase-dependent pathways, enhances SM α-actin filament polymerization. In contrast, PDGFRβ signalling inhibits SM α-actin filaments by up-regulating RhoE, which inhibits ROCK and by PDGFB induced cofilin-mediated filament destabilization [93].

As previously reported, VEGFA can stimulate PDGFRs exerting its effect on MSC migration and proliferation. Moreover, it has been demonstrated that a low concentration of $VEGFA_{165}$ at the cell surface can inhibit the chemotaxis

mediated by both PDGFA and -B, indicating that $VEGFA_{165}$ competes with PDGF ligands for PDGFRs occupancy.

**Fibroblast Growth Factor (FGF)**. This growth factor is another important direct pro-angiogenic molecule actively up-regulated during angiogenesis. The two most commonly studied forms FGF-2 or basic FGF (bFGF), and FGF-1 or acidic FGF (aFGF), bind the receptor tyrosine kinases FGFR-1 or FGFR-2 [80]. bFGF enhances endogenous VEGFA production, as well as VEGFA is required for the bFGF-induced expression of placental growth factor, proving the existence of a specific cross talk between bFGF and other pro-angiogenic growth factors [94,95]. bFGF has also effects on ECM remodelling during angiogenesis enhancing the proteolysis of matrix components (via up-regulation of urokinase receptors), and inducing the synthesis of collagen, fibronectin and proteoglycans by ECs [96]. However, unlike $VEGFA_{165}$, FGF binds with a high degree of affinity and saturation to ECM proteins, potentiating therefore its angiogenic activity.

In the mesenchymal context, it has been proved that FGF has proliferative effects on multipotent human stem cells and, more interestingly, it seems to control the differentiation of adipose-derived stromal cells (ASCs) towards ECs [97]. Recently it has been demonstrated that this process is enhanced in the presence of both FGF and VEGF [98], underlying once again the synergistic effect of these two pro-angiogenic growth factors.

**Interleukin-6 (IL6)**. IL6 is a glycosylated polypeptide secreted by different cell types, and considered one of the most important mediators of both inflammatory and immunity response. However, IL6 is also involved in other biological processes, including generation and maintenance of stem/progenitor cells, as well as invasion, metastasis and angiogenesis [99,100]. The pro-angiogenic activity of IL6 is predominantly mediated through STAT3 signalling. Indeed, STAT3 activation by IL6 facilitates angiogenesis in several cancer types by inducing the expression of *VEGF*, *bFGF* and *MMP9* in tumour-associated ECs [101,102]. Moreover, IL6 may also promote resistance to anti-angiogenic agents through influencing the phenotype of immune cells, which secrete numerous angiogenic factors [103]. The IL6/STAT3 signalling also functions as a transcriptional repressor of P53 expression, whilst blocking STAT3 up-regulates the expression of P53, and leading to P53-mediated apoptosis [104].

MSCs exert a paracrine activity on ECs by synthesizing and secreting IL6. Particularly, recent work suggests that BM-MSCs-produced IL6 may control the endothelial response via NF-kB pathway and, following this stimulation, ECs activate P-selectin, producing some of the main key molecules involved in both EC motility and activity and, therefore, potentiating angiogenesis [105]. Moreover, it has been proved that cultured medium (CM) of BM-MSCs enriched of IL6 appears to strongly influence nascent bone formation [106], as well as mediates the regulatory effect on macrophages [107].

**P53 and thrombospondin-1 (THBS1)**. P53 protein is the most important tumour suppressor factor, inactivated by mutations or deletions in approximately 50% of all malignancies. P53 is triggered by various types of stress, and able to cause multiple outcomes by the transcriptional activation of different target genes [108]. For example, P53 induces cell cycle arrest and DNA repair when cells are exposed to low levels of DNA damage, whereas it brings to cell death when cells are exposed to extensive DNA damages. Although some P53 effects may be independent of transcription, transcriptional regulation by P53 is important for tumour suppression, and loss of its function strongly promotes tumour development [108]. The P53 tumour suppressor protein is also able to stimulate several anti-angiogenic mechanisms; not surprisingly, tumour inhibition mediated by gene therapy carriers expressing P53 appears to be due in part to angiogenesis inhibition. Indeed, P53 may affect angiogenesis either by inducing the expression of thrombospondin-1 (THBS1) and/or down-regulating VEGFA [109,110]. Several studies have correlated the presence of wild-type P53 and increased levels of THBS1 with an anti-angiogenic effect on tumours. Moreover, it has been demonstrated that loss of functional P53 in small cell lung cancer specimens correlates with increases in VEGFA expression [111]. There is also evidence in suggesting that P53 could affect the growth of tumours by inducing the expression of THBS1 and, in a variety of cell lines, low levels of THBS1 correlate with a more malignant phenotype [112]. Recently, it

has been proved a novel role of THBS1 in stimulating MSC proliferation and migration via different pathways either in combination with PDGF or by activating latent TGFβ1 [113]. Particularly, this mechanism seems to be highly specific since THBS1 did not increase the activity of other growth factors such as bFGF, confirming previous studies showing that THBS1 potentiates only PDGF- but not bFGF-dependent migration of vascular smooth muscle cells [114].

**Chemokine (C-X-C motif) ligand 9 (CXCL9)**. This chemokine is a member of the C-X-C family and exerts mainly a significant role in the chemotaxis of immune cells. CXCL9 has also a versatile and controversial role in tumorigenesis since accumulating evidence suggest that CXCL9 is closely associated with both prognosis and tumour-derived angiogenesis [115]. CXCL9 is also considered a direct counter-regulatory molecule of VEGFA signalling due to its strong anti-proliferative and anti-migratory effect on VEGF-stimulated ECs [116]. CXCL9 produced by OBs is even involved both *in vivo* and *in vitro* suppression of angiogenesis and osteogenesis [117]. CXCL9 secreted by BM-MSCs was indeed identified to be an angiostatic factor able to counter-regulate VEGFA and prevented its binding to HUVECs, thus abrogated angiogenesis of MSCs-ECs co-culture [118]. These data revealed the critical role of CXCL9 in both angiogenesis and osteogenesis processes, and how its inhibition could be considered as a useful tool to target the impaired angiogenesis and, on the other hand, to prevent bone loss-related diseases.

**Angiopoietins (ANGs)**. ANGs form a family of secreted glycoproteins comprising ANG1, ANG2, and ANG4, acting primarily on the vasculature to control blood vessel development and stability [119]. While ANG1 has been widely accepted as an agonist for the tyrosine kinase with Ig and EGF homology domains (TIE2) receptor, ANG2 has been described as a context-dependent antagonist interfering with ANG1-induced TIE2 phosphorylation and eliciting, therefore, very different biological responses. Indeed, ANG1 has a significant role in stabilizing vessels by activating TIE2 receptor and subsequently promoting ECs survival and inhibition of ANG2 expression. Conversely, ANG2, mainly acting by the inhibition of the ANG1/TIE2 complex, leads to a destabilizing effect [119]. This latter outcome was demonstrated in a three-dimensional co-culture model of ECs and SMCs, where co-cultures were stimulated with ANG1, ANG2, and VEGFA. Interestingly, ANG2 disturbed the EC monolayer integrity by acting through an autocrine loop mechanism, and this effect was rescued by ANG1, VEGFA, or soluble TIE2 treatment [120]. Moreover, CM from transfected cells over-expressing ANG2 led to modest induction of both cell proliferation and capillary-like structures of HUVECs seeded on fibrin matrices in a dose-dependent manner, as well as in the absence of ANG1 [121]. Many other studies, instead, have also demonstrated the angiogenic role of ANG2 in an indirect fashion, through ANG2 inhibition in pathological angiogenesis [122].

ANG2 expression is triggered by inflammatory mediators, for example thrombin, and specific environmental conditions, such as hypoxia-derived molecules (i.e. VEGFA) and cancer [119]. Not surprisingly, the biological function of ANG2 has been closely linked to the bioavailability of VEGFA. Specifically, during development, ANG2 causes apoptosis of the vessel in the absence of VEGFA, whereas when VEGFA is available, ANG2 stimulates angiogenesis perhaps by disrupting the vessels' integrity. Moreover, the expression patterns of VEGFA and ANG2 correlate to the changes seen in the tumour: in early tumour development, the levels of VEGFA are low, whereas ANG2 is up-regulated and diffusely scattered throughout the tumour. Thus, in the absence of VEGFA, ANG2 may mark the ECs for destruction. At a later stage or when the tumour is large with evident central necrosis, both ANG2 and VEGFA are up-regulated primarily in the peripheral zones of the growth and, not surprisingly, marked angiogenesis and tumour development in these zones are present. Therefore, VEGFA determines whether ANG2 induces apoptosis of ECs or stimulates angiogenesis and tumour growth [119;122-126]. However, a clear understanding of the role of angiopoietins remains elusive and hard to define, as their highly context-dependent functions vary with the relative levels of ANG1, ANG2, VEGFA, as well as the cellular sources of angiogenic molecules under specific physiologic and pathologic conditions.

In MSCs, the angiogenic role of ANGs was studied mainly in cerebral ischemia [127,128]. Particularly, in a rat

model of middle cerebral artery occlusion it has been demonstrated that the therapeutic use of human MSCs significantly up-regulated both ANG1 and ANG2 mRNAs. Specifically, the expression of ANG2 was up-regulated earlier than ANG1, suggesting that ANG2-derived from human MSCs may be considered the early mediator of the angiogenesis process of the ischemic brain [127].

### 1.6.4 Transforming growth factor-beta family

The transforming growth factor- beta (TGFβ) superfamily members consist of > 30 cytokines including TGFβ1/2/3, activins/inhibins/ Müllerian-inhibiting substances (MIS), bone morphogenetic proteins (BMPs), Nodal, growth/ differentiation factors (GDFs), and the distantly related glial cell line-derived neurotrophic factors (GDNF) family [129]. TGFβ1/2/3 are present only in mammals and distinct genes encode for the relative isoforms, which are expressed in unique, occasionally overlapping patterns, and can perform many different *in vivo* functions [130-133]. TGFβ1 is the most abundant and ubiquitously expressed isoform [134], mainly recognized in cartilage and endochondral tissue, and involved in the development of bone and skin [131]. TGFβ2, also known as glioblastoma-derived T-cell suppressor factor, was first discovered in human glioblastoma cells, whereas TGFβ3 was first identified from a cDNA library of a human rhabdomyosarcoma cell line. Particularly, TGFβ2 is expressed by neurons and astrocytes, whereas pathologically it is involved

in tumorigenesis by enhancing cell proliferation and reducing the host immune surveillance against tumour development [135]. TGFβ3, instead, has an essential role in the development of the palate and lungs, mainly through the regulation of epithelial-mesenchymal interactions during embryonic, foetal, and neonatal development [132,136]. TGFβ family members are typically secreted and deposited in the ECM in its latent form, and their biological effects can only be delivered upon ligand activation. For example, TGFβ1 has to be activated by plasmin, MMPs (i.e. MMP2 and MMP9), THBS1, lower pH, integrins or reactive oxygen species [137], before assuming its role of signalling molecule. Consequently, the magnitude and duration of TGFβ1 signalling is closely controlled at many different levels.

TGFβ superfamily ligands bind to and signal through specific transmembrane serine-threonine kinases, type I (TGFβRI also known as ALK5) and type II receptor (TGFβRII). Auxiliary receptors, including the type III receptor (also known as β-glycan), and endoglin (also known as CD105) have been subsequently identified [138]. Nevertheless, neither β-glycan nor CD105 is directly involved in intracellular TGFβ signalling due to the deficiency of the kinase domain. Instead, they affect the access of TGFβ ligands to its receptors, and consequently modulate the intracellular signalling [138]. All the three TGFβ isoforms have affinity for β-glycan, with a particular higher affinity for TGFβ2. However, CD105 binds TGFβ1 and TGFβ3 with identical affinity, and it has also a weak affinity for TGFβ2

[138]. In most of the cellular context, active forms of TGFβ signal through a canonical Smad-mediated pathway. Particularly, TGFβ1 binds to TGFRβII first and then cross-links to ALK5. This pattern was also adopted by activin, suggesting that TGFβs/activins assemble their receptors in an ordered manner. However, upon ligand activation, TGFRβII phosphorylates its type I receptor partner, which then transmits the signal by the phosphorylation of intracellular small mother against decapentaplegic (Smad) proteins. Eight Smads (Smad1 to Smad8) have been identified in vertebrates. Specifically, Smad1/5/8 are activated by BMP receptors, whereas Smad2/3 are activated by TGFβ/activin/nodal receptors. These receptor-activated Smads form heterotrimers with a common Smad (Smad4) shared by the TGFβ/activin/nodal and BMP signalling pathways, and translocate into the nucleus [138,139]. On the other hand, TGFβ1 could also activates the non-Smad pathways through the interactions of signalling mediators with the type I/II receptors, either directly or through adaptor proteins. Following this signalling, TGFβ1 can directly activate the Ras-Raf-MEK-ERK/MAPK pathway through the interaction of ShcA and the TGFβ receptor complex. In response to TGFβ1, ALK5 mediates tyrosine phosphorylation of ShcA, which then recruits Grb2 and Sos, to form a complex, initiating Ras activation and consequently ERK/MAPK signalling cascade. TGFβ1 can also activate TAK1 through TRAF6, a ubiquitin ligase, which interacts with the TGFβ receptor complex, leading to induction of p38 and JNK MAPK signalling.

Even if the exact mechanism still remains to be explored, TGFβ1 can modulate the activities of the small GTPase proteins Rho, Rac, and Cdc42, which regulate cytoskeletal organization and gene expression. TGFβ1 also activates Akt pathway through the phospho-inositol 3 kinase (PI3K), and consequently, initiates signalling pathways, through for example mTOR, which have roles in cell survival, growth, migration, and invasion [139,140]. Although in most cell types TGFβ1 signalling is conveyed through ALK5, during angiogenesis multiple studies have identified the activin receptor-like kinase-1 (ALK1) as an alternative type I receptor for TGFβ1. In ECs, indeed, TGFβ1 has been shown to signal via both ALK5 and ALK1 receptors and, depending on which type I receptor is recruited, different Smad signalling cascades are activated (**Figure 1.5**) [141]. Particularly, ALK1 activation induces the phosphorylation of Smad1/5/8, whereas ALK5 leads to Smad 2/3 activation. The ALK5 and ALK1 pathways mediates opposite effects: ALK5 inhibits, whereas, ALK1 stimulates both endothelial cell growth and migration [141,142]. In addition, ALK5, but not ALK1, mediates TGFβ1 induction of EC apoptosis [143]. However, in these cells TGFβ1/ALK1/Smad1 signalling mediates the expression of VEGFA [144], which is required for TGFβ1 induction of apoptosis [78]. In this context, CD105, one of the two TGFβ auxiliary receptors as well as the highly up-regulated gene during actively angiogenesis, efficiently modulates TGFβ1/ALK1 but not TGFβ1/ALK5 signalling [145]. It has been demonstrated that the multiple

functions exerted by CD105 during physiological and pathological angiogenesis [146] are mediated through both canonical and non-canonical TGFβ1 signalling pathways. Therefore, it is not a surprise that ECs are characterized by a specific correlation between the expression of platelet endothelial cell adhesion molecule (PECAM-1, also known as CD31), one of the most important EC markers, and CD105, where the reduced expression of this latter brings to the related down-regulation of the first. In other words, through undetermined mechanisms, CD31 and endoglin influence the expression of each other, and their altered expression generate defective angiogenic properties of ECs through the intracellular signalling pathways induced by TGFβ1 [147].

The dual role of ALK5 and ALK1 were also studied in MSCs. Recently, it has been demonstrated that *in vitro*-expanded human BM-MSCs as well as chondrogenically differentiating human BM-MSC pellet cultures express both *ALK5* and *ALK1* gene. More interestingly, TGFβ1, besides inducing chondrogenic differentiation of BM-MSCs, regulates the expression of its receptors by enhancing ALK5 expression whilst down-regulates ALK1 expression, and therefore skewing the balance between its two receptors towards ALK5 [148].

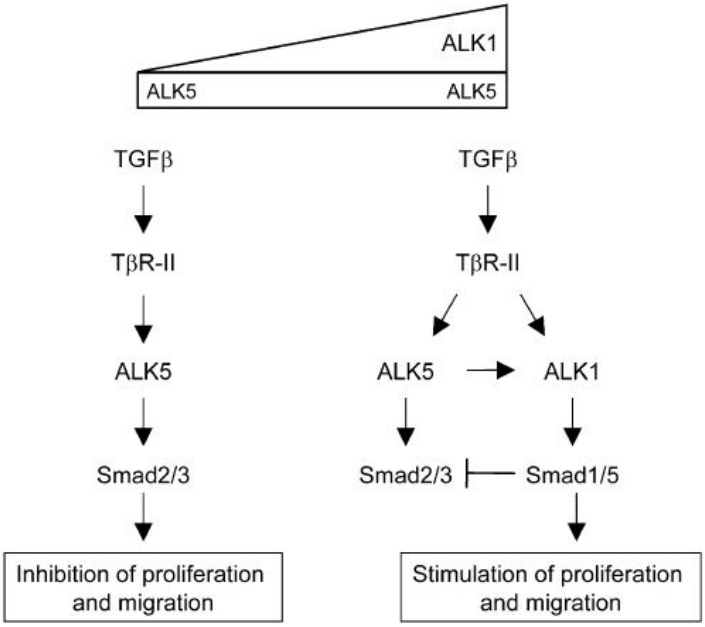


**Figure 1.5**: *Schematic Model for Activation of TGFβRs in ECs*

TGFβ1 first binds to TGFβRII, which subsequently recruits ALK5. ALK5 is phosphorylated and activated by TGFβRII kinase. ALK5 can recruit ALK1 into the complex, and for its activation both ALK5 and TGFβRII kinase are required. Activated ALK1 and activated ALK5 induce phosphorylation of Smad1/5 and Smad2/3, respectively. ALK1 and ALK5 have opposite effects on EC migration and proliferation. In addition, ALK1 directly inhibits ALK5/Smad3 signalling. The ratio between ALK1 and ALK5 expression will determine whether TGFβ1 will induce activation or quiescence of the endothelium.

*Abbreviations*: ALK1, activin receptor-like kinase-1; ALK5, activin receptor-like kinase-5 also known as TGFβRI; Smad, small mother against decapentaplegic protein; TGFβ, transforming growth factor beta; TGβR-II, transforming growth factor beta receptor II [adapted from Goumans J., et al. “Activin Receptor-Like Kinase (ALK)1 Is an Antagonistic Mediator of Lateral TGFbeta/ALK5 Signaling”. Mol Cell. 2003 Oct;12(4):817-28]

TGFβ1 is mainly considered as an important regulator of tissue morphogenesis and as a strong inhibitor of proliferation for most cell types. In MSCs, TGFβ1 is involved in osteoclastic

bone resorption, and orchestrates the migration of these cells to the bone resorptive surface [139]. Moreover, active TGFβ1 also controls both mobilization and recruitment of MSCs to injured tissues [140], stimulating MSC proliferation and differentiation [141,142]. As an indirect pro-angiogenic factor, TGFβ1 plays a pivotal role in the regulation of vasculogenesis and angiogenesis. Particularly, TGFβ1 can exert effects on angiogenesis by regulating the expression of other important pro-angiogenic factors, such as VEGFA, and components of the ECM, including MMPs (i.e. MMP2) and integrins [149]. In MSCs, indeed, TGFβ1 stimulates the VEGFA synthesis through Akt and ERK1/2 pathways [150], and it has been proved that this mechanism could be responsible for the enhanced tumour angiogenesis seen in hepatocellular carcinoma [151]. Moreover, the dual cooperation between TGFβ1 and VEGFA was also found in a nerve regeneration study performed with ASCs and xenogeneic acellular nerve matrix in combination with TGFβ1 [152]. Not surprisingly, in this *in vivo* model it has been demonstrated that the inhibition of VEGFA with a neutralizing antibody, affected the protective role of TGFβ1 on ASCs apoptosis, supporting the hypothesis that this effect was achieved through the promotion of VEGF-dependent angiogenesis.

**Matrix metalloproteinases (MMPs) and tissue inhibitors of metalloproteinases (TIMPs)**. MMPs are a family of proteases able to degrade ECM proteins, and exerting a critical role in vascular remodelling, cellular migration, and sprout formation

[153]. The observation that there is significant up-regulation of MMP activity in ECs during inflammation, wound healing and tumour growth reflects their important role in both physiologic and pathologic angiogenesis [154]. Protein inhibitors of MMP2 and MMP9 have been shown to greatly attenuate the migration of both ECs and tumour cells and have been proposed as therapeutic targets in oncology [155]. The anti-tumour effects of targeted MMP inhibition is likely due to the dual benefits of inhibiting tumour angiogenesis and metastasis, as these processes both require significant ECM degradation [155,156]. While the presence of growth factors can modulate the activity and expression of ECM proteolytic pathways, it is clear that the interaction between growth factors and proteases is bidirectional. Proteolytic growth factors activation or release from ECM reservoirs can propagate the angiogenic response by allowing a sustained cell-demanded local concentration of active pro- (or anti-) angiogenic *stimuli* within the tissue. In addition, MMP2 has been shown to directly cleave the extracellular domain of the FGF-1 receptor, which releases a soluble extracellular receptor domain that binds FGF-1 and may modulate angiogenesis *in vivo* [157]. Matrix remodelling proteins also appear to be involved in formation of luminal and tubular structures during the morphogenic differentiation of ECs in a manner that is specific to the type of MMP involved, with the membrane-bound forms appearing to be more critical in these events than secreted MMPs [158,159].

In MSCs, instead, it has been demonstrated that despite the secretion of MMP active forms, MMP enzyme activity was not detected in the CM of these cells due to TIMP-mediated inhibition. Therefore, MSC-secreted growth factors protect vascular matrix molecules and EC structures from MMP-induced disruption. Furthermore, MSCs remained matrix-protective even when exposed to pro-inflammatory cytokines and hypoxia, countering these stresses with increased TIMP1 expression and augmented MMP-inhibition. Thus, MSCs are an efficient source of TIMP-mediated MMP-inhibition, capable of protecting the perivascular niche from high levels of MMPs even under pathological conditions [160].

## 1.7 Scope of the thesis

Using both *in vitro* and *in vivo* models, our research group recently demonstrated that SDS-MSCs display a marked impairment in their angiogenic potential [47]. However, further studies are needed to understand whether the altered SDS angiogenesis could be the marrow promoting factor of the progression of malignant clones.

The general aim of my PhD project was to better elucidate the cellular and molecular mechanisms underlying haematological defects typically observed in SDS patients.

In particular, we focused our attention on two different lines of research:

1. The study of the altered *in vitro* capillary-like capability of SDS-MSCs;
2. The analysis of the involvement of mTOR-STAT3 signalling in SDS lymphoid lineage (in collaboration with Dr. Cipolli and Dr. Bezzerri).

# REFERENCES


[1] Shwachman H., et al. The syndrome of pancreatic insufficiency and bone marrow dysfunction. J Pediatr. 1964 nov;65:645-63.
[2] Burke V., et al. Association of pancreatic insufficiency and chronic neutropenia in childhood. Arch Dis Child. 1967 Apr;42(222):147-57.
[3] Doe W.F. Two brothers with congenital pancreatic exocrine insufficiency, neutropenia and dysgammaglobulinaemia. Proc R Soc Med. 1973 Nov;66(11):1125-26.
[4] Brueton M.J., et al. Hepatic dysfunction in association with pancreatic insufficiency and cyclical neutropenia. Shwachman-Diamond syndrome. Arch Dis Child. 1977 Jan;52(1):76-8.
[5] Cipolli M. Shwachman-Diamond syndrome: clinical phenotypes. Pancreatology. 2001;1:543-48.
[6] Dror Y., Freedman M.H. Shwachman-diamond syndrome. Br J Haematol. 2002 Sep;118(3):701-13.
[7] Nelson A.S., Myers K.C. Diagnosis, Treatment, and Molecular Pathology of Shwachman-Diamond Syndrome. Hematol Oncol Clin North Am. 2018 Aug;32(4):687-700.
[8] Nelson A., Myers K. Shwachman-Diamond Syndrome. 2008 Jul 17 [Updated 2018 Oct 18]. In: Adam M.P., et al., editors. GeneReviews® [Internet]. Seattle (WA): University of Washington, Seattle; 1993-2020.
[9] Minelli A., et al. Incidence of Shwachman-Diamond syndrome. Pediatr Blood Cancer. 2012 Dec;59(7)1334-35.
[10] Boocock G.R., et al. Mutations in SBDS are associated with Shwachman-Diamond syndrome. Nat Genet. 2003 Jan;33(1):97-101.
[11] Dhanraj S., et al. Biallelic mutations in DNAJC21 cause Shwachman-Diamond syndrome. Blood. 2017 Mar;129(11):1557-62.
[12] Tummala H., et al. DNAJC21 mutations link a cancer-prone bone marrow failure syndrome to corruption in 60S ribosome subunit maturation. Am J Hum Genet. 2016 Jul;99(1):115-24.
[13] Aggett P.J., et al. Shwachman's syndrome. A review of 21 cases. Arch Dis Child. 1980 May;55(5):331-47.
[14] Ip W.F., et al. Serum pancreatic enzymes define the pancreatic phenotype in patients with Shwachman-Diamond syndrome. J Pediatr. 2002 Aug;141(2):259-65.
[15] Rosendahl J., et al. Compound heterozygous mutations of the SBDS gene in a patient with Shwachman-Diamond syndrome, type 1 diabetes mellitus and osteoporosis. Pancreatology. 2006;6(6):549-54.

[16] Terlizzi V., et al. Can continuous subcutaneous insulin infusion improve health-related quality of life in patients with Shwachman-Bodian-Diamond syndrome and diabetes? Diabetes Technol Ther. 2015 Jan;17(1):64-7.
[17] Dror Y. Shwachman-Diamond syndrome. Pediatr Blood Cancer. 2005 Dec;45(7):892-901.
[18] Dror Y., Freedman M.H. Shwachman-Diamond syndrome: An inherited preleukemic bone marrow failure disorder with aberrant hematopoietic progenitors and faulty marrow microenvironment. Blood. 1999 Nov 1;94(9):3048-54.
[19] Dror Y., Freedman M.H. Shwachman-Diamond syndrome marrow cells show abnormally increased apoptosis mediated through the Fas pathway. Blood. 2001 May 15;97(10):3011-16.
[20] Rujkijyanont P., et al. SBDS-deficient cells undergo accelerated apoptosis through the Fas-pathway. Haematologica. 2008 Mar;93(3):363-71.
[21] Smith A., et al. Intermittent 20q- and consistent i(7q) in a patient with Shwachman-Diamond syndrome. Pediatr Hematol Oncol. 2002 Oct-Nov;19(7):525-28.
[22] Valli R., et al. Novel recurrent chromosome anomalies in Shwachman-Diamond syndrome. Pediatr Blood Cancer. 2017 Aug;64(8).
[23] McLennan T.W., Steinbach H.L. Schwachman's syndrome: the broad spectrum of bony abnormalities. Radiology. 1974 Jul;112(1):167-73.
[24] Makitie O., et al. Skeletal phenotype in patients with Shwachman-Diamond syndrome and mutations in SBDS. Clin Genet. 2004 Feb;65(2):101-12.
[25] Perobelli S., et al. Diffuse alterations in grey and white matter associated with cognitive impairment in Shwachman–Diamond syndrome: Evidence from a multimodal approach. Neuroimage Clin. 2015 Feb;7:721-31.
[26] Kent A., et al. Psychological characteristics of children with Shwachman syndrome. Arch Dis Child. 1990 Dec;65(12):1349-52.
[27] Cipolli M., et al. Shwachman's syndrome: Pathomorphosis and long-term outcome. J Pediatr Gastroenterol Nutr. 1999 Sep;29(3):265-72.
[28] Toiviainen-Salo S., et al. Shwachman-Diamond syndrome is associated with structural brain alterations on MRI. Am J Med Genet A. 2008 Jun;146A(12):1558-64.
[29] Booij J., et al. Increase in central striatal dopamine transporters in patients with Shwachman-Diamond syndrome: additional evidence of a brain phenotype. Am J Med Genet A. 2013 Jan;161A(1):102-07.

[30] Boocock G.R., et al. Mutations in SBDS are associated with Shwachman-Diamond syndrome. Nat Genet. 2003 Jan;33(1):97-101.
[31] Warren A.J. Molecular basis of the human ribosomopathy Shwachman-Diamond syndrome. Adv Biol Regul. 2018 Jan;67:109-27.
[32] Stepensky P., et al. Mutations in EFL1, an SBDS partner, are associated with infantile pancytopenia, exocrine pancreatic insufficiency and skeletal anomalies in a Shwachman-Diamond like syndrome. J Med Genet. 2017 Aug;54(8):558-66.
[33] Carapito R., et al. Mutations in signal recognition particle SRP54 cause syndromic neutropenia with Shwachman-Diamond-like features. J Clin Invest. 2017 Nov;127(11):4090-4103.
[34] Ball H.L., et al. Shwachman-Bodian Diamond syndrome is a multi-functional protein implicated in cellular stress responses. Hum Mol Genet. 2009 Oct;18(19):3684-95.
[35] Finch A.J., et al. Uncoupling of GTP hydrolysis from eIF6 release on the ribosome causes Shwachman-Diamond syndrome. Genes Dev. 2011 May;25(9):898-900.
[36] Yamaguchi M., et al. Shwachman-Diamond syndrome is not necessary for the terminal maturation of neutrophils but is important for maintaining viability of granulocyte precursors. Exp Hematol. 2007 Apr;35(4):579-86.
[37] Orelio C., Kuijpers T.W. Shwachman-Diamond syndrome neutrophils have altered chemoattractant-induced F-actin polymerization and polarization characteristics. Haematologica. 2009 Mar;94(3):409-13.
[38] Austin K.M., et al. Mitotic spindle destabilization and genomic instability in Shwachman-Diamond syndrome. J Clin Invest. 2008 Apr;118(4):1511-18.
[39] Bezzerri V., et al. New insights into the Shwachman-Diamond Syndrome-related haematological disorder: hyper-activation of mTOR and STAT3 in leukocytes. Sci Rep. 2016 Sep 23;6:33165.
[40] Vella A., et al. mTOR and STAT3 Pathway Hyper-Activation is Associated with elevated Interleukin-6 Levels in Patients with Shwachman-Diamond Syndrome: Further Evidence of Lymphoid Lineage Impairment. Cancers (Basel). 2020 Mar 5;12(3):597.
[41] Weis F., et al. Mechanism of eIF6 release from the nascent 60S ribosomal subunit. Nat Struct Mol Biol. 2015 Nov;22(11):914-19.
[42] Bernardo M.E., Fibbe W.E. Mesenchymal stromal cells: sensors and switchers of inflammation. Cell Stem Cell. 2013 Oct;13(4):392-402.
[43] Lee M.W., et al. Mesenchymal stem cells in suppression or progression of hematologic malignancy: current status and challenges. Leukemia. 2019 Mar;33(3):597-611.

[44] Raaijmakers M.H., et al. Bone progenitor dysfunction induces myelodysplasia and secondary leukaemia. Nature. 2010 Apr;464(7290):852-57.
[45] Santamaria C., et al. Impaired expression of DICER, DROSHA, SBDS and some microRNAs in mesenchymal stromal cells from myelodysplastic syndrome patients. Haematologica. 2012 Aug;97(8):1218-24.
[46] Andre' V., et al. Mesenchymal stem cells from Shwachman-Diamond syndrome patients display normal functions and do not contribute to hematological defects. Blood Cancer J. 2012 Oct;2(10), e94.
[47] Bardelli D., et al. Mesenchymal stromal cells from Shwachman-Diamond syndrome patients fail to recreate a bone marrow niche in vivo and exhibit impaired angiogenesis. Br J Haematol. 2018 Jul;182(1):114-24.
[48] Kuzu I., et al. Bone marrow microvessel density (MVD) in adult acute myeloid leukemia (AML): therapy induced changes and effects on survival. Leuk Lymphoma. 2004 Jun;45(6):1185-90.
[49] Leung E.W., et al. Shwachman-Diamond Syndrome: An Inherited Model of Aplastic Anaemia With Accelerated Angiogenesis. Br J Haematol. 2006 Jun;133(5):558-61.
[50] Papadaki H.A., Eliopoulos G.D. The role of apoptosis in the pathophysiology of chronic neutropenias associated with bone marrow failure. Cell Cycle. Sep-Oct 2003;2(5):447-51.
[51] Dale D.C., et al. Cyclic neutropenia. Semin Hematol. 2002 Apr;39(2):89-94.
[52] Zeidler C., Welte K. Kostmann syndrome and severe congenital neutropenia. Semin Hematol. 2002 Apr;39(2):82-8.
[53] Aprikyan A.A., et al. Myelokathexis, a congenital disorder of severe neutropenia characterized by accelerated apoptosis and defective expression of bcl-x in neutrophil precursors. Blood. 2000 Jan 1;95(1):320-17.
[54] Elghetany M.T., Alter B.P. p53 protein overexpression in bone marrow biopsies of patients with Shwachman-Diamond syndrome has a prevalence similar to that of patients with refractory anemia. Arch Pathol Lab Med. 2002 Apr;126(4):452-55.
[55] Semenza G.L. Vasculogenesis, angiogenesis, and arteriogenesis: mechanisms of blood vessel formation and remodeling. J Cell Biochem. 2007 Nov;102(4):840-47.
[56] Nwajei F., Konopleva M. The bone marrow microenvironment as niche retreats for hematopoietic and leukemic stem cells. Adv Hematol. 2013;953982.

[57] Shirzad R., et al. Signaling and molecular basis of bone marrow niche angiogenesis in leukemia. Clin Transl Oncol. 2016 Oct;18(10):957-71.
[58] Nakamura Y., et al. Isolation and characterization of endosteal niche cell populations that regulate hematopoietic stem cells. Blood. 2010 Sep;116(9):1422-32.
[59] Pelus L.M., Broxmeyer H.E. Peripheral blood stem cell mobilization; a look ahead. Curr Stem Cell Rep. 2018 Dec;4(4):273-81.
[60] Nervi B., et al. Cytokines and hematopoietic stem cell mobilization. J Cell Biochem. 2006 Oct;99(3):690-705.
[61] Ogawa M. Differentiation and proliferation of hematopoietic stem cells. Blood. 1993 Jun;81(11):2844-53.
[62] Schröder H.C., et al. Silicate modulates the cross-talk between osteoblasts (SaOS-2) and osteoclasts (RAW 264.7 cells): inhibition of osteoclast growth and differentiation. J Cell Biochem. 2012 Oct;113(10):3197-206.
[63] Mansour A., et al. Osteoclasts promote the formation of hematopoietic stem cell niches in the bone marrow. J Exp Med. 2012 Mar;209(3):537-49.
[64] Yang L., et al. Expansion of myeloid immune suppressor Gr+CD11b+ cells in tumor-bearing host directly promotes tumor angiogenesis. Cancer Cell. 2004 Oct;6(4):409-21.
[65] Ziegelhoeffer T., et al. Bone marrow-derived cells do not incorporate into the adult growing vasculature. Circ Res. 2004 Feb;94(2):230-38.
[66] Burger J.A., Kipps T.J. CXCR4: A key receptor in the crosstalk between tumor cells and their microenvironment. Blood. 2006 Mar;107:1761-67.
[67] Ruiz de Almodovar C., et al. An SDF-1 trap for myeloid cells stimulates angiogenesis. Cell. 2006 Jan;124(1):18-21.
[68] Hattori, K., et al. Vascular endothelial growth factor and angiopoietin-1 stimulate postnatal hematopoiesis by recruitment of vasculogenic and hematopoietic stem cells. J Exp Med. 2001 May;193(1):1005-14.
[69] Seandel M., et al. A catalytic role for proangiogenic marrow-derived cells in tumor neovascularization. Cancer Cell. 2008 Mar;13(3):181-83.
[70] Brandi M.L., Collin-Osdoby P. Vascular biology and the skeleton. J Bone Miner Res. 2006 Feb;21(2):183-92.
[71] Kusumbe A.P., et al. Coupling of angiogenesis and osteogenesis by a specific vessel subtype in bone. Nature. 2014 Mar;507(3):323-28.

[72]. Cheung W.Y., et al. Osteocyte apoptosis is mechanically regulated and induces angiogenesis in vitro. J Orthop Res. 2010 Apr;29(4):523-30.
[73] Ramasamy S.K., et al. Endothelial notch activity promotes angiogenesis and osteogenesis in bone. Nature. 2014 Mar;507(3):376-80.
[74] Caplan A.I., Dennis J.E. Mesenchymal stem cells as trophic mediators. J Cell Biochem. 2006 Aug;98(5):1076-84.
[75] Xia X., et al. Growth Hormone-Releasing Hormone and Its Analogues: Significance for MSCs-Mediated Angiogenesis. Stem Cells Int. 2016;8737589.
[76] Zheng W., et al. Mechanisms of coronary angiogenesis in response to stretch: role of VEGF and TGF-beta. Am J Physiol Heart Circ Physiol. 2001 Feb;280(2):H909-17.
[77] Nakagawa T., et al. TGF-beta Induces Proangiogenic and Antiangiogenic Factors via Parallel but Distinct Smad Pathways. Kidney Int. 2004 Aug;66(2):605-13.
[78] Ferrari G., et al. VEGF, a Prosurvival Factor, Acts in Concert With TGF-beta1 to Induce Endothelial Cell Apoptosis. Proc Natl Acad Sci U S A. 2006 Nov;103(46):17260-65.
[79] Ferrari G., et al. TGF-β1 Induces Endothelial Cell Apoptosis by Shifting VEGF Activation of p38(MAPK) From the Prosurvival p38β to Proapoptotic p38α. Mol Cancer Res. 2012 May;10(5):605-14.
[80] Acuzian A.A., et al. Molecular Mediators of Angiogenesis. J Burn Care Res. 2010 Jan-Feb;31(1):158-75.
[81] Ferrara N., et al. The biology of VEGF and its receptors. Nat Med. 2003 Jun;9(6):669-76.
[82] Neufeld G., et al. Vascular endothelial growth factor and its receptors. Prog Growth Factor Res. 1994;5(1):89-97.
[83] Gerhardt H., et al. Neuropilin-1 is required for endothelial tip cell guidance in the developing central nervous system. Dev Dyn Nov. 2004 Nov;231(3):503-09.
[84] Ball S.G. et al. Mesenchymal stem cells and neovascularization: role of platelet-derived growth factor receptors. J Cell Mol Med. 2007 Sep-Oct;11(5):1012-30.
[85] Ball S.G., et al. Platelet-derived Growth Factor Receptors Regulate Mesenchymal Stem Cell Fate: Implications for Neovascularization. Expert Opin Biol Ther. 2010 Jan;10(1):57-71.
[86] Oswald J., et al. Mesenchymal Stem Cells Can Be Differentiated Into Endothelial Cells in Vitro. Stem Cells. 2004;22(3):377-84.
[87] Wang N., et al. Vascular Endothelial Growth Factor Stimulates Endothelial Differentiation From Mesenchymal Stem Cells via Rho/myocardin-related Transcription Factor--A Signaling Pathway. Int J Biochem Cell Biol. 2013 Jul;45(7):1447-56.

[88] Beckermann B.M., et al. VEGF expression by mesenchymal stem cells contributes to angiogenesis in pancreatic carcinoma. Br. J. Cancer. 2008 Aug;99(4):622-31.
[89] Andrae J., et al. Role of platelet-derived growth factors in physiology and medicine. Genes Dev. 2008 May;22(10):1276-12.
[90] Clowes A.W. Regulation of smooth muscle cell proliferation and migration. Transplant Proc. 1999 Feb-Mar;31(12):810.
[91] Fredriksson L., et al. The PDGF family: four gene products form five dimeric isoforms. Cytokine Growth Factor Rev. 2004 Aug;15(4):197-204.
[92] Ball S.G., et al. Direct cell contact influences bone marrow mesenchymal stem cell fate. Int J Biochem Cell Biol. 2004 Apr;36:714-27.
[93] Ball S.G., et al. Platelet-derived Growth Factor Receptor-Alpha Is a Key Determinant of Smooth Muscle Alpha-Actin Filaments in Bone Marrow-Derived Mesenchymal Stem Cells. Int J Biochem Cell Biol. 2007;39(2):379-91.
[94] Couper L.L., et al. Vascular endothelial growth factor increases the mitogenic response to fibroblast growth factor-2 in vascular smooth muscle cells in vivo via expression of fms-like tyrosine kinase-1. Circ Res. 1997 Dec;81(6):932-39.
[95] Faraone D., et al. Heterodimerization of FGF-receptor 1 and PDGF-receptor-alpha: a novel mechanism underlying the inhibitory effect of PDGF-BB on FGF-2 in human cells. Blood. 2006 Mar;107(5):1896-902.
[96] Pepper M.S., et al. Upregulation of urokinase receptor expression on migrating endothelial cells. J Cell Biol. 1993 Aug;122(3):673-84.
[97] Cherubino M., Marra K.G. Adipose-derived stem cells for soft tissue reconstruction. Regen Med. 2009 Jan;4(1):109-17.
[98] Khan S., et al. Fibroblast growth factor and vascular endothelial growth factor play a critical role in endotheliogenesis from human adipose-derived stem cells. J Vasc Surg. 2017 May;65(5):1483-92.
[99] Taniguchi K., Karin M. IL-6 and Related Cytokines as the Critical Lynchpins Between Inflammation and Cancer. Semin Immunol. 2014 Feb;26(1):54-74.
[100] Kumari N., et al. Role of interleukin-6 in Cancer Progression and Therapeutic Resistance. Tumour Biol. 2016 Sep;37(9):11553-72.
[101] Nagasaki T., et al. Interleukin-6 released by colon cancer-associated fibroblasts is critical for tumour angiogenesis: anti-interleukin-6 receptor antibody suppressed angiogenesis and inhibited tumour-stroma interaction. Br J Cancer. 2014 Jan;110(2):469-78.

[102] Zou M., et al. IL6-induced metastasis modulators p-STAT3, MMP-2 and MMP-9 are targets of 3,3′-diindolylmethane in ovarian cancer cells. Cell Oncol (Dordr). 2015 Feb;39(1):47-57.
[103] Middleton K., et al. Interleukin-6. An angiogenic target in solid tumours. Crit Rev Oncol Hematol. 2014 Jan;89(1):129-39.
[104] Niu G., et al. Role of Stat3 in regulating p53 expression and function. Mol Cell Biol. 2005 Sep;25(17):7432-40.
[105] Li J., et al. Transcriptional Profiling Reveals Crosstalk Between Mesenchymal Stem Cells and Endothelial Cells Promoting Prevascularization by Reciprocal Mechanisms. Stem Cells Dev. 2015 Mar;24(5):610-23.
[106] Ando Y., et al. Stem cell-conditioned medium accelerates distraction osteogenesis through multiple regenerative mechanisms. Bone. 2014 Apr;61:82-90.
[107] Luz-Crawford P., et al. Mesenchymal Stem Cells Direct the Immunological Fate of Macrophages. Results Probl Cell Differ. 2017;62:61-72.
[108] Levine A.J. P53, the Cellular Gatekeeper for Growth and Division. Cell. 1997 Feb;88(3):323-31.
[109] Volpert O.V., et al. Sequential development of an angiogenic phenotype by human fibroblasts progressing to tumorigenicity. Oncogene. 1997 Mar;14(12):1495-502.
[110] Dameron K.M., et al. The p53 tumor suppressor gene inhibits angiogenesis by stimulating the production of thrombospondin. Cold Spring Harb Symp Quant Biol. 1994;59:483-89.
[111] Giatromanolaki A., et al. Vascular endothelial growth factor, wild-type p53, and angiogenesis in early operable non-small cell lung cancer. Clin Cancer Res. 1998 Dec;4(12):3017-24.
[112] Zabrenetzky V., et al. Expression of the extracellular matrix molecule Thrombospondin inversely correlates with malignant progression in melanoma, lung, and breast carcinoma. Int J Cancer. 1994 Oct;59(2):191-95.
[113] Belotti D., et al. Thrombospondin-1 Promotes Mesenchymal Stromal Cell Functions via TGFβ and in Cooperation With PDGF. Matrix Biol. 2016 Sep;55:106-16.
[114] Isenberg J.S., et al. Endogenous thrombospondin-1 is not necessary for proliferation but is permissive for vascular smooth muscle cell responses to platelet-derived.growth factor. Matrix Biol. 2005 Apr;24:110-23.
[115] Ding Q., et al. CXCL9: Evidence and Contradictions for Its Role in Tumor Progression. Cancer Med. 2016 Nov;5(11):3246-59.
[116] Sahin H., et al. Chemokine Cxcl9 attenuates liver fibrosis-associated angiogenesis in mice. Hepatology. 2012 May;55(5):1610-19.

[117] Huang B., et al. Osteoblasts secrete Cxcl9 to regulate angiogenesis in bone. Nat. Commun. 2016 Dec;7:13885.
[118] Shen Q., et al. Inhibiting Expression of Cxcl9 Promotes Angiogenesis in MSCs-HUVECs Co-Culture. Arch Biochem Biophys. 2019 Oct;675:108108.
[119] Fagiani E., Christofori G. Angiopoietins in angiogenesis. Cancer Lett. 2013 Jan;328(1):18-26.
[120] Scharpfenecker M., et al. The Tie-2 ligand angiopoietin-2 destabilizes quiescent endothelium through an internal autocrine loop mechanism. J. Cell Sci. 2005 Feb;118(Pt 4):771-80.
[121] Teichert-Kuliszewska K., et al. Biological action of angiopoietin-2 in a fibrin matrix model of angiogenesis is associated with activation of Tie2. Cardiovasc Res. 2001 Feb;49(3):659-70.
[122] Oliner J., et al. Suppression of angiogenesis and tumor growth by selective inhibition of angiopoietin-2. Cancer Cell. 2004 Nov;6(5):507-16.
[123] Krikun G., et al. Expression of angiopoietin-2 by human endometrial endothelial cells: regulation by hypoxia and inflammation. Biochem Biophys Res Commun. 2000 Aug;275(1):159-63.
[124] Oh H., et al. Hypoxia and vascular endothelial growth factor selectively up-regulate angiopoietin-2 in bovine microvascular endothelial cells. J Biol Chem. 1999 May;274(22):15732-29.
[125] Thomas M., Augustin H.G. The role of the Angiopoietins in vascular morphogenesis. Angiogenesis. 2009;12(2):125-37.
[126] Post S., et al. Balance between angiopoietin-1 and angiopoietin-2 is in favor of angiopoietin-2 in atherosclerotic plaques with high microvessel density. J Vasc Res. 2008;45(3):244-50.
[127] Ma X., et al. Human Mesenchymal Stem Cells Increases Expression of α-Tubulin and Angiopoietin 1 and 2 in Focal Cerebral Ischemia and Reperfusion. Curr Neurovasc Res. 2013 May;10(2):103-11.
[128] Vu N.B., et al. Allogeneic Adipose-Derived Mesenchymal Stem Cell Transplantation Enhances the Expression of Angiogenic Factors in a Mouse Acute Hindlimb Ischemic Model. Adv Exp Med Biol. 2018;1083:1-17.
[129] Kingsley D.M. The TGF-beta superfamily: new members, new receptors, and new genetic tests of function in different organisms. Genes Dev. 1994 Jan;8(2):133-46.
[130] Letterio J.J., Roberts A.B. Transforming growth factor-beta1-deficient mice: identification of isoform-specific activities in vivo. J Leukoc Biol. 1996 Jun;59(6):769-74
[131] Dickinson M.E., et al. Chromosomal localization of seven members of the murine TGF-beta superfamily suggests close linkage

to several morphogenetic mutant loci. Genomics. 1990 Mar;6(3):505-20.
[132] Proetzel G., et al. Transforming growth factor-beta 3 is required for secondary palate fusion. Nat Genet. 1995 Dec;11(4);409-14.
[133] Sanford L.P., et al. TGFbeta2 knockout mice have multiple developmental defects that are non-overlapping with other TGF beta knockout phenotypes. Development. 1997 Jul;124(13):2659-70.
[134] Derynck R., et al. Human transforming growth factor-beta complementary DNA sequence and expression in normal and transformed cells. Nature. 1985 Aug;316(6030):701-05.
[135] Flanders K.C., et al. Localization and actions of transforming growth factor-beta S in the embryonic nervous system. Development. 1991 Sep;113(1):183-91.
[136] Kaartinen V., et al. Abnormal lung development and cleft palate in mice lacking TGF-beta 3 indicates defects of epithelial–mesenchymal interaction. Nat Genet. 1995 Dec;11(4):415-21.
[137] Annes J.P., et al. Making sense of latent TGF beta activation. J Cell Sci. 2003 Jan;116(Pt 2);217-24.
[138] de Caestecker M. The transforming growth factor-beta superfamily of receptors. Cytokine Growth Factor Rev. 2004 Feb;15(1):1-11.
[139] Wrana J.L. Signaling by the TGFb Superfamily. Cold Spring Harb Perspect Biol. 2013;5:a011197.
[140] Xian L., et al. Matrix IGF-1 maintains bone mass by activation of mTOR in mesenchymal stem cells. Nat Med. 2012 Jul;18(7):1095-101.
[141] Orlova V.V., et al. Controlling Angiogenesis by Two Unique TGF-β Type I Receptor Signaling Pathways. Histol Histopathol. 2011 Sep;26(9):1219-30.
[142] Goumans J., et al. Activin Receptor-Like Kinase (ALK)1 Is an Antagonistic Mediator of Lateral TGFbeta/ALK5 Signaling. Mol Cell. 2003 Oct;12(4):817-28.
[143] Ota T., et al. Targets of Transcriptional Regulation by Two Distinct Type I Receptors for Transforming Growth Factor-Beta in Human Umbilical Vein Endothelial Cells. J Cell Physiol. 2002 Dec;193(3):299-318.
[144] Boström K., et al. Matrix GLA protein stimulates VEGF expression through increased transforming growth factor-beta1 activity in endothelial cells. J Biol Chem. 2004 Dec;279(51):52904-13.
[145] Lebrin F., et al. Endoglin promotes endothelial cell proliferation and TGF-beta/alk1 signal transduction. EMBO J. 2004 Oct;23(20):4018-28.
[146] ten Dijke P., et al. Endoglin in angiogenesis and vascular diseases. Angiogenesis. 2008;11(1):79-89.

[147] Park S., et al. PECAM-1 Isoforms, eNOS and Endoglin Axis in Regulation of Angiogenesis. Clin Sci (Lond). 2015 Aug;129(3):217-34.
[148] de Kroon L.M.G., et al. Activin Receptor-Like Kinase Receptors ALK5 and ALK1 Are Both Required for TGFβ-Induced Chondrogenic Differentiation of Human Bone Marrow-Derived Mesenchymal Stem Cells. PLoS One. 2015 Dec;10(12):e0146124.
[149] Liu Z., et al. VEGF and inhibitors of TGFbeta type-I receptor kinase synergistically promote blood-vessel formation by inducing alpha5-integrin expression. J Cell Sci. 2009 Sep;122(Pt 18):3294e302.
[150] Wang X.J., et al. Transforming Growth factor-beta1 Enhanced Vascular Endothelial Growth Factor Synthesis in Mesenchymal Stem Cells. Biochem Biophys Res Commun. 2008 Jun;365(3):548-54.
[151] Li G.C., et al. Mesenchymal Stem Cells Promote Tumor Angiogenesis via the Action of Transforming Growth Factor β1. Oncol Lett. 2016 Feb;11(2):1089-94.
[152] Luo H., et al. The Protection of MSCs From Apoptosis in Nerve Regeneration by TGFβ1 Through Reducing Inflammation and Promoting VEGF-dependent Angiogenesis. Biomaterials. 2012 Jun;33(17):4277-87.
[153] Visse R., Nagase H. Matrix metalloproteinases and tissue inhibitors of metalloproteinases: structure, function, and biochemistry. Circ Res. 2003 May;92(8):827-39.
[154] van Hinsbergh V.W., Koolwijk P. Endothelial sprouting and angiogenesis: matrix metalloproteinases in the lead. Cardiovasc Res. 2008 May;78(2):203-12.
[155] Montesano R., et al. Phorbol ester induces cultured endothelial cells to invade a fibrin matrix in the presence of fibrinolytic inhibitors. J Cell Physiol. 1987 Sep;132(3):509-16.
[156] Wilson C.L., et al. Intestinal tumorigenesis is suppressed in mice lacking the metalloproteinase matrilysin. Proc Natl Acad Sci U S A. 1997 Feb;94(4):1402-07.
[157] Levi E., et al. Matrix metalloproteinase 2 releases active soluble ectodomain of fibroblast growth factor receptor 1. Proc Natl Acad Sci U S A. 1996 Jul;93(14):7069-74.
[158] Saunders W.B., et al. Coregulation of vascular tube stabilization by endothelial cell TIMP-2 and pericyte TIMP-3. J Cell Biol. 2006 Oct;175(1):179-91.
[159] Bayless K.J., Davis G.E. Sphingosine-1-phosphate markedly induces matrix metalloproteinase and integrin-dependent human endothelial cell invasion and lumen formation in three-dimensional collagen and fibrin matrices. Biochem Biophys Res Commun. 2003 Dec;312(4):903-13.

[160] Lozito T.P., Tuan R.S. Mesenchymal Stem Cells Inhibit Both Endogenous and Exogenous MMPs via Secreted TIMPs. J Cell Physiol. 2011 Feb;226(2):385-96.

# Chapter 2

# The altered TGFβ1/VEGFA axis hampers *in vitro* angiogenic capability of Shwachman-Diamond Syndrome - mesenchymal stromal cells

Gloria Bedini[1], C. Gervasoni[1], E. Dander[1], C. Bugarin[1], A. Pegoraro[2], S. Cesaro[3], P. Farruggia[4], C. Dufour[5], M. Cipolli[2], V. Bezzerri[6], A. Biondi[1,7], G. D'Amico[1]

**Manuscript in preparation**

[1]Department of Paediatrics, Centro Ricerca Tettamanti, University of Milano-Bicocca, Fondazione MBBM, Monza; [2]Cystic Fibrosis Center, Azienda Ospedaliera Universitaria Integrata Verona, Verona; [3]Department of Paediatrics, Paediatric Haematology Oncology, Azienda Ospedaliera Universitaria Integrata Verona, Verona; [4]Department of Paediatric Haemato-Oncology, ARNAS Ospedali Civico, G Di Cristina, Palermo; [5]Haematology Unit, Giannina Gaslini Children's Research Hospital, Genoa; [6]Cystic Fibrosis Center, Azienda Ospedaliero Universitaria Ospedali Riuniti, Ancona; [7]Department of Paediatrics, University of Milano-Bicocca, San Gerardo Hospital/Fondazione MBBM, Monza (Italy)

## 2.1 Abstract

Shwachman-Diamond Syndrome (SDS; OMIM # 260400) is an inherited bone marrow (BM) failure disorder associated with leukaemia predisposition. Approximately 90% of patients meeting clinical criteria for the diagnosis of SDS harbour mutations in Shwachman-Bodian-Diamond Syndrome (*SBDS*) gene. Although the role of SBDS protein is yet to be fully established, it is thought to be involved in multiple important cellular pathways including ribosomal maturation, mitosis, and stromal microenvironment. Using both *in vitro* and *in vivo* models, our research group recently demonstrated that SDS-MSCs display a marked impairment in their angiogenic potential. Here, we confirm that SDS-derived cells obtained from a cohort of 10 patients show impaired angiogenic properties in response to angiogenic *stimuli*. Moreover, we demonstrate that the expression of several growth factors able to increase the endogenous release of VEGFA and to be induced by TGFβ1 is down-regulated in SDS- *vs* HD-MSCs. Our data also reveal that under angiogenic stimulation, P53 protein levels are 2-fold increase in SDS- *vs* HD-MSCs, as well as the number of early/late apoptotic cells. Interestingly, by providing the exogenous administration of VEGFA or TGFβ1, only SDS-MSCs from severely neutropenic patients are able to restore their angiogenic properties. Moreover, our preliminary results also show that VEGFA treatment leads to the normalization of P53 protein levels only in MSCs derived from severely neutropenic patient. Collectively, our results suggest

that the defective *in vitro* SDS-MSC tube formation is associated to TGFβ1/VEGFA signalling abnormalities. Moreover, we provide a rational to investigate whether the defective angiogenesis driven by SDS-MSCs could be related to patients' neutropenia. The better comprehension of the molecular mechanisms regulating neutrophil number and functionality may lead to novel strategies for the management of SDS recurrent infections.

**Keywords**: angiogenesis; mesenchymal stromal cells; neutropenia; VEGFA; TGFβ1

## 2.2 Rationale

Shwachman-Diamond Syndrome (SDS, OMIM # 260400) is a genetic multisystem disorder associated with bone marrow (BM) failure and increased risk of transformation to myelodysplastic syndrome (MDS) and acute myeloid leukaemia (AML) [1,2]. Hematological abnormalities are present in all SDS patients, where neutropenia is the most common deficiency frequently associated with other cytopenias, such as normochromic anaemia and thrombocytopenia [1,2]. SDS is also characterised by several other developmental anomalies including intrinsic growth abnormality, pancreatic insufficiency and cognitive impairment. SDS is a rare disease, considering an incidence of 1/168,000 new-borns with a mean of 3.0 new cases/year in Italy [3], and no ethnic-specific predilection.

SDS is an autosomal recessive disorder with approximately 90% of affected patients having biallelic mutations in Shwachman-Bodian-Diamond Syndrome (*SBDS*) gene [4,5]. Recently, it has also been reported that other genes, including 60S ribosome assembly factor *DNAJC21* (yeast *JJJ1*), elongation factor-like GTPase 1 (*EFL1*) [6,7] and signal recognition particle 54 (*SRP54*) [8], are associated with SDS-like phenotype. Even if all these genes play a role in ribosome biogenesis and function [4], thus defining SDS as ribosomopathy, the functional defect responsible of SDS phenotype has not yet been defined. However, it was demonstrated that both molecular and genetic alterations in one

or more cellular elements of the BM niche could promote the progression of haematological malignancies usually seen in SDS patients [9-11].

Angiogenesis plays an important role in the pathogenesis and progression of haematological malignancies. Indeed, BM stromal cells including osteoblasts, osteoclasts and mesenchymal stromal cells (MSCs), promote the proliferation of leukemic cells and angiogenesis by secreting cytokines and chemokines [12]. In 2006, it was demonstrated that BM biopsies of SDS patients are characterized by an increased number of microvessels compared to those found in healthy BM of the same age [13]. However, the increased microvessel density did not correlate with severe aplastic anaemia, MDS or leukaemia, probably because SDS patients who develop MDS and/or AML collect multiple molecular and cellular abnormalities until transformation becomes evident.

Mesenchymal stromal cells are the key component of the BM stroma and inhibit or promote tumour growth by suppressing either proliferation or apoptosis of tumour cells, respectively [14]. Particularly, MSCs can potentiate angiogenesis via direct cell differentiation, cell-cell interaction, and autocrine or paracrine effects [15,16]. In 2010, our research group isolated and characterized BM-MSCs from SDS patients demonstrating that SDS-derived cells are similar to healthy donor (HD)-MSCs in terms of morphology and growth kinetics [17]. However, our unpublished gene expression data also revealed that several genes are differentially modulated

between SDS- and HD-MSCs, suggesting that these molecular differences could underlying a possible alteration in the functional properties of SDS-MSCs. Indeed, by applying an *in vivo* model of hematopoietic niche able to recreate the BM microenvironment [18], we further demonstrated that *in vivo* implanted cartilaginous pellets derived from SDS-MSCs display a marked impairment in their angiogenic potential, resulting in the formation of dysfunctional BM niches [19]. Moreover, we showed that the ability of SDS-MSCs to form correct tube-networks under specific angiogenic *stimuli* is severely affected in comparison to HD-MSCs. Interestingly, the defective *in vitro* SDS-MSCs angiogenic capability was associated to a specific decreased in the expression of vascular endothelial growth factor A (*VEGFα*) gene [19], one of the main regulators of angiogenesis.

Here, we deeply analysed the cellular and molecular mechanisms underlying the defective *in vitro* angiogenic capability of SDS-MSCs. Our data provide new evidence supporting the involvement of TGFβ1/VEGFA axis in dictating the *in vitro* angiogenic properties of SDS-MSCs.

## 2.3 Experimental procedures

### 2.3.1 Shwachman-Diamond Syndrome patients and healthy controls

Mesenchymal stromal cells (MSCs) were derived from bone marrow (BM) samples of 13 SDS patients and 12 age-gender-matched healthy donors (HD; median age at enrolment 11 years, range from 3 to 15 years old; 50% male), as previously reported [17,19].

SDS diagnosis was based on clinical and genetics criteria. The median age at enrolment was 9 years (range from 1 to 19 years old; 38% male), and all patients were carriers of classical *SBDS* mutations associated with normal karyotype or cytogenetic abnormalities isochromosome 7q/20q deletion (**Table 2.1**). Almost all SDS patients were also neutropenic. Neutropenia is usually considered as a blood neutrophil count < 1500 cells/μL. Particularly, mild neutropenia is defined as the absolute neutrophil count (ANC) < 1500 cells/μL, whereas moderate neutropenia represents a count less than 1000 cells/μL. ANC < 500 cells/μL, instead, characterizes the severe degree of neutropenia [1,20].

### 2.3.2 Ethical issues

The study design was approved by the Ethics Committee of San Gerardo Hospital (Monza, Italy; approval No. 504 4/9/2012), and performed in accordance with the 2013 WMA

Declaration of Helsinki. Samples were obtained after informed consent was released by the legal guardians or, whenever eligible, by patients/donors themselves. Privacy procedures were also applied to protect personal identities of subjects.

### 2.3.3 BM-MSC isolation, culture and expansion

Bone marrow-MSCs were isolated and cultured as previously described [17,19]. Briefly, mononuclear cells (MNCs) were isolated using Ficoll-Paque PLUS (GE Healthcare, Waukesha, WI, USA) and seeded at 0.16 x $10^6$ cells/$cm^2$ in Dulbecco's Modified Eagle's Medium Low Glucose (DMEM LG, Lonza, Basel, Switzerland) supplemented with 10% of foetal bovine serum (FBS, Biosera, Heathfield, Sussex, UK), 1% of L-glutamine (EuroClone, Pero, Italy) and 1% of penicillin and streptomycin (EuroClone). BM-MNCs were incubated at 37°C in humidified atmosphere, with 5% $CO_2$, and after 48 hours the culture medium was replaced and non-adherent cells were removed, whereas adherent cells were maintained with medium replacement twice a week. As the culture reached around 80-90% of confluence, cells were detached with 0.25% trypsin-EDTA (EuroClone) and seeded at 0.10 x $10^6$ cells/$cm^2$. Cell number and viability were assessed using trypan blue exclusion count. Cell growth, between passage 3 (P3) and 5 (P5), was analysed by cumulative population doublings (CPD) following the formula $\log_{10}$ (harvested cells/seeded cells)/$\log_{10}$ (2) [21]. After P3, MSCs phenotype was assessed using the following

monoclonal antibodies (mAb): phycoerythrin (PE)-labelled anti-CD14 (eBioscience, San Diego, CA, USA); PE-labelled anti-CD34 (BD Biosciences, San Jose, CA, USA); PE-labelled anti-CD45 (BD); PE-labelled anti-CD73 (BD); PE-labelled anti-CD90 (eBioscience); PE-labelled anti-CD105 (eBioscience); fluorescein isothiocyanate-labelled anti-HLA-ABC (BD); PE-labelled anti-HLA-DR (BD), and allophycocyanin-(APC)-labelled anti-CD54 (ICAM1) (BD). Staining of at least 0.05 x $10^6$ cells was performed at 4°C for 30 min in the dark, and in presence of 1% FBS to avoid unspecific binding. Samples were acquired by FACSCanto II (BD) and post-acquisition analyses were performed using FlowJo Software (BD). To evaluate the osteogenic and adipogenic differentiation ability, BM-MSCs were stimulated for 14 and 21 days with specific differentiation inductive media. Adipogenic inductive medium consisted of DMEM-High Glucose (EuroClone) supplemented with 10% FBS, penicillin (100 U/mL), streptomycin (100 µg/mL) and L-glutamine (2 mM), dexamethasone (1 µM), indomethacin (1 µM), 3-isobutyl-1-methylxantine (IBMX) (500 µM) and human recombinant insulin (10 µg/mL) (SigmaAldrich, St Louis, MO, USA). Lipid droplets were stained with Oil Red O (SigmaAldrich). Osteogenic inductive medium, instead, consisted of DMEM LG, 10% FBS, 2-phosphate-ascorbic acid (50 µM), β-glycerol phosphate (10 mM) and dexamethasone (100 nM) (SigmaAldrich). The presence of calcium deposits was detected by Alizarin Red staining (SigmaAldrich).

### 2.3.4 Matrigel angiogenesis assay

Matrigel *in vitro* angiogenesis assay was performed as previously described [19], with slight modifications. Briefly, after an overnight starvation in DMEM LG (Lonza) supplemented with 2% of FBS (Biosera), 1% of L-glutamine (EuroClone) and 1% of penicillin and streptomycin (EuroClone) (referred as basal condition), 0.22 x $10^6$ cells/$cm^2$ were seeded in 24- or 6-well plates, pre-coated with Matrigel (Corning, New York USA). To stimulate angiogenesis (stimulated condition, referred also as angiogenic *stimuli*), MSCs were then resuspended in vascular cell medium (Vascular Cell Basal Medium PCS-100-030; American Type Culture Collection, Manassas, VA, USA) supplemented with 5% FBS and different pro-angiogenic factors: ascorbic acid (50 µg/mL), bFGF (5 ng/mL), EGF (5 ng/mL), heparan sulphate (0.75 U/mL), hydrocortisone (1 µg/mL), IGF (15 ng/mL), VEGFA (5 ng/mL), and L-glutamine (10 mM). After 2- and 3-hours incubation at 37°C, capillary tube formation was assessed with a phase-contrast microscope. Where specified, TGFβ1 (10 ng/mL) (R&D System, Minneapolis, MN, USA), or VEGFA ($VEGF_{165}$; 50 ng/mL) (SigmaAldrich) were further added to the above-mentioned stimulation medium. Three photographs for each well were acquired by means of a phase-contrast microscope (Zeiss Axiovert40C; Zeiss, Obercocken, Germany), and analysed using *ImageJ Angiogenesis Analyzer* (http://rsb.info.nih.gov/ij). Supernatants were collected and cryopreserved at -80°C for further analysis. To isolate MSCs from the cellular matrix,

Matrigel was digested with Hank's Balanced Salt Solution (Gibco/Invitrogen, Thermo Fisher Scientific) containing 10 U/mL dispase (Roche Diagnostics, Basel, Switzerland). After the enzymatic incubation, MSCs were washed with ice-cold PBS supplemented with 2% FBS (Biosera), and processed for gene expression or protein analysis.

### 2.3.5 Viability assay

For the detection of viable, early/late apoptotic, and necrotic cells, the GFP-Certified® Apoptosis/Necrosis Detection Kit (Enzo Life Sciences, Farmingdale, NY, USA) was used following the manufacturer's instructions. Briefly, at least 0.2 x $10^6$ MSCs pre- and post-Matrigel assay were washed and resuspended in binding buffer (1:10 in $H_2O$). Then, the annexin V-PE and 7-AAD were added for 15 min in the dark at room temperature. For every condition, at least 50,000 events were collected and analysed. Samples were acquired by FACSCanto II (BD) and post-acquisition analyses were performed using FlowJo Software (BD).

### 2.3.6 RNA isolation and Quantitative Real-Time polymerase chain reaction (qPCR)

Total RNA was isolated using TRIzol reagent (Invitrogen, Carlsbad, CA, USA) following the manufacturer's instructions. RNA concentration was determined using NanoDrop ND-2000 Spectrophotometer (Thermo Scientific, Waltham, USA), and

500 ng of total RNA was used to perform first strand cDNA synthesis by Superscript (Invitrogen). The qPCR was run in triplicate with SYBR® Green PCR Master Mix (Thermo Scientific) on 7500/7500 Fast Real-Time PCR System (Thermo Scientific). The ABI PRISM 7300 SDS software (relative quantification study) was used to determine the cycle threshold (CT) for each reaction, and the specificity of qPCR products was checked by melting curve analysis. Total cDNA from human telomerase-immortalized microvascular endothelial (TIME) cells was used as positive control, and reverse transcription negative controls were also included in all amplification experiments. Primer sequences, listed in **Table 2.2**, were designed using Primer-BLAST Software (http://www.ncbi.nlm.nih.gov/tools/primer-blast) [22].

Gene expression determined for each gene was normalized to the expression of the endogenous housekeeping gene *Tata Binding Protein* (*TBP*) [23]. The relative expression intensity was estimated using the comparative CT method [24].

*Signal transducer and activator of transcription-3* (*STAT3*) and *P53* gene expression was instead quantified by QuantiTect Primer Assays (Qiagen, Hilden, Germany) (STAT3: Hs_STAT3_1_SG, NM_003150; P53: Hs_P53_1_SG, NM_000546).

**Table 2.2**: *Quantitative Real-Time polymerase chain reaction primers (listed in alphabetical order)*

| *target gene* | *primers* | $T_m$ (°C) | *product lenght (bp)* |
|---|---|---|---|
| h*ALK1* (activin receptor-like kinase-1) | F: ccatcgtgaatggcatcgt | 58 | 63 |
| | R: ggtcattgggcaccacatc | | |
| h*ALK5* (transforming growth factor beta receptor-1) | F: tgggctctgctttgtctctg | 60 | 202 |
| | R: tgaaaaagggccagtagttgga | | |
| h*ANG1* (angiopoietin-1) | F: tttgccattaccagtcagagg | 60 | 184 |
| | R: cagcaccgtgtaagatcagg | | |
| h*ANG2* (angiopoietin-2) | F: ttatcacagcaccagcaagc | 60 | 221 |
| | R: cgcgagaacaaatgtgagaa | | |
| h*bFGF* (basic fibroblast growth factor) | F: ggctgtactgcaaaaacggg | 61 | 94 |
| | R: agcttgatgtgagggtcgc | | |
| h*CD31* (platelet endothelial cell adhesion molecule-1) | F: gtgtcttgagtgggtgggag | 60 | 70 |
| | R: aggcgtggttctcatctgtg | | |
| h*CD105* (endoglin) | F: aggaggtcgctacctgtgta | 60 | 61 |
| | R: tgaatgtggacccggttctt | | |
| h*CXCL9* (C-X-C motif chemokine ligand-9) | F: gtgcaaggaaccccagtagt | 60 | 110 |
| | R: gggcttggggcaaattgttt | | |
| h*INHBA* (activin-a) | F: cattgctccctctggctatcat | 60 | 161 |
| | R: gcacacagcacgatttgaggtt | | |
| h*IL-6* (interleukin-6) | F: accgggaacgaaagagaagc | 60 | 74 |
| | R: cgaaggcgcttgtggaga | | |
| h*MMP2* (matrix metalloproteinase-2) | F: tacgatggaggcgctaatgg | 60 | 166 |
| | R: caggtattgcactgccaactc | | |
| h*NRP1* (neurophilin-1) | F: cgcaaggcgaagtcttttga | 60 | 266 |
| | R: ccacctgtgagctggaagtc | | |
| h*PDGFA* (platelet-derived growth factor subunit-A) | F: cgtagggagtgaggattctttg | 60 | 117 |
| | R: gcttcctcgatgcttctctt | | |
| h*PDGFR* α (platelet-derived growth factor receptor-alpha) | F: gaagctgtcaacctgcatga | 60 | 187 |
| | R: cttccttagcacggatcagc | | |
| h*PDGFR* β (platelet-derived growth factor receptor beta) | F: atgctcagcagagtgtcatcc | 60 | 73 |
| | R: gggtgatgttctcaccctgg | | |
| h*SMAD1* (small mother against decapentaplegic-1) | F: gcgtgagagacagatgtggg | 60 | 275 |
| | R: acccagtcagcacgaaaagg | | |
| h*SMAD3* (small mother against decapentaplegic-3) | F: catcgagccccagagcaata | 60 | 88 |
| | R: gtggttcatctggtggtcact | | |
| h*SMAD4* (small mother against decapentaplegic-4) | F: tgtggcttccacaagtcagc | 60 | 283 |
| | R: aggctggaatgcaagctcat | | |
| h*TBP* (tata binding protein) | F: gcaccactccactgtatccc | 61 | 79 |
| | R: ccagaactctccgaagctgg | | |
| h*TGF β 1* (trasforming growth factor-beta 1) | F: acctgccacagatcccctat | 60 | 176 |
| | R: ctcccggcaaaaggtaggag | | |
| h*TGF β2* (trasforming growth factor-beta 2) | F: ctgtgggtaccttgatgcca | 61 | 170 |
| | R: gctcaatccgttgttcaggc | | |
| h*TGF β3* (trasforming growth factor-beta 3) | F: agcgctatatcggtggcaagaatc | 65 | 390 |
| | R: cctccaagttgcggaagcagtaat | | |
| h*THBS1* (thrombospondin-1) | F: gtccccgtggtcatcttgtt | 60 | 158 |
| | R: ctccattgatggggcaggc | | |
| h*TIE-2* (tyrosin-protein kinase receptor-2) | F: tgtgctgttccttcttgcct | 61 | 212 |
| | R: gcaccttccacagttccaga | | |
| h*TIMP1* (tissue inhibitor of metalloproteinases-1 ) | F: ctgttgttgctgtggctgat | 60 | 104 |
| | R: aacttggccctgatgacg | | |
| h*VEGF* α (vascular endothelial growth factor-alpha) | F: tacatcttcaagccatcctgtg | 58 | 169 |
| | R: tgttgtgctgtaggaagctcat | | |

*Abbreviations*: bp, base pair; F, forward primer; h, human; R, reverse primer; $T_m$, melting temperature

### 2.3.7 TGFβ1 intracellular staining

For the detection of intracellular TGFβ1, MSCs pre- and post-Matrigel assay were incubated with APC-conjugated human TGFβ1 mAb (R&D System). Briefly, MSCs were firstly permeabilized with Cytofix/Cytoperm (BD), and then incubated with mAb. Staining of at least 0.1 x $10^6$ cells was performed at 4°C for 30 min in the dark, in presence of 1% FBS to avoid unspecific binding. Samples were acquired by FACSCanto II (BD) and post-acquisition analyses were performed using FlowJo Software (BD).

### 2.3.8 ELISA assay for quantification of IL6 and CXCL9

Levels of IL6 and CXCL9 were assessed in MSC culture supernatants pre- and post-Matrigel assay using commercially available ELISA kits (R&D Systems), according to the manufacturer's instructions. Absorbance was read on a Genios microplate reader (Tecan, Switzerland) using Magellan Software. When the value obtained resulted below the detection limit of the kit, a value equal to half of the last concentration of the standard curve was assigned.

### 2.3.9 Western blot analysis

Western blot analysis was performed as previously reported [25]. Briefly, a total of 35-50 µg of MSC extract pre- and post- Matrigel assay was denatured for 5 min at 95°C in 4X Laemmli Sample Buffer (277.8 mM Tris-HCl, pH 6.8, 44.4%

glycerol, 4.4% LDS, 0.02% bromophenol blue) (Bio-Rad Laboratories, Philadelphia, PA, USA), supplemented with 355 mM 2-mercaptoethanol. The samples were loaded on 11% polyacrylamide SDS-PAGE gel in Tris-glycine Buffer (25 mM Tris, 192 mM glycine, and 0.1% SDS). Primary antibodies were: anti-human P53 rabbit polyclonal antibody (Ab131442, Abcam; dilution 1:500), and monoclonal anti-β-Actin clone AC-15 (Sigma-Aldrich, diluted 1:2000). Secondary antibodies were obtained from SigmaAldrich. Band intensity was calculated by scanning video densitometry using the ChemiDoc imaging system (UVP, LCC, Upland, CA, USA).

### 2.3.10 STAT3 flow cytometry

After an overnight starvation in DMEM LG (Lonza) supplemented with 2% of FBS (Biosera), 1% of L-glutamine (EuroClone) and 1% of penicillin and streptomycin (EuroColne) (referred as basal condition), SDS- and HD-MSCs were firstly detached with 0.25% trypsin-EDTA (EuroClone), washed with Dulbecco's Phosphate Buffered Saline (PBS; EuroClone), and then stimulated with angiogenic *stimuli* for various lengths of time. After fixation in 16% paraformaldehyde (SigmaAldrich), MSCs were permeabilized with 90% cold methanol (SigmaAldrich) according to Nolan's Lab protocol (http:// www.cytobank.org/nolanlab/experiment_protocols/general_prot ocol.html). Samples were then stored in 90% methanol at -20°C until usage. After recovery, MSCs were washed with PBS and

stained with anti-STAT3-APC (BD), anti-pS727-STAT3-488 (BD), anti-Y705-STAT3-PE (BD), or isotype control-conjugated mAbs for 30 min in the dark. Samples were acquired on FACS Aria (BD) and post-acquisition analyses were performed using FlowJo Software (BD).

### 2.3.11 Statistical analysis

All values are expressed as mean ± sd or sem. Normal distribution was tested in each experiment using the Shapiro-Wilk Test. Based on that, independent groups were tested using Mann-Whitney U Test, while Wilcoxon was used in case of pair data. Data were analysed through GraphPad Prism 6.1 (GraphPad Software Inc, La Jolla, CA, USA) assuming a p-value less than 0.05 as the limit of significance (see figure legends for details). Figures show data from representative experiments.

## 2.4 Results

### 2.4.1 SDS- and HD-bone marrow mesenchymal stromal cell characterization

Mesenchymal stromal cells (MSCs) were obtained from the bone marrow of 13 SDS patients (**Table 2.1**), and 12 age-gender-matched healthy donors (HD). Following the classical ISCT characterization [26], SDS-MSCs resulted comparable in terms of immunophenotype and adipogenic/osteogenic differentiation to HD-MSCs (**Supplementary Figure 2.1 A and B**), as previously reported [17]. From P3 to P5, MSCs were further characterised by evaluating their growth capacity in terms of cumulative population doublings (CPDs) [21]. As shown in **Supplementary Figure 2.1 C**, CPDs obtained from both SDS- and HD-MSCs were similar at each passage (P3: 3.82±0.13 *vs* 3.14±0.67, P4: 7.15±0.70 *vs* 6.86±0.82, and P5: 9.75±1.45 *vs* 9.81±0.82, respectively). Particularly, an average of 3 days was necessary to double the cell number of SDS- and HD-derived cells. During the entire culture period, the viability of SDS- and HD-MSCs resulted comparable, as assessed by trypan blue exclusion test (data not shown). Moreover, before performing the *in vitro* angiogenesis assay (P6), annexin V staining showed that the number of viable cells was similar between SDS- and HD-MSCs (92.60% *vs* 94.50%, respectively), as well as the value of early/late apoptotic and necrotic cells (4.90% *vs* 4.30%, and 2.50% *vs* 1.10,

respectively; SDS- *vs* HD-MSCs) (**Supplementary Figure 2.1 D**).

**Table 2.1**: *Clinical and demographic features of SDS patients. All SDS subjects included in this study are enrolled in the SDS Italian registry*

| UPN | Age at study (y), gender | ANC/ µL | *SBDS* mutations (genotype) | Cytogenetics |
|---|---|---|---|---|
| UPN06 | 8, F | 100 | c.258+2T>C; c.183_184TA>CT | 46,XXi(7)(q10)[5]/ 46,XX[16] |
| UPN13 | 13, M | 800 | c.258+2T>C; c.183_184TA>CT; c.258+2T>C | 46, XY, del(20)(q11,21q13,32)[6]/ 46, XY [7](q10)[1]/ 46, XY [6] |
| UPN16 | 9, F | 1000 | c.258+2T>C; c.258+2T>C | 46,XX[23] |
| UPN35 | 7, F | 1760 | c.258+2T>C; c.183_184TA>CT | 46,XX[22] |
| UPN37* | 4, F | 1100 | c.258+2T>C; c.183_184TA>CT | 46,XX[9] |
| UPN40* | 15, F | | c.258+2T>C; c.183_184TA>CT | *n.a.* |
| UPN48 | 1, F | 260 | c.258+2T>C; c.183_184TA>CT;c.258+2T>C | 46,XX[17] |
| UPN55 | 11, M | 310 | c.258+2T>C; c.183_184TA>CT | 46, XY, i(7)(q10)[4]/ 46, XY [16] |
| UPN58* | 13, M | 480 | c.183_184TA>CT; c.258+2T>C | *n.a.* |
| UPN63 | 6, M | 1600 | c.258+2T>C; c.183_184TA>CT;c.258+2T>C | 46,XY[15] |
| UPN67* | 5, M | 480 | c.183_184TA>CT; c.258+2T>C | *n.a.* |
| UPN72 | 18, M | 380 | c.258+2T>C; c.183_184TA>CT | 46,XY[20] |
| UNP105 | 15, F | 278 | c.258+2T>C; c.652>CT | *n.a.* |

*Abbreviations*: ANC/µL, absolute neutrophil count per µL; F, female; M, male; n.a., not available; *SBDS*, Shwachman-Bodian-Diamond Syndrome gene; UPN, unique patient number; y, years.
All the mutations are described according to the mutation nomenclature (www.hgvs.org/mutnomen).

*Fresh samples

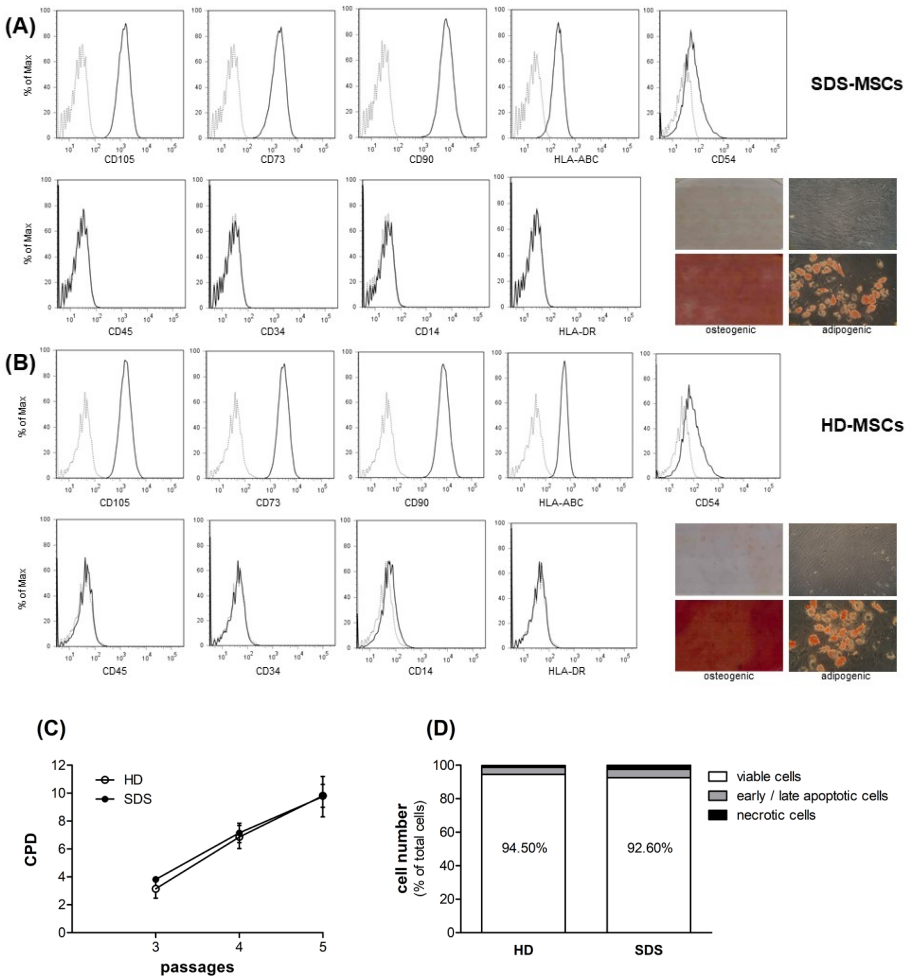


**Supplementary Figure 2.1**: *SDS- and HD-MSC characterization*

(**A**-**B**) Representative immunophenotype and differentiation capability of (**A**) SDS- and (**B**) HD-MSCs. (**C**) Growth curve of three representative SDS and HD primary MSC cultures. Data are expressed as mean ± sd (CPD, cumulative population doublings). (**D**) SDS- and HD-MSC viability was evaluated by Annexin V staining at passage 6, before the *in vitro* angiogenesis assay. Data are expressed as mean of five SDS- and four HD-MSC samples of 3 independent experiments.

### 2.4.2 SDS-MSCs show a defective *in vitro* ability to form correct tube networks after specific angiogenic *stimuli*

Our research group previously demonstrated that the angiogenic potential of SDS-MSCs was severely impaired compared to HD-derived cells [19]. Therefore, to deeper investigate this phenomenon, we evaluated the *in vitro* angiogenic capability of SDS- and HD-MSCs at different time points. As shown in **Figure 2.1 A**, at 2- and 3-hours after angiogenic *stimuli*, almost all HD-MSCs were able to assemble well-spread and defined tubular structures across the entire cell culture at both evaluated time points (**panels i-iv**). On the other hand, SDS-MSCs were able to recreate few small tube networks (**panels v-viii**), form disorganized cell aggregates (**panels ix-xii**), and/or not able at all to organise themself into capillary-like structures (**panels xiii-xvi**). Notably, all SDS-MSCs showed also cell-substratum detachment at 2- and 3-hours after angiogenic *stimuli*. Accordingly, the number of junctions, meshes and segments derived was reduced in SDS-*vs* HD-MSCs (**Figure 2.1 B-G**). Specifically, 2-hours after angiogenic *stimuli*, a mean of 74.10 ± 32.66 junctions and 36.25 ± 16.03 master junctions was observed in SDS-MSCs, whereas at 3-hours they resulted 57.16 ± 20.12, and 22.89 ± 8.18, respectively. These values were significantly lower than those observed in HD-MSCs (2-hours: 212.30 ± 40.10, and 120.80 ± 28.31, respectively; 3-hours: 208.90 ± 39.24, and 114.20 ± 23.17, respectively) ($P < 0.05$) (**Figure 2.1 B and C**). The number of segments and master segments was also

significantly reduced in SDS- *vs* HD-MSCs (2-hours: 84.07 ± 37.22, and 61.51 ± 27.02 *vs* 255.70 ± 58.49, and 195.40 ± 45.32, respectively; 3-hours: 212.30 ± 40.10, and 212.30 ± 40.10 *vs* 212.30 ± 40.10, and 201.80 ± 39.65, respectively; SDS- *vs* HD-MSCs) ($P < 0.05$) (**Figure 2.1 D and E**). Moreover, the number of meshes and mean mesh size, two angiogenic parameters underlying the complexity of the *in vitro* tubular structures, were the most affected (2-hours: 16.24 ± 7.21, and 2313 ± 1054 *vs* 57.17 ± 13.58, and 5648 ± 1255, respectively; 3-hours: 10.24 ± 3.68, and 1922 ± 719.30 *vs* 50.84 ± 10.80, and 6625 ± 11.91, respectively; SDS- *vs* HD-MSCs), ($P < 0.05$, and $P < 0.01$, respectively) (**Figure 2.1 F and G**).

Given the predisposition to apoptosis of haematopoietic stem/progenitor cells reported in SDS patients [27], we investigated whether this characteristic could be responsible of the angiogenic defect observed in SDS-MSCs. Interestingly, at 2-hours the number of viable cells was significantly lower in SDS- *vs* HD-MSCs (85.40% and 93.68%, respectively; $P < 0.05$) (**Figure 2.1 H**), whereas the fraction of early/late apoptotic cells resulted more than doubled (11.18% *vs* 4.02; $P < 0.05$). A trend of increase was observed also after 3-hours of angiogenic *stimuli*, when the number of apoptotic SDS- was almost doubled *vs* HD-MSCs (12.64 *vs* 5.97; $P = 0.063$) (**Figure 2.1 I**).

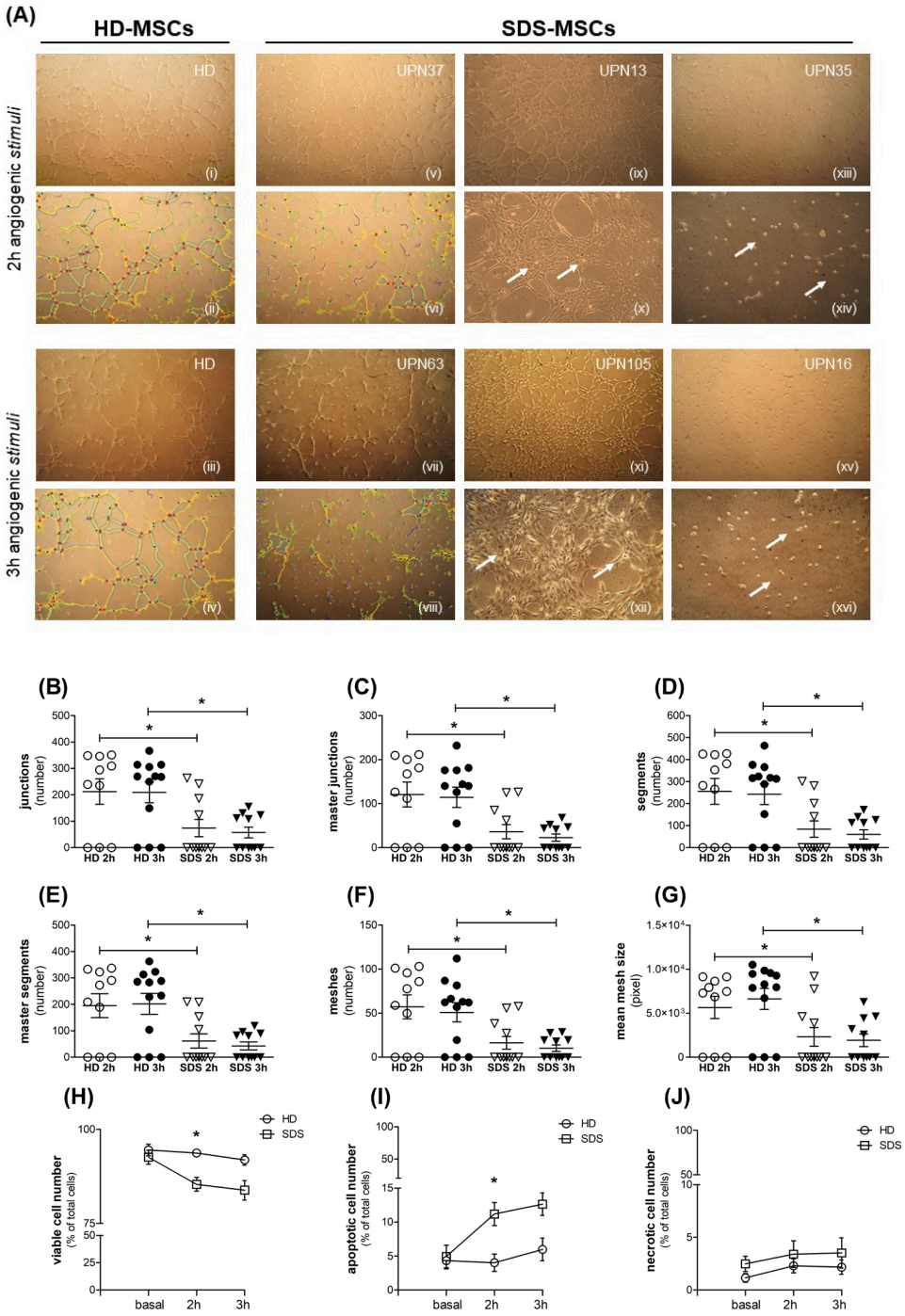


**Figure 2.1**: *SDS altered in vitro angiogenic capillary-like capability is associated to a higher apoptotic rate*

*In vitro* angiogenesis assay was performed on HD- and SDS-MSCs (P5 to P6) stimulated with angiogenic factors. After 2- and 3-hours incubation at 37°C, capillary tube formation was assessed and analysed using *ImageJ Angiogenesis Analyzer*. (**A**) Representative images of HD- and SDS-MSCs (magnification 5X and 10X). At each time point after angiogenic *stimuli*, SDS- exhibited a drastic decrease of tubular structures *vs* HD-MSCs. Moreover, all SDS-MSCs showed cell-substratum detachment (see white arrows). (**B-G**) Evaluation of angiogenesis parameters analysed with *ImageJ Angiogenesis Analyzer*. Data are expressed as mean ± sem (2h: HD=10, and SDS=10; 3h: HD=12, and SDS=10) of 5 independent experiments. *P < 0.05. Statistical analysis was performed using Mann-Whitney U Test. (**H-J**) Cell viability following the angiogenic *stimuli*. Data are expressed as mean ± sem of 3 independent experiments (HD=4, and SDS=5). *P < 0.05. Statistical analysis was performed using Mann-Whitney U Test.

### 2.4.3 Under angiogenic *stimuli*, the expression of *VEGFα* and related pro-angiogenic molecules is down-regulated in SDS- *vs* HD-MSCs

Recently, our research group demonstrated that the defective *in vitro* angiogenic capability of SDS-MSCs is associated with a specific decrease in *VEGFα* expression [19]. Since it has been reported that VEGFA can stimulate angiogenesis itself or through the regulation of other angiogenesis-associated molecules [15;28-30], we deeply investigated the deregulation of VEGF pathway in SDS-MSCs. As previously reported, after 3-hours of angiogenic *stimuli*, we observed a 0.78-fold down-regulation of *VEGFα* expression in SDS- *vs* HD-MSCs ($P < 0.0001$) (**Figure 2.2 A**). Even though MSCs do not express vascular endothelial growth factor receptors (VEGFRs), VEGFA can stimulate angiogenesis by binding platelet-derived growth factor receptors (PDGFRs) [31,32], and by influencing several molecular pathways. In our angiogenic assay, while PDGF receptor-beta (*PDGFRβ*) was slightly up-regulated in SDS- *vs* HD-MSCs (1.16-fold; $P < 0.001$) (**Figure 2.2 B**), the expression of both PDGF receptor-alpha (*PDGFRα*) and neurophilin-1 (*NRP1*), an additional VEGF receptor mainly involved in capillary morphogenesis [33], resulted unaltered between SDS- and HD-MSCs (**Supplementary Figure 2.2 A and B**). Based on the differences observed in SDS patients in terms of *VEGFα*, we also evaluated the expression of other growth factors able to modulate the endogenous release of VEGF [30;34-38]. Interestingly, while the levels of interleukin-6 (IL6) did not result

differentially expressed between SDS- and HD-MSCs (**Supplementary Figure 2.2 C and D**), mRNA of both platelet derived growth factor-A (*PDGFA*) and basic fibroblast growth factor (*bFGF*) were down-regulated in SDS- *vs* HD-MSCs (0.38-fold and 0.57-fold, respectively; $P < 0.0001$, and $P < 0.001$, respectively) (**Figure 2.2 C and D**). Among the angiostatic factors acting as counter-regulators of VEGFA, chemokine (C-X-C motif) ligand 9 (CXCL9) is emerging as a strong anti-proliferative and anti-migratory molecule secreted by BM-MSCs, able to abrogate both *in vivo* and *in vitro* angiogenesis [39-42]. Of note, after 3-hours of angiogenic *stimuli*, we did not find any difference in CXCL9 mRNA expression and protein release between SDS- and HD-MSCs (**Supplementary Figure 2.2 E and F**), suggesting that in our angiogenic assay the down-regulation of *VEGFα* is not driven by CXCL9.

Since during vascular development, angiopoietin-2 (ANG2) can induce programmed cell death of ECs in the absence of VEGFA [43], we sought to understand if angiopoietins could be involved in the altered angiogenic capillary-like ability of SDS-derived cells. Interestingly, we found that while *ANG2* and its biological inhibitor angiopoietin-1 (*ANG1*) were not differently modulated between SDS- and HD-MSCs (**Supplementary Figure 2.2 G and H**), after angiogenic *stimuli* SDS-MSCs showed a down-regulation in the expression of endothelial specific receptor tyrosine kinase-2 (*TIE2*) *vs* HD-derive cells (0.68-fold; $P < 0.05$) (**Figure 2.2 E**).

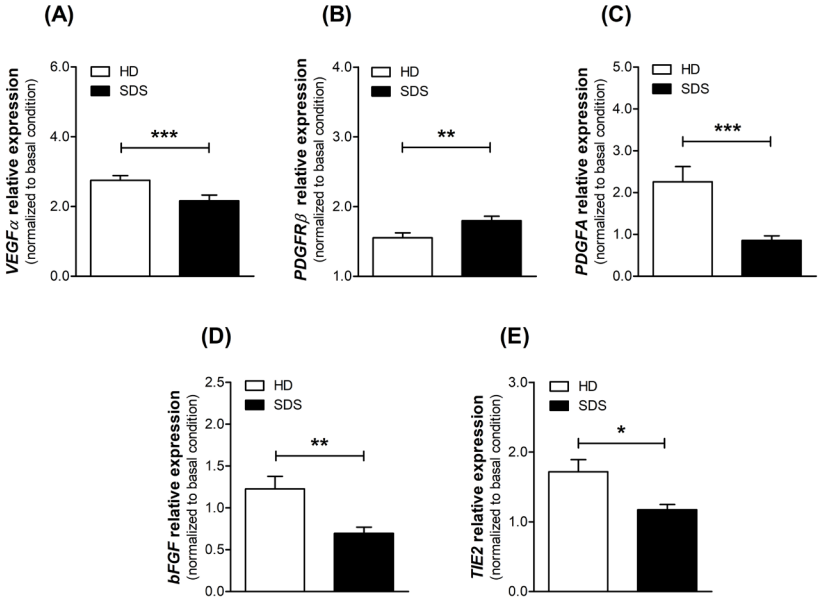


**Figure 2.2**: *Molecular expression of VEGF family and related pro-angiogenic molecules in SDS- and HD-MSCs after angiogenic condition*

(**A**) *VEGFα*, (**B**) *PDGFRβ*, (**C**) *PDGFA*, (**D**) *bFGF*, and (**E**) *TIE2* mRNA expression in SDS- (black bar; n=10) and HD-MSCs (white bar; n=12) evaluated by qPCR. Data are expressed as mean ± sem normalized to basal condition. *P < 0.05; **P < 0.001; ***P < 0.0001. Statistical analysis was performed using Mann-Whitney U Test.

### 2.4.4 Angiogenic *stimuli* induces P53 protein expression in SDS-MSCs

Activation of P53 has been proposed as a common mechanism in the pathogenesis of various ribosomopathies, including SDS [44]. Previous studies showed that *SBDS*-deficient cells undergo accelerated apoptosis through Fas-mediated and generally P53-dependent pathway [27;44-46]. Concerning angiogenesis, P53 has the ability to inhibit the synthesis of several pro-angiogenic molecules (i.e. VEGFA and bFGF), and/or directly increasing the production of the endogenous angiogenesis inhibitor thrombospondin-1 (THBS1) [47]. Although mRNA expression did not differ between SDS- and HD-MSCs (**Supplementary Figure 2.2 I**), after 3-hours of angiogenic *stimuli* we showed that P53 protein levels were elevated in SDS- *vs* HD-MSCs (**Figure 2.3 A-C**). Specifically, we found that P53 protein was doubled in SDS-derived cells after stimulation ($P < 0.05$) (**Figure 2.3 D**). However, the expression of *THBS1* was similar among SDS- and HD-MSCs (**Supplementary Figure 2.2 J**), indicating a possible link between P53 level and *VEGFα* and *bFGF* gene expression in altered SDS-MSCs angiogenic capability.

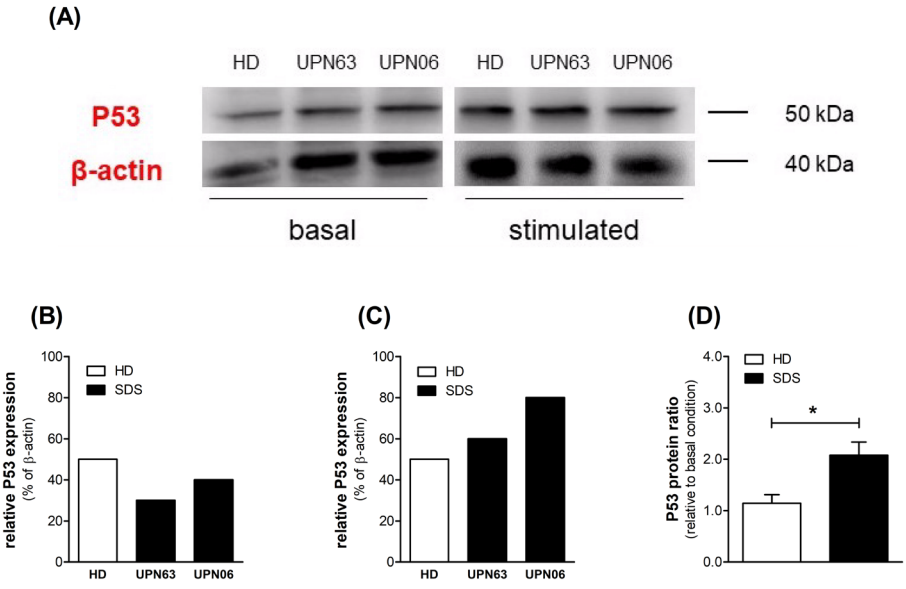


**Figure 2.3**: *Under angiogenic stimuli, P53 protein is differently modulated between SDS- and HD-MSCs*

(**A**) P53 protein was measured in SDS- and HD-MSCs both in basal and stimulated condition by Western blot analysis (representative images from one out of three independent experiments performed). (**B**) Densitometric analysis of Western blots showed in panel **A** – basal condition (overnight starvation with DMEM supplemented with 2% FBS). (**C**) Densitometric analysis of Western blots showed in panel **A** – stimulated condition. (**D**) Analysis of Western blots expressed as P53 protein ratio (stimulated/basal condition). SDS- are presented in black bar (n=5), and HD-MSCs in white bar (n=4). Data are expressed as mean ± sem of three independent experiments. *P < 0.050. Statistical analysis was performed using Mann-Whitney U Test.

### 2.4.5 The expression of TGFβ1 is down-regulated in SDS- *vs* HD-MSCs after angiogenic stimulation

Transforming growth factor beta-1 (TGFβ1) is able to induce the expression of many pro-angiogenic factors [48,49]. Particularly, TGFβ1 mediates both *in vitro* and *in vivo* angiogenesis through the autocrine or paracrine activation of vascular endothelial growth factor receptor-2 (VEGFR2 or KDR) induced by VEGFA [49,50]. We therefore investigated its involvement in the altered angiogenic capability of SDS-MSCs. Interestingly, 3-hours after angiogenic *stimuli*, the expression of *TGFβ1* was specifically down-regulated at mRNA level in SDS- *vs* HD-MSCs (0.63-fold; P < 0.001) (**Figure 2.4 A, and Supplementary Figure 2.2 K-M**), along with *VEGFα*. Even if with a high inter-patient variability, TGFβ1 showed a trend of decrease also at protein level in the cytoplasm of SDS- compared to HD-MSCs (Δ relative to basal condition -103.10 ± 122.7 MFI and 62.94 ± 1.17 MFI, respectively; P = 0.114) (**Figure 2.4 B and C**). Particularly, only SDS- able to form few tubular structures released an amount of TGFβ1 quite comparable to HD-MSCs (UNP63 Δ = 68.10 MFI, UNP55 Δ = 44.38 MFI, and UPN37 Δ = 5.45 MFI, highlighted in blue in **Figure 2.4 B and C**).

Regarding TGFβ receptors, we further observed a 0.44-fold down-regulation of the transmembrane serine-threonine kinases, type I receptor (*TGFβRI* also known as *ALK5*) in SDS- *vs* HD-MSCs (P < 0.001) (**Figure 2.4 D**), while the activin receptor-like kinase-1 (*ALK1*) was not differentially expressed in

the two groups (**Supplementary Figure 2.2 N**). In most of the cellular context, active forms of TGFβ signal through the canonical small mother against decapentaplegic (Smad)-mediated pathway [51,52]. After 3-hours of angiogenic *stimuli*, we found that *SMAD4* and *-3* were expressed at comparable level between SDS- and HD-MSCs (**Supplementary Figure 2.2 O and P**), whereas *SMAD1* was poorly expressed both at basal and under stimulated condition in the two group (data not shown).

During physiological and pathological angiogenesis, TGFβ1-auxiliary receptor endoglin (CD105) exert multiple functions through both canonical and non-canonical TGFβ1 signalling pathways [53]. Particularly, CD105 and platelet endothelial cell adhesion molecule (PECAM-1, or CD31) influence the expression of each other, and their altered expression generate defective angiogenic properties of ECs through the intracellular signalling pathways induced by TGFβ1 [54]. In our angiogenic assay, we found that mRNA of both *CD105* and *CD31* was down-regulated in SDS- *vs* HD-MSCs (0.59-fold, and 0.62-fold, respectively; $P < 0.050$) (**Figure 2.4 E and F**), suggesting that the lack TGFβ1 influences the angiogenic properties of SDS-MSCs.

TGFβ1 can also influence angiogenesis by regulating the expression of extracellular matrix components, including matrix metalloproteinases and inhibitors [55]. After 3-hours of angiogenic *stimuli*, the expression of tissue inhibitor of metalloproteinases-1 (*TIMP1*) was 0.66-fold down-regulated in

SDS- *vs* HD-MSCs ($P < 0.001$) (**Figure 2.4 G**). On the contrary, the matrix metalloproteinase-2 (*MMP2*) resulted unaltered (**Supplementary Figure 2.2 Q**) between groups.

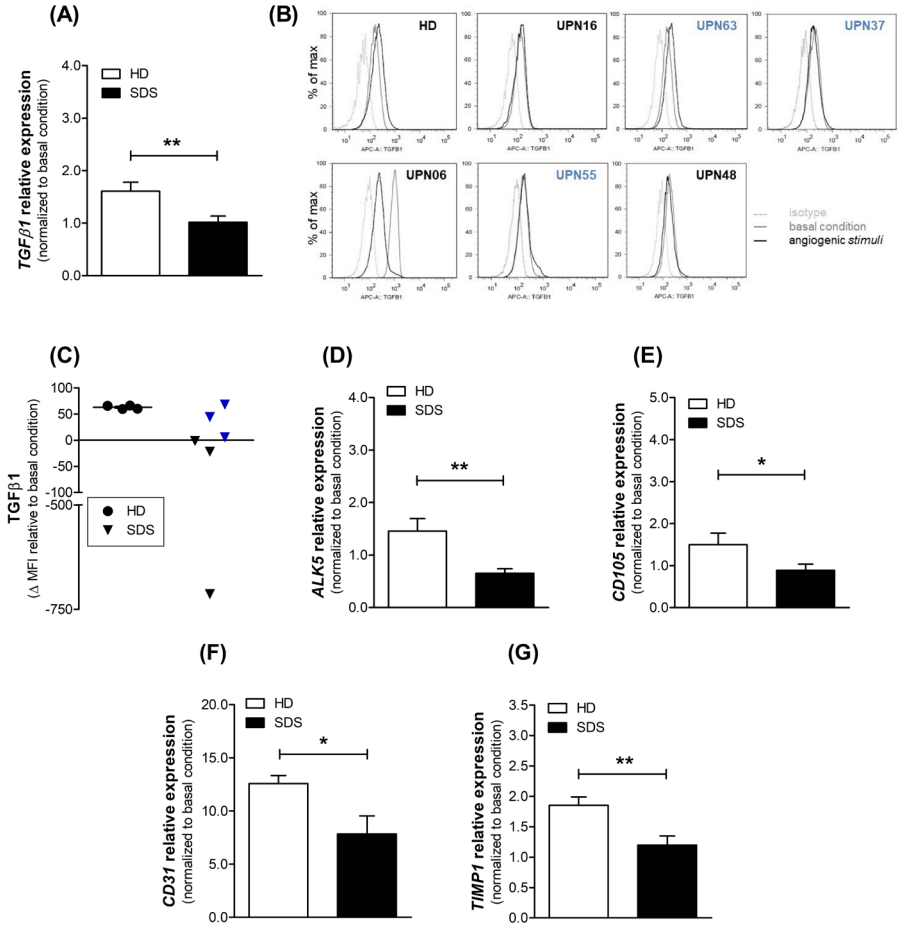


**Figure 2.4**: *TGFβ1 and related molecules are down-regulated in SDS- vs HD-MSCs*

(**A**) *TGFβ1* mRNA expression in SDS- (black bar; n=10) and HD-MSCs (white bar; n=12) evaluated by qPCR. Data are expressed as mean ± sem normalized to basal condition. **P < 0.001. Statistical analysis was performed using Mann-Whitney U Test. (**B**) Analysis of intracellular TGFβ1 staining in SDS- (n=6) and HD-MSCs (n=4; figure show data from one representative sample) underwent angiogenic *stimuli*. In blue are highlighted SDS-MSCs that were able to recreate few small tube networks after angiogenic *stimuli* (UPN63, UPN37, and UPN55). (**C**) TGFβ1 mean fluorescence intensity as measured by intracellular staining. Data are expressed as Δ mean ± sem relative to basal condition of six SDS- and four HD-MSCs after 3-hours of angiogenic *stimuli*. In blue are highlighted the mean MFI value derived from SDS-MSCs that were able to recreate few small

tube networks. Of note, if we excluded the MFI values derived from these three SDS samples, we reached a P value of 0.057 (Mann-Whitney U Test). (**D**) *ALK5*, (**E**) *CD105*, (**F**) *CD31*, and (**G**) *TIMP1* mRNA expression in SDS- (black bar; n=10) and HD-MSCs (white bar; n=12) evaluated by qPCR. Data are expressed as mean ± sem normalized to basal condition. *P < 0.050; **P < 0.001. Statistical analysis was performed using Mann-Whitney U Test.

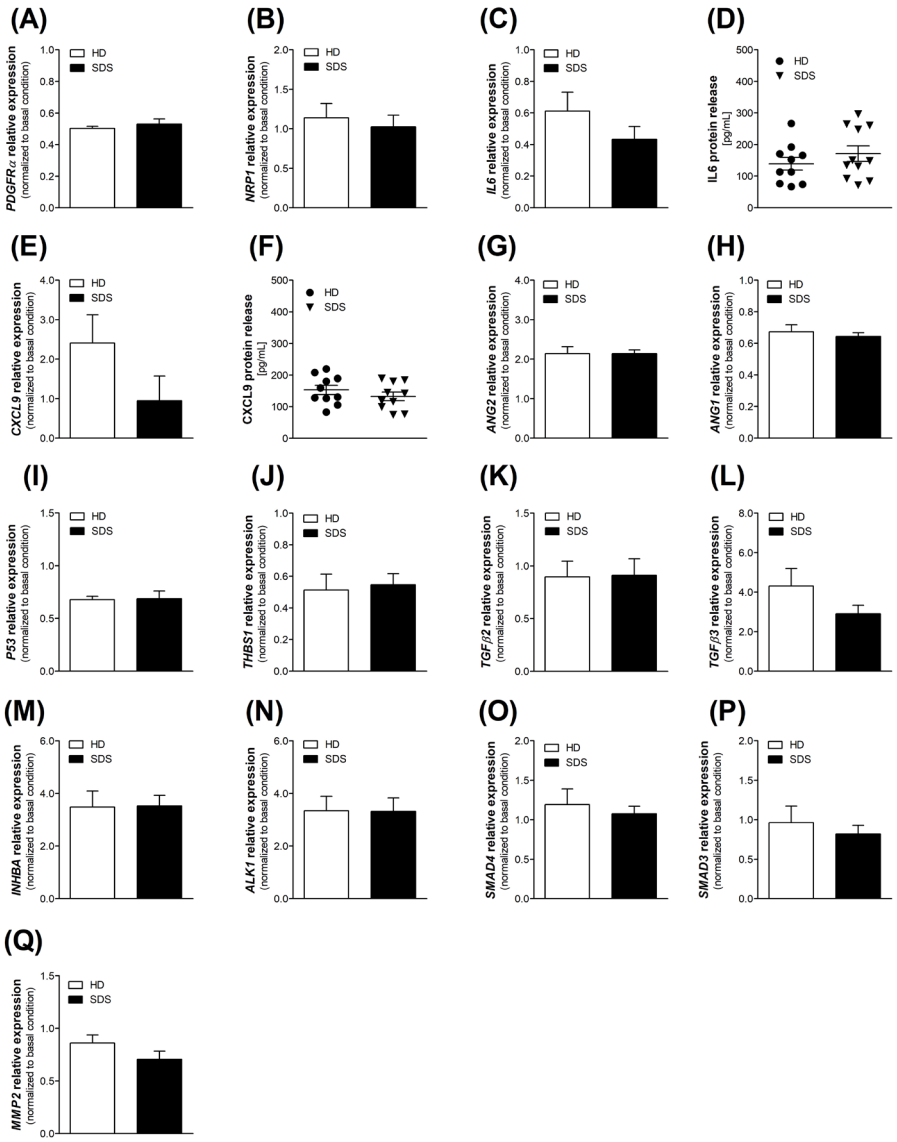


**Supplementary Figure 2.2:** *Expression of different molecules involved in the regulation of angiogenesis process after 3-hours of angiogenic stimuli*

(**A**) *PDGFRα*, (**B**) *NRP1*, and (**C**) *IL6* mRNA expression in SDS- and HD-MSCs evaluated by qPCR. (**D**) Measurement of IL6 released in supernatants collected after the *in vitro* angiogenesis assay. (**E**) *CXCL9* mRNA expression in SDS- and HD-MSCs evaluated by qPCR. (**F**) Measurement of CXCL9 released in supernatants

collected after the *in vitro* angiogenesis assay. (**G**) *ANG2*, (**H**) *ANG1*, (**I**), *P53*, (**J**) *THSB1*, (**K**) *TGFβ2*, (**L**) *TGFβ3*, (**M**) *INHBA*, (**N**) *ALK1*, (**O**) *SMAD4*, (**P**) *SMAD3,* and (**Q**) *MMP2* mRNA expression in SDS- and HD-MSCs evaluated by qPCR.

mRNA expression data are shown as mean ± sem normalized to basal condition; SDS- are presented in black bar (n=10), and HD-MSCs in white bar (n=12).

ELISA results are expressed as mean ± sem of eleven SDS- and ten HD-MSCs stimulated with pro-angiogenic factors.

### 2.4.6 STAT3 expression and activation during angiogenic *stimuli*

Signal transducer and activator of transcription-3 (STAT3) is a critical signalling intermediate activated by several cytokines. STAT3 has also been reported to be a direct transcriptional activator of both *VEGFα* and *TGFβ1* genes [56,57]. Specifically, it has two different phosphorylation sites, tyrosine 705 (Y705) and serine 727 (S727), which can yield similar, enhancing or even opposite cellular effects depending on cell types and organs [58,59]. Recently, it has been demonstrated that different SDS-derived cell subsets present a constitutive hyper-activation of STAT3 [25,60]. Thus, we sought to evaluate the possible involvement of STAT3 in driving the altered *in vitro* angiogenic capability of SDS-MSCs. After 3-hours of angiogenic stimulation, STAT3 mRNA expression did not change between SDS- and HD-MSCs (**Figure 2.5 A**). However, preliminary time course experiments demonstrated that phospho-STAT3 levels seem to be dissimilar between SDS- and HD-MSCs. Specifically, at different time-points after angiogenic *stimuli*, total STAT3 levels were comparable between SDS- and HD-MSCs (0': 3297 ± 446 MFI, and 3462 ± 637 MFI, respectively; 2'30'': 2505 ± 218 MFI, and 3489 ± 930 MFI, respectively; 5': 2483 ± 267 MFI, and 2482 ± 995 MFI, respectively; SDS- *vs* HD-MSCs) (**Figure 2.5 B**). STAT3-Y705, instead, basally (before stimulation) demonstrated a 2.1-fold increase in SDS- *vs* HD-MSCs (**Figure 2.5 C**), whereas after 5 minutes of stimulation, it reached values comparable to HD-

derived cells (**Figure 2.5 D**). STAT3-S727 showed over time a trend of increase in both SDS- and HD-MSCs (**Figure 2.5 E**). Interestingly, it resulted basically increased in SDS- *vs* HD-derived cells (1.43-fold) (**Figure 2.5 F**). Although these results partially confirmed the hyper-phosphorylation state of STAT3 in SDS-derived cells [25,60], further experiments are needed to better understand its role in the altered angiogenic properties of SDS-MSCs.

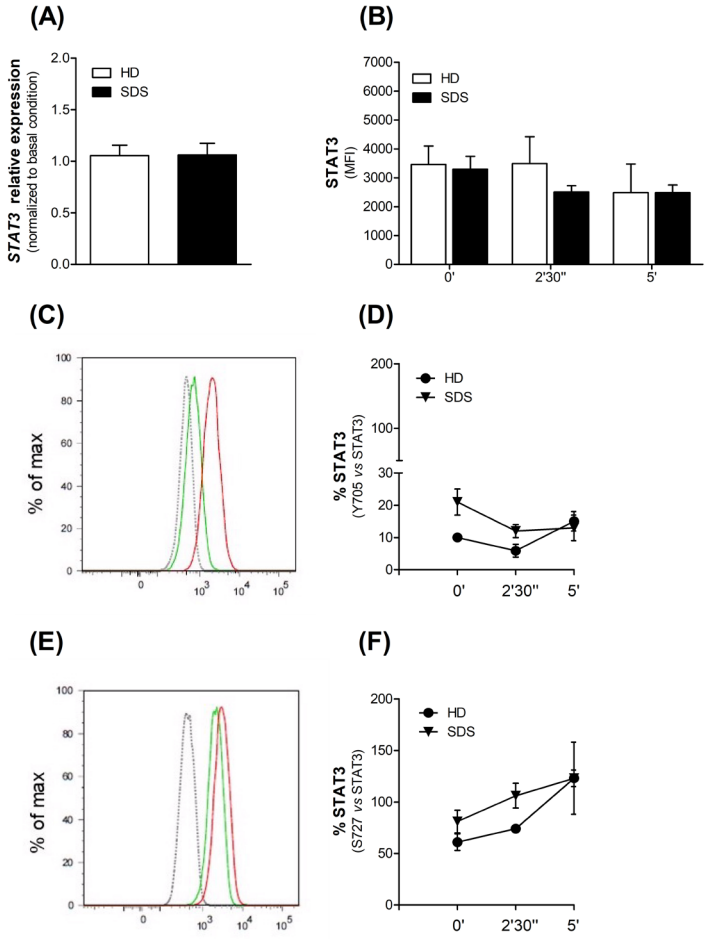


**Figure 2.5**: *STAT3 expression and activation in SDS- and HD-MSCs under angiogenic stimuli*

(**A**) *STAT3* mRNA expression in SDS- and HD-MSCs evaluated by qPCR. Data are expressed as mean ± sem normalized to basal condition; SDS- are presented in black bar (n=10), and HD-MSCs in white bar (n=12). (**B**) STAT3 mean fluorescence intensity as measured by intracellular staining. SDS- and HD-MSCs were treated with angiogenic *stimuli* and STAT3 analysed at different time-points. Data are expressed as mean ± sd of two experiments performed on four SDS- and three HD-MSCs. (**C**) Representative analysis of STAT3-Y705 in SDS- and HD-MSCs at time zero (basal condition, overnight starvation with DMEM supplemented with 2% FBS). Green histogram represents age-matched HD-MSCs, red histogram represents SDS-derived cells, and grey histogram represents isotype

control. (**D**) STAT3-Y705 time course levels. Data are expressed as mean ± sd of the percentage derived from the ratio (phospho-STAT3 / total STAT3). Two experiments performed on three HD- and four SDS-MSCs (UPN13, UPN35, UPN48, and UPN40) were represented. (**E**) Representative analysis of STAT3-S727 in SDS- and HD-MSCs at time zero (basal condition, overnight starvation with DMEM supplemented with 2% FBS). Green histogram represents age-matched HD-MSCs, red histogram represents SDS-derived cells, and grey histogram represents isotype control. (**F**) STAT3-S727 time course levels. Data are expressed as mean ± sd of the percentage derived from the ratio (phospho-STAT3 / total STAT3). Two experiments performed on three HD- and four SDS-MSCs (UPN13, UPN35, UPN48, and UPN40) were represented.

### 2.4.7 VEGFA and TGFβ1 treatments restore the capillary-like capability of severe neutropenic SDS-MSCs

Based on our results indicating the involvement of both *VEGFα* and *TGFβ1* in the *in vitro* capillary-like capacity of SDS-MSCs, we wanted to check whether the exogeneous addition of these molecules could restore tube network formation in our *in vitro* angiogenesis assay. As previously reported, under angiogenic condition HD-MSCs were able to recreate well-spread and defined tubular structures (**Figure 2.6 A, panel i**), whereas after 50 ng/mL of $VEGF_{165}$ treatment, they formed only disorganized cell aggregates (**Figure 2.6 A, panel ii**). On the other hand, SDS-MSCs were once again characterized by an altered *in vitro* angiogenic capability after 3-hours of angiogenic *stimuli* (**Figure 2.6 A, panel iii and v**). Particularly, 6/9 SDS-MSCs recreated few small tube networks, whereas 3/9 shaped disorganized cell aggregates. Notably, after $VEGF_{165}$ treatment, 5/9 of SDS-derived cells were able to restore their capillary-like ability. Accordingly, the number of junctions, master junctions, segments, master segments and meshes, as well as the mean mesh size value derived from *ImageJ Angiogenesis Analyzer*, further demonstrated that only this specific SDS-subgroup reached comparable angiogenic parameters to those derived from HD-MSCs treated with angiogenic condition alone (**Figure 2.6 B-G**). By the analysis of SDS clinical features, we noticed that MSCs derived from neutropenic patients (N SDS; 1760/μL < absolute neutrophil count < 500/μL) were only able to recreate few small tube-networks and/or not able at all to

organise themself into capillary-like structures as reported under angiogenic *stimuli* alone (**Figure 2.6 A, panel iv**), whereas 3/4 SDS-derived cells from severely neutropenic patients (SN SDS; absolute neutrophil count < 500/μL) recreated a well-defined tubular structure after exogenous $VEGF_{165}$ addition (**Figure 2.6 A, panel vi**). Specifically, a mean value of 263.70 ± 24.78 junctions and 143.90 ± 22.18 master junctions was observed in SN SDS-MSCs (**Figure 2.6 H and I**). After treatment, the number of segments and master segments was also significantly improved in SN SDS-derived cells (311.00 ± 37.30, and 243.80 ± 31.46, respectively) (**Figure 2.6 J and K**), along with the number of meshes and mean mesh size (66.16 ± 11.49, and 8090.00 ± 987.40, respectively) (**Figure 2.6 L and M**). These results were also supported by the preliminary data obtained from the evaluation of P53 protein levels after $VEGF_{165}$ treatment. Interestingly, the exogenous addition of VEGFA protein restored normal level of P53 only in MSCs derived from severely neutropenic patient UPN67 (480 absolute neutrophil count/μL) (**Figure 2.6 N-Q**).

TGFβ1 treatment partially confirmed the results previously reported. Under angiogenic condition, the ability of SDS- to form correct tube-networks was severely impaired *vs* HD-MSCs (**Figure 2.7 A, panel i, iii and v**). However, after the administration of TGFβ1 (10 ng/mL), HD-derived cells were not able to organise capillary-like structures, displaying also cell-substratum detachment (**Figure 2.7, A panel ii**). On the other hand, 3/7 SDS-MSCs did not restore their angiogenic capability

whereas 4/7 SDS-derived cells recreated well-defined tube networks (**Figure 2.7 A, panel iv and vi**) (**Figure 2.7 B-G**). Particularly, by the comparative morphometric analysis derived from *ImageJ Angiogenesis Analyzer*, only MSCs derived from SN SDS patients underwent TGFβ1 treatment (4/4) were able to recreate similar capillary-like structures found in HD-MSCs under stimulated condition alone. Indeed, severely neutropenic SDS-MSCs reported a mean value of 265.20 ± 14.11 and 140.70 ± 8.41 for junctions and master junctions, respectively (**Figure 2.7 H and I**). The number of segments and master segments was also significantly enhanced in severely neutropenic SDS-MSCs (318.80 ± 11.22, and 234.30 ± 8.28, respectively) (**Figure 2.7 J and K**), in addition to number of meshes and mean mesh size (62.80 ± 4.23, and 7777.00 ± 958.30, respectively) (**Figure 2.7 L and M**).

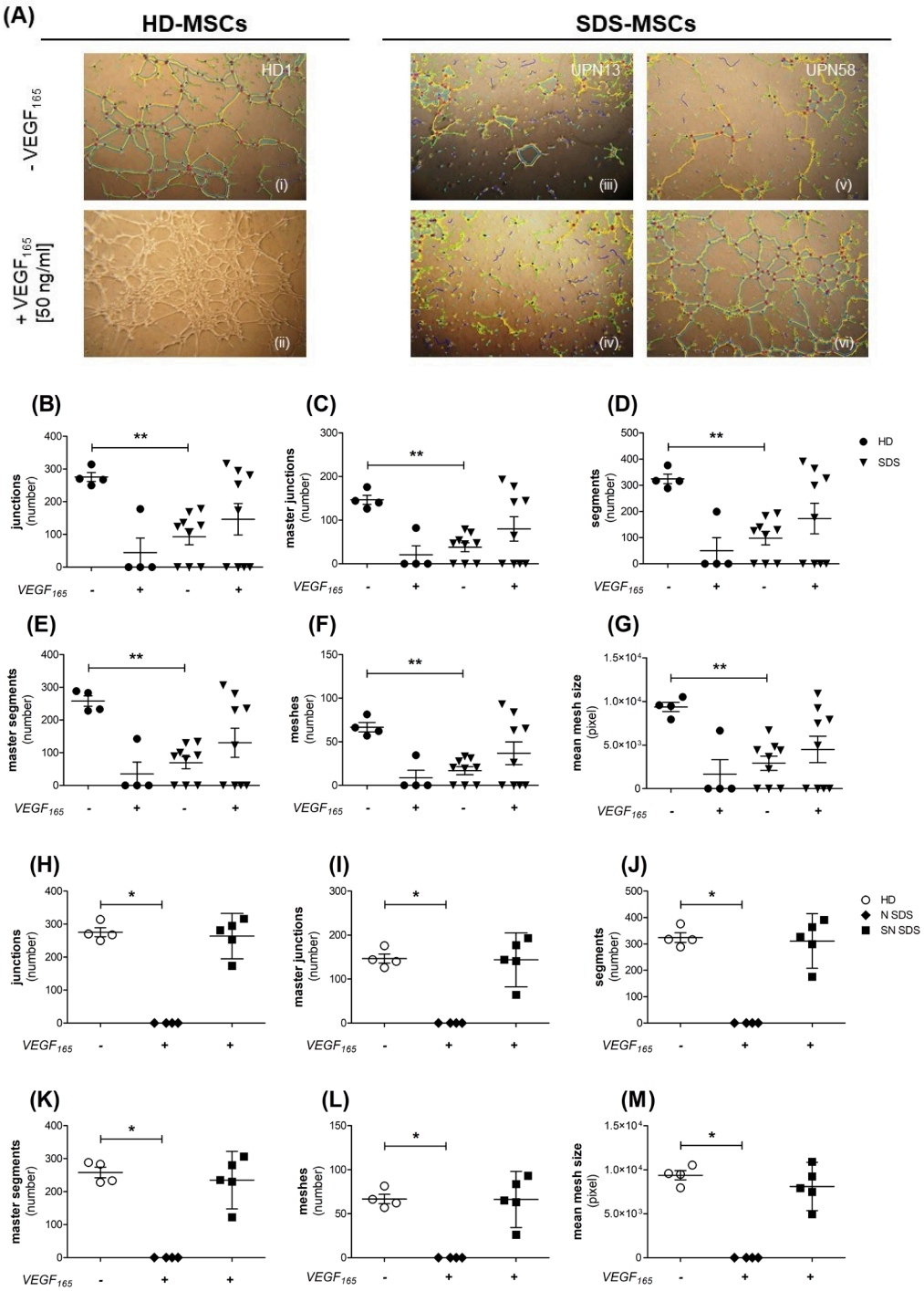
(A)
HD-MSCs
SDS-MSCs
- VEGF165
+ VEGF165 [50 ng/ml]
HD1
UPN13
UPN58
(i)
(ii)
(iii)
(iv)
(v)
(vi)
(B)
(C)
(D)
(E)
(F)
(G)
(H)
(I)
(J)
(K)
(L)
(M)
junctions (number)
master junctions (number)
segments (number)
master segments (number)
meshes (number)
mean mesh size (pixel)
VEGF165
HD
SDS
N SDS
SN SDS
**
*

*Figure 2.6 A - M*

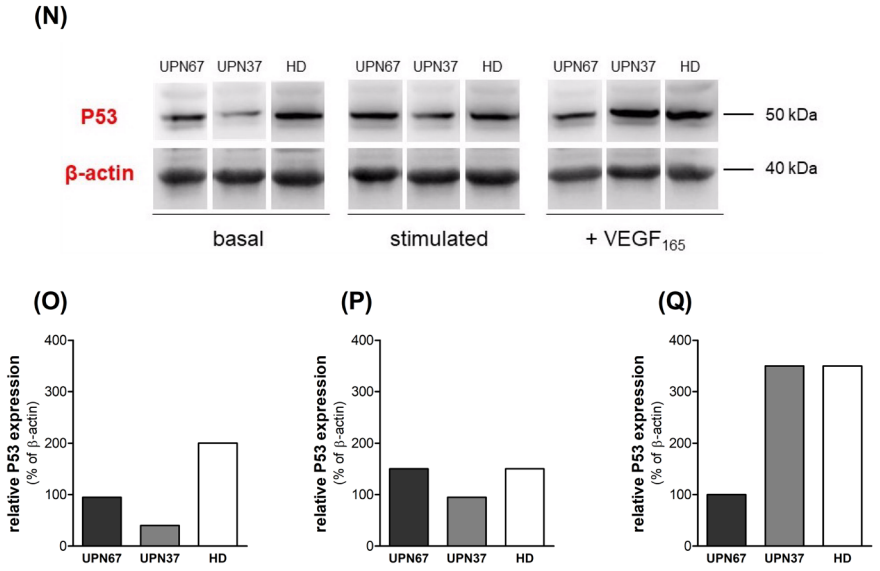


**Figure 2.6**: *Only MSCs derived from severe neutropenic SDS patients are able to recovery their capillary-like ability after VEGFA treatment*

*In vitro* angiogenesis assay was performed on HD- and SDS-MSCs stimulated with angiogenic factors in the presence or absence of $VEGF_{165}$ protein (50 ng/mL). After 3-hours incubation at 37°C, capillary tube formation was assessed and analysed using *ImageJ Angiogenesis Analyzer*. (**A**) Representative images of HD- and SDS-MSCs (magnification 5X). Cell-substratum detachment is highlighted with white arrows. (**B-G**) Evaluation of angiogenesis parameters analysed with *ImageJ Angiogenesis Analyzer*. Data are expressed as mean ± sem (HD=4, and SDS=9) of 4 independent experiments. **P < 0.001. Statistical analysis was performed using Mann-Whitney U Test. (**H-M**) Evaluation of angiogenesis parameters analysed with *ImageJ Angiogenesis Analyzer* taking into account of neutrophil count. Data are expressed as mean ± sem (HD=4 not treated; N SDS=4, and SN SDS=5) of 4 independent experiments. *P < 0.05. Statistical analysis was performed using Mann-Whitney U Test. Neutropenic patients (N SDS) = 1760 cells/µL < absolute neutrophil count < 500 cells/µL; severely neutropenic patients (SN SDS) = absolute neutrophil count < 500 cells/µL. (**N**) P53 protein was measured in basal, stimulated, and stimulated condition supplemented with $VEGF_{165}$ protein (50 ng/mL) by Western blot analysis. One preliminary experiment is shown. (**O**) Densitometric analysis of Western blots showed in panel **N** – basal condition (overnight starvation with DMEM supplemented with 2% FBS). (**P**)

Densitometric analysis of Western blots showed in panel **N** – stimulated condition. (**Q**) Densitometric analysis of Western blots showed in panel **N** – stimulated with angiogenic factors in the presence of $VEGF_{165}$ protein (50 ng/mL).

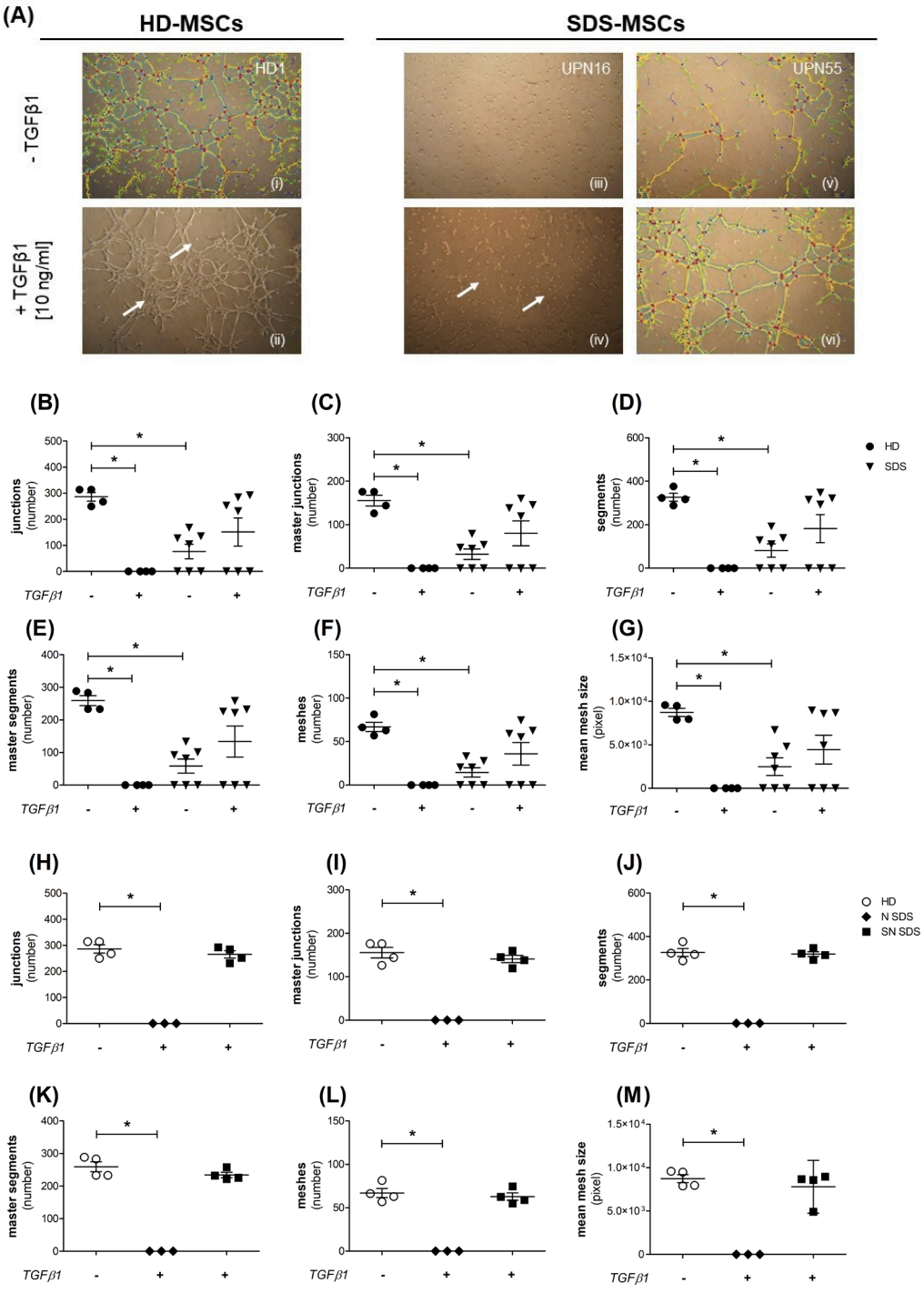
(A)
HD-MSCs
SDS-MSCs
- TGFβ1
+ TGFβ1 [10 ng/ml]
HD1
UPN16
UPN55
(i)
(ii)
(iii)
(iv)
(v)
(vi)
(B)
(C)
(D)
(E)
(F)
(G)
(H)
(I)
(J)
(K)
(L)
(M)
junctions (number)
master junctions (number)
segments (number)
master segments (number)
meshes (number)
mean mesh size (pixel)
TGFβ1
HD
SDS
N SDS
SN SDS

**Figure 2.7**: *Only MSCs derived from severe neutropenic SDS patients are able to recovery their capillary-like ability after TGFβ1 treatment*

*In vitro* angiogenesis assay was performed on HD- and SDS-MSCs stimulated with angiogenic factors in the presence or absence of TGFβ1 protein (10 ng/mL). After 3-hours incubation at 37°C, capillary tube formation was assessed and analysed using *ImageJ Angiogenesis Analyzer*. (**A**) Representative images of HD- and SDS-MSCs (magnification 5X). Cell-substratum detachment is highlighted with white arrows. (**B-G**) Evaluation of angiogenesis parameters analysed with *ImageJ Angiogenesis Analyzer*. Data are expressed as mean ± sem (HD=4, and SDS=7) of 4 independent experiments. *P < 0.05. Statistical analysis was performed using Mann-Whitney U Test. (**H-M**) Evaluation of angiogenesis parameters analysed with *ImageJ Angiogenesis Analyzer* taking into account of neutrophil count. Data are expressed as mean ± sem (HD=4 not treated; N SDS=3, and SN SDS=4) of 4 independent experiments. *P < 0.05. Statistical analysis was performed using Mann-Whitney U Test. Neutropenic patients (N SDS) = 1760 cells/µL < absolute neutrophil count < 500 cells/µL; severely neutropenic patients (SN SDS) = absolute neutrophil count < 500 cells/µL.

## 2.5 Discussion

Although SBDS protein has been associated with critical cellular pathways including ribosomal biogenesis [61-64], microtubule stabilization [10], and actin polymerization [66], accumulating evidence demonstrated also its involvement in the regulation of stromal microenvironment [11,19;66,67]. Mesenchymal stromal cells are not only considered an inert and structural element of the bone marrow. Indeed, it has been shown their involvement in supporting, driving and maintaining several haematopoietic disorders, such as myelodysplasia and aplastic anaemia [14]. During the last years, using both *in vitro* and *in vivo* models, our research group has deepened the characterization of SDS-MSCs, demonstrating that these cells display a marked impairment in their angiogenic potential [17,19]. Here, we firstly confirmed the altered *in vitro* angiogenic capability of SDS-MSCs on a large cohort of SDS-derived cells. Specifically, we showed that after 2- and 3-hours of angiogenic *stimuli*, none of SDS-derived cells are able to recreate well-defined tubular structures, suggesting that the defective angiogenic ability of SDS-MSCs is time-independent. We also demonstrated that after both time-points the number of early/late apoptotic cells is doubled in SDS- *vs* HD-MSCs. Inhibition of growth factors signalling can induce apoptosis and subsequently block angiogenesis [68]. We recently reported that under angiogenic stimulation SDS-MSCs display a specific down-regulation in the expression of *VEGFα* [19], one of the

most important MSC pro-angiogenic factors [29]. Here, we demonstrated that TGFβ1 mRNA and protein production are down-regulated in SDS- compared to HD-derived cells. Interestingly, we also found that the expression of other several growth factors able to increase the endogenous release of VEGFA [30;34-38] and to be induced by TGFβ1 [48,49] is down-regulated in SDS- *vs* HD-MSCs. Conversely to HD-derived cells, after angiogenic stimulation, SDS-MSCs display also a different modulation of both *CD105* and *CD31*, suggesting that the intrinsic angiogenic capability of SDS-MSCs could be related to the lack of TGFβ1 [54]. Indeed, by providing the exogenous administration of TGFβ1, we demonstrated that a subgroup of SDS-derived cells is able to recovery its capillary-like ability. Particularly, by the analysis of the clinical data, we found that only MSCs from severely neutropenic patients recreate well-defined tubular structures after TGFβ1 treatment. Similarly, upon $VEGF_{165}$ administration, only 75% of SDS-derived cells from severely neutropenic patients restore their angiogenic properties, reaching comparable angiogenic parameters to those derived from HD-MSCs treated with angiogenic condition alone. However, VEGFA treatment did not rescue the impaired angiogenesis only in one severely neutropenic derived-MSCs (UNP06, absolute neutrophils count = 100/μL) (**Supplementary Figure 2.3**). Of note, this patient subsequently progressed to a myelodysplastic syndrome. Collectively, these findings seem to sustain the hypothesis that, under angiogenic stimulation, the inhibition of TGFβ1 and

VEGFA signalling is responsible for the altered angiogenic capability of SDS-MSCs. Moreover, it seems that defective SDS-MSC angiogenic properties could be related to the degree of neutropenia. Neutropenia and impaired neutrophil chemotaxis are likely the most critical contributors to recurrent infections seen in young SDS children [1,2;69]. Vascularization is not necessarily driven by ECs recruitment alone. Once activated and extravasated, ECs become VEGF-dependent, and the absence of this specific pro-angiogenic growth factor leads to the apoptotic death of activated ECs [68]. Neutrophils are migrating cells acting as the first-line of response under acute inflammatory *stimuli*. It has been demonstrated that these cells help to prepare a suitable environment for subsequent EC invasion, releasing pro-angiogenic factors such as VEGFA [70]. Therefore, neutrophils could not only condition the bone marrow environment, but physically open a passage for ECs towards a particular site of acute angiogenesis, with the introduction of an avascular tissue containing pluripotent angiogenic factors. Given the persistent or intermittent neutropenia which characterised SDS patients [1,2] as well as the aberrant chemoattractant-induced F-actin properties of SDS neutrophils [65], we speculate that SDS neutrophils are not able to migrate to the BM niche and, therefore, sustain the angiogenic potential of SDS-MSCs. On the other hand, the identification of neutropenia driving-cells within *SBDS*-deficient haematopoietic hierarchy could allow to define the cellular and molecular events underlying SDS neutropenia. Therefore, further *in vitro*

studies on the different fine-tuning molecular responses of neutropenic and severely neutropenic SDS-MSCs to pro-angiogenic *stimuli* could be useful to recognise the role of MSCs in driving haematological SDS defects, and whether neutropenia is a cause rather than an effect of the BM failure of these patients. Moreover, given the dual role of neutrophils, that can be either pro-angiogenic by contributing to VEGFA production, or anti-angiogenic [71,72], future experiments are also needed to understand how different degree of neutropenia could influence SDS-MSCs angiogenic capability.

SDS hematopoietic progenitors exhibit higher apoptosis rates than normal marrow progenitor cells, being hyper-sensitive to direct Fas-stimulation [27]. Recently, it has also been demonstrated that apoptosis of $KDR^{+}CD34^{+}$ hemoangiogenic progenitor cells was at least partially P53-independent [73]. Our data show that under basal condition, the number of early/late apoptotic cells is similar between SDS- and HD-MSCs. Moreover, also P53 protein levels are comparable between the two groups, suggesting that basally SDS-MSCs are not prone to programmed cell death. Interestingly, elevated P53 levels may also be responsible for aberrant angiogenesis either by inducing the expression of *THBS1*, and/or down-regulating both *VEGFα* and *bFGF* [47]. Indeed, we demonstrated that under angiogenic *stimuli*, P53 protein levels are 2-fold increase in SDS- *vs* HD-MSCs, despite the unaltered expression of *THBS1*. Interestingly, our preliminary experiments also showed that $VEGF_{165}$ exogenous administration restores

normal levels of P53 only in MSCs derived from severely neutropenic patient, i.e. cells able to recreate a well-defined tubular structure after treatment. Therefore, these results sustain that under angiogenic stimulation, the altered *in vitro* angiogenic capacity of severely neutropenic SDS-MSCs could be exerted by the up-regulation of P53, which in turn brings to the down-regulation of *VEGFα*. Wild-type P53 has been reported to reduce STAT3 tyrosine phosphorylation and interfere with its DNA binding activity in prostate cancer cell lines displaying a constitutive STAT3 activation [74]. On the other hand, STAT3 may inhibit P53, repressing its pro-apoptotic activity [75]. STAT3 has also the ability to directly activate the transcription of both *VEGFα* and *TGFβ1* genes [56,57], depending on the activation of tyrosine 705 (Y705) [58] or serine 727 (S727) [59], respectively. Concerning SDS, it has been demonstrated that different cellular subsets are characterised by an increased hyper-activation of STAT3 [25,60]. Here, our preliminary results seem to demonstrate that basally (before angiogenic stimulation) STAT3 is hyper-activated at both residues also in SDS-MSCs. At different time-points after angiogenic stimulation, instead, even if phospho-STAT3 levels show a trend of increase in both groups, SDS- seem to present a constitutive STAT3 hyper-activation compared to HD-MSCs. Since wild-type P53 is typically anti-proliferative and pro-apoptotic [76], whereas STAT3 signalling is usually pro-proliferative and anti-apoptotic [77], our data suggest that under angiogenic *stimuli* the up-regulation of P53

along with the persistent induction of STAT3 activity could lead to changes in gene expression patterns able to alter cell survival, proliferation and functionality of SDS-MSCs. However, further studies are needed to better understand the possible involvement of STAT3 in dictating the altered angiogenic capability of SDS-MSCs, as well as its molecular correlation to P53.

In this study we successfully increased the functional *in vitro* characterization of SDS-MSCs. In summary, our results suggest a strong link between TGFβ1 and VEGFA in dictating the altered *in vitro* angiogenic capability of SDS-MSCs. Moreover, our data also provide a rational to investigate whether the defective angiogenesis driven by SDS-MSCs could be related to patients' neutropenia. The identification of down-stream transcriptional factors in TGFβ1/VEGFA axis may lead to the discovery of a possible link between aberrant angiogenesis and haematological abnormalities observed in SDS patients, finally providing new highly targeted strategies for the treatment and cure of this rare bone marrow failure syndrome.

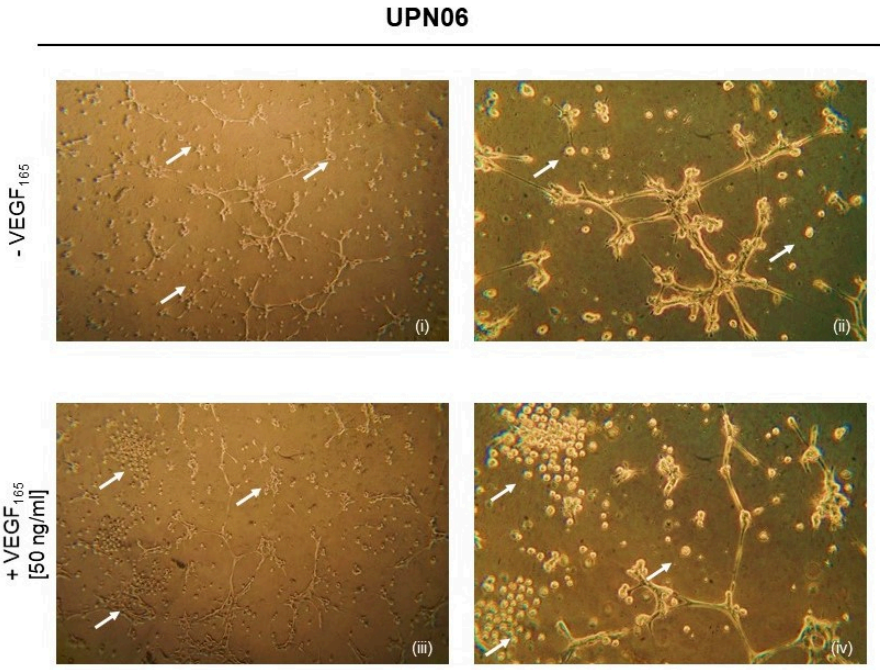


**Supplementary Figure 2.3**: *In vitro angiogenesis assay performed on SDS-MSCs derived from UPN06*

Representative images of SDS-MSCs (magnification 5X and 10X) derived from UPN06 (absolute neutrophils count = 100/µL) stimulated with angiogenic factors or angiogenic factors supplemented with $VEGF_{165}$ protein (50 ng/mL). Cell-substratum detachment is highlighted with white arrows.

# REFERENCES


[1] Dror Y., et al. Draft consensus guidelines for diagnosis and treatment of Shwachman-Diamond syndrome. Ann N Y Acad Sci. 2011 Dec;1242:40-55.

[2] Nelson A.S., Myers K.C. Diagnosis, Treatment, and Molecular Pathology of Shwachman-Diamond Syndrome. Hematol Oncol Clin North Am. 2018 Aug;32(4):687-700.

[3] Minelli A., et al. Incidence of Shwachman-Diamond syndrome. Pediatr Blood Cancer. 2012 Dec;59(7)1334-35.

[4] Bezzerri V., Cipolli M. Shwachman-Diamond Syndrome: Molecular Mechanisms and Current Perspectives. Mol Diagn Ther. 2019 Apr;23(2):281-90.

[5] Boocock G.R., et al. Mutations in SBDS are associated with Shwachman-Diamond syndrome. Nat Genet. 2003 Jan;33(1):97-101.

[6] Dhanraj S., et al. Biallelic mutations in DNAJC21 cause Shwachman-Diamond syndrome. Blood. 2017 Mar;129(11):1557-62.

[7] Stepensky P., et al. Mutations in EFL1, an SBDS partner, are associated with infantile pancytopenia, exocrine pancreatic insufficiency and skeletal anomalies in a Shwachman-Diamond like syndrome. J Med Genet. 2017 Aug;54(8):558-66.

[8] Carapito R., et al. Mutations in signal recognition particle SRP54 cause syndromic neutropenia with Shwachman-Diamond-like features. J Clin Invest. 2017 Nov;127(11):4090-03.

[9] Rawls A.S., et al. Lentiviral-mediated RNAi inhibition of Sbds in murine hematopoietic progenitors impairs their hematopoietic potential. Blood. 2007 Oct;110(7):2414-22.

[10] Austin K.M., et al. Mitotic spindle destabilization and genomic instability in Shwachman-Diamond syndrome. J Clin Invest. 2008 Apr; 118(4):1511-18.

[11] Raaijmakers M.H., et al. Bone progenitor dysfunction induces myelodysplasia and secondary leukaemia. Nature. 2010 Apr;464(7290):852-57.

[12] Shirzad R., et al. Signaling and molecular basis of bone marrow niche angiogenesis in leukemia. Clin Transl Oncol. 2016 Oct;18(10):957-71.

[13] Leung E.W., et al. Shwachman-Diamond Syndrome: An Inherited Model of Aplastic Anaemia With Accelerated Angiogenesis. Br J Haematol. 2006 Jun;133(5):558-61.

[14] Lee M.W., et al. Mesenchymal stem cells in suppression or progression of hematologic malignancy: current status and challenges. Leukemia. 2019 Mar;33(3):597-611.
[15] Caplan A.I., Dennis J.E. Mesenchymal stem cells as trophic mediators. J Cell Biochem. 2006 Aug;98(5):1076-84.
[16] Watt S.M., et al. The angiogenic properties of mesenchymal stem/stromal cells and their therapeutic potential. British Medical Bulletin. 2013;108(1):25-53.
[17] Andre' V., et al. Mesenchymal stem cells from Shwachman-Diamond syndrome patients display normal functions and do not contribute to hematological defects. Blood Cancer J. 2012 Oct;2(10), e94.
[18] Serafini M., et al. Establishment of bone marrow and hematopoietic niches in vivo by reversion of chondrocyte differentiation of human bone marrow stromal cells. Stem Cell Res. 2014 May;12(3):659-72.
[19] Bardelli D., et al. Mesenchymal stromal cells from Shwachman-Diamond syndrome patients fail to recreate a bone marrow niche in vivo and exhibit impaired angiogenesis. Br J Haematol. 2018 Jul;182(1):114-24.
[20] Dale C.D. How I Manage Children With Neutropenia. Br. J. Haematol. 2017 Aug;178(3):351-63.
[21] Avanzini M.A., et al. Generation of mesenchymal stromal cells in the presence of platelet lysate: a phenotypic and functional comparison of umbilical cord blood- and bone marrow-derived progenitors. Haematologica. 2009 Dec;94(12):1649-60.
[22] Jian Y.E., et al. Primer-BLAST: A Tool to Design Target-Specific Primers for Polymerase Chain Reaction. BMC Bioinformatics. 2012 Jun;13(6):134.
[23] Ragni E., et al. What is beyond a qRT-PCR study on mesenchymal stem cell differentiation properties: how to choose the most reliable housekeeping genes. J Cell Mol Med. 2013 Jan;17(1):168-80.
[24] Livak K.J., Schmittgen T.D. Analysis of relative gene expression data using real-time quantitative PCR and the 2(-Delta Delta C(T)) Method. Methods. 2001 Dec;25(4):402-08.
[25] Vella A., et al. mTOR and STAT3 Pathway Hyper-Activation is Associated with elevated Interleukin-6 Levels in Patients with Shwachman-Diamond Syndrome: Further Evidence of Lymphoid Lineage Impairment. Cancers (Basel). 2020 Mar 5;12(3):597.
[26] Dominici M., et al. Minimal criteria for defining multipotent mesenchymal stromal cells. The International Society for Cellular Therapy position statement. Cytotherapy. 2006;8(4):315-17.

[27] Dror Y., Freedman M.H. Shwachman-Diamond syndrome marrow cells show abnormally increased apoptosis mediated through the Fas pathway. Blood. 2001 May;97(10):3011-6.
[28] Zheng W., et al. Mechanisms of coronary angiogenesis in response to stretch: role of VEGF and TGF-beta. Am J Physiol Heart Circ Physiol. 2001 Feb;280(2):H909-17.
[29] Xia X., et al. Growth Hormone-Releasing Hormone and Its Analogues: Significance for MSCs-Mediated Angiogenesis. Stem Cells Int. 2016;8737589.
[30] Acuzian A.A., et al. Molecular Mediators of Angiogenesis. J Burn Care Res. 2010 Jan-Feb;31(1):158-75.
[31] Ball S.G., et al. Mesenchymal stem cells and neovascularization: role of platelet-derived growth factor receptors. J Cell Mol Med. 2007 Sep-Oct;11(5):1012-30.
[32] Ball S.G., et al. Platelet-derived Growth Factor Receptors Regulate Mesenchymal Stem Cell Fate: Implications for Neovascularization. Expert Opin Biol Ther. 2010 Jan;10(1):57-71.
[33] Gerhardt H., et al. Neuropilin-1 is required for endothelial tip cell guidance in the developing central nervous system. Dev Dyn Nov. 2004 Nov;231(3):503-09.
[34] Nagasaki T., et al. Interleukin-6 released by colon cancer-associated fibroblasts is critical for tumour angiogenesis: anti-interleukin-6 receptor antibody suppressed angiogenesis and inhibited tumour-stroma interaction. Br J Cancer. 2014 Jan;110(2):469-78.
[35] Zou M., et al. IL6-induced metastasis modulators p-STAT3, MMP-2 and MMP-9 are targets of 3,3′-diindolylmethane in ovarian cancer cells. Cell Oncol (Dordr). 2015 Feb;39(1):47-57.
[36] Middleton K., et al. Interleukin-6. An angiogenic target in solid tumours. Crit Rev Oncol Hematol. 2014 Jan;89(1):129-39.
[37] Couper L.L., et al. Vascular endothelial growth factor increases the mitogenic response to fibroblast growth factor-2 in vascular smooth muscle cells in vivo via expression of fms-like tyrosine kinase-1. Circ Res. 1997 Dec;81(6):932-39.
[38] Faraone D., et al. Heterodimerization of FGF-receptor 1 and PDGF-receptor-alpha: a novel mechanism underlying the inhibitory effect of PDGF-BB on FGF-2 in human cells. Blood. 2006 Mar;107(5):1896-902.
[39] Ding Q., et al. CXCL9: Evidence and Contradictions for Its Role in Tumor Progression. Cancer Med. 2016 Nov;5(11):3246-59.
[40] Sahin H., et al. Chemokine Cxcl9 attenuates liver fibrosis-associated angiogenesis in mice. Hepatology. 2012 May;55(5):1610-19.

[41] Huang B., et al. Osteoblasts secrete Cxcl9 to regulate angiogenesis in bone. Nat Commun. 2016 Dec;7:13885.
[42] Shen Q., et al. Inhibiting Expression of Cxcl9 Promotes Angiogenesis in MSCs-HUVECs Co-Culture. Arch Biochem Biophys. 2019 Oct;675:108108.
[43] Fagiani E., Christofori G. Angiopoietins in angiogenesis. Cancer Lett. 2013 Jan;328(1):18-26.
[44] Sieff C.A., et al. Pathogenesis of the erythroid failure in Diamond Blackfan anaemia. Br J Haematol. 2010 Feb;148(4):611-22.
[45] Rujkijyanont P., et al. SBDS-deficient cells undergo accelerated apoptosis through the Fas-pathway. Haematologica. 2008 Mar;93(3):363-71.
[46] Watanabe K., et al. SBDS-deficiency results in specific hypersensitivity to Fas stimulation and accumulation of Fas at the plasma membrane. Apoptosis. 2009 Jan;14(1):77-89.
[47] Chiarugi V, et al. P53: radiosensitivity and antiangiogenic effects. Mol Genet Metab. 1998 May;64(1):7-11.
[48] Nakagawa T., et al. TGF-beta Induces Proangiogenic and Antiangiogenic Factors via Parallel but Distinct Smad Pathways. Kidney Int. 2004 Aug;66(2):605-13.
[49] Ferrari G., et al. VEGF, a Prosurvival Factor, Acts in Concert With TGF-beta1 to Induce Endothelial Cell Apoptosis. Proc Natl Acad Sci U S A. 2006 Nov;103(46):17260-65.
[50] Ferrari G., et al. TGF-β1 Induces Endothelial Cell Apoptosis by Shifting VEGF Activation of p38(MAPK) From the Prosurvival p38β to Proapoptotic p38α. Mol Cancer Res. 2012 May;10(5):605-14.
[51] de Caestecker M. The transforming growth factor-beta superfamily of receptors. Cytokine Growth Factor Rev. 2004 Feb;15(1):1-11.
[52] Wrana J.L. Signaling by the TGFb Superfamily. Cold Spring Harb Perspect Biol. 2013;5:a011197
[53] ten Dijke P., et al. Endoglin in angiogenesis and vascular diseases. Angiogenesis. 2008;11(1):79-89.
[54] Park S., et al. PECAM-1 Isoforms, eNOS and Endoglin Axis in Regulation of Angiogenesis. Clin Sci (Lond). 2015 Aug;129(3):217-34.
[55] Liu Z., et al. VEGF and inhibitors of TGFbeta type-I receptor kinase synergistically promote blood-vessel formation by inducing alpha5-integrin expression. J Cell Sci. 2009 Sep;122(Pt 18):3294e302.
[56] Wei D., et al. STAT3 activation regulates the expression of vascular endothelial growth factor and human pancreatic cancer angiogenesis and metastasis. Oncogene. 2003 Jan;22(3):319-29.

[57] Kinjyo I., et al. Loss of SOCS3 in T helper cells resulted in reduced immune responses and hyperproduction of interleukin 10 and transforming growth factor-beta 1. J Exp Med. 2006 Apr;203(4):1021-31.
[58] Sehgal P.B. Paradigm shifts in the cell biology of STAT signaling. Semin Cell Dev Biol. 2008 Aug;19(4):329-40.
[59] Li C., et al. Noncanonical STAT3 activation regulates excess TGF-β1 and collagen I expression in muscle of stricturing Crohn's disease. J Immunol. 2015 Apr 1;194(7):3422-31.
[60] Bezzerri V., et al. New insights into the Shwachman-Diamond Syndrome-related haematological disorder: hyper-activation of mTOR and STAT3 in leukocytes. Sci Rep. 2016 Sep 23;6:33165.
[61] Ng C., et al. Conformational flexibility and molecular interactions of an archaeal homologue of the Shwachman-Bodian-Diamond syndrome protein. BMC Struct Biol. 2009 May;9:32.
[62] Ganapathi K.A., et al. The human Shwachman-Diamond syndrome protein, SBDS, associates with ribosomal RNA. Blood. 2007 Sep 1;110(5):1458-65.
[63] Finch A.J., et al. Uncoupling of GTP hydrolysis from eIF6 release on the ribosome causes Shwachman-Diamond syndrome. Genes Dev. 2011 May 1;25(9):917-29.
[64] Wong C.C., et al. Defective ribosome assembly in Shwachman-Diamond syndrome. Blood. 2011 Oct 20;118(16):4305-12.
[65] Orelio C., Kuijpers T.W. Shwachman-Diamond syndrome neutrophils have altered chemoattractant-induced F-actin polymerization and polarization characteristics. Haematologica. 2009 Mar;94(3):409-13.
[66] Dror Y., Freedman M.H. Shwachman-Diamond syndrome: An inherited preleukemic bone marrow failure disorder with aberrant hematopoietic progenitors and faulty marrow microenvironment. Blood. 1999 Nov 1;94(9):3048-54.
[67] Santamaria C., et al. Impaired expression of DICER, DROSHA, SBDS and some microRNAs in mesenchymal stromal cells from myelodysplastic syndrome patients. Haematologica. 2012 Aug;97(8):1218-24.
[68] Chavakis E., Dimmeler S. Regulation of endothelial cell survival and apoptosis during angiogenesis. Arterioscler Thromb Vasc Biol. 2002 Jun 1;22(6):887-93.
[69] Stepanovic V., et al. The chemotaxis defect of Shwachman-Diamond Syndrome leukocytes. Cell Motil Cytoskeleton. 2004 Mar;57(3):158-74.
[70] Vené R., et al. HIV-Tat dependent chemotaxis and invasion, key aspects of tat mediated pathogenesis. Clin Exp Metastasis. 2000;18(7):533-8.

[71] Gaudry M., et al. Intracellular pool of vascular endothelial growth factor in human neutrophils. Blood. 1997;90:4153-61.
[72] Ai S., et al. Angiogenic activity of bFGF and VEGF suppressed by proteolytic cleavage by neutrophil elastase. Biochem Biophys Res Commun. 2007;364:395-401.
[73] Hamabata T., et al. Pluripotent stem cell model of Shwachman-Diamond syndrome reveals apoptotic predisposition of hemoangiogenic progenitors. Sci Rep. 2020 Sep 9;10(1):14859.
[74] Lin J., et al. p53 regulates Stat3 phosphorylation and DNA binding activity in human prostate cancer cells expressing constitutively active Stat3. Oncogene. 2002 May 2;21(19):3082-8.
[75] Niu G., et al. Role of Stat3 in regulating p53 expression and function. Mol Cell Biol. 2005 Sep;25(17):7432-40.
[76] Vogelstein B., et al. Surfing the p53 network. Nature. 2000 Nov 16;408(6810):307-10.
[77] Yu H., Jove R. The STATs of cancer - new molecular targets come of age. Nat Rev Cancer. 2004 Feb;4(2):97-105.

## Chapter 3

# mTOR and STAT3 pathway hyper-activation is associated with elevated interleukin-6 levels in patients with Shwachman-Diamond Syndrome: further evidence of lymphoid lineage impairment

Cancers (Basel). 2020 Mar 5;12(3):597
doi: 10.3390/cancers12030597

A. Vella[1], E. D'Aversa[2], M. Api[3], G. Breveglieri[2], M. Allegri[3], A. Giacomazzi[1], E. Marinelli Busilacchi[4], B. Fabrizzi[3], T. Cestari[1], C. Sorio[5], Gloria Bedini[6], G. D'Amico[6], V. Bronte[1], A. Poloni[4], A. Benedetti[7], C. Bovo[8], S.J. Corey[9], M. Borgatti[2,10], M. Cipolli[11] and V. Bezzerri[3]

[1]Unit of Immunology, Azienda Ospedaliera Universitaria Integrata, 37134 Verona, Italy; [2]Department of Life Sciences and Biotechnology, University of Ferrara, 44100 Ferrara, Italy; [3]Cystic Fibrosis Center, Azienda Ospedaliero Universitaria Ospedali Riuniti, 60126 Ancona, Italy; [4]Hematology Clinic, Università Politecnica delle Marche -AOU Ospedali Riuniti, 60126 Ancona, Italy; [5]Department of Medicine, University of Verona, 37134 Verona, Italy; [6]Immunology and Cell Therapy Unit, Tettamanti Research Center, University of Milano-Bicocca, 20900 Monza, Italy; [7]Department of Gastroenterology and Hepatology, Università Politecnica delle Marche, 60126 Ancona, Italy; [8]Hospital Health Direction, Azienda Ospedaliera Universitaria Integrata, 37126 Verona, Italy; [9]Department of Pediatric Hematology/Oncology and Stem Cell Transplantation, Cleveland Clinic, Cleveland, OH 44195, USA; [10]Biotechnology Center, University of Ferrara, 44100 Ferrara, Italy; [11]Cystic Fibrosis Center, Azienda Ospedaliera Universitaria Integrata, 37126 Verona, Italy

## 3.1 Abstract

Shwachman-Diamond syndrome (SDS) is a rare inherited bone marrow failure syndrome, resulting in neutropenia and a risk of myeloid neoplasia. A mutation in a ribosome maturation factor accounts for almost all of the cases. Lymphoid involvement in SDS has not been well characterized. We recently reported that lymphocyte subpopulations are reduced in SDS patients. We have also shown that the mTOR-STAT3 pathway is hyper-activated in SDS myeloid cell populations. Here, we show that mTOR-STAT3 signalling is markedly up-regulated in the lymphoid compartment of SDS patients. Furthermore, our data reveal elevated IL6 levels in cellular supernatants obtained from lymphoblasts, bone marrow mononuclear and mesenchymal stromal cells, and plasma samples obtained from a cohort of 10 patients. Of note, everolimus-mediated inhibition of mTOR signalling is associated with basal state of phosphorylated STAT3. Finally, inhibition of mTOR-STAT3 pathway activation leads to normalization of IL6 expression in SDS cells. Altogether, our data strengthen the hypothesis that SDS affects both lymphoid and myeloid blood compartment and suggest everolimus as a potential therapeutic agent to reduce excessive mTOR-STAT3 activation in SDS.

**Keywords:** STAT3; mTOR; Bone Marrow Failure Syndromes; lymphocytes

## 3.2 Rationale

Shwachman-Diamond Syndrome (SDS) is one of the most common inherited bone marrow failure syndromes (IBMFS), occurring in almost 1 out of 75,000 live births [1]. SDS results from biallelic mutations in the Shwachman-Bodian-Diamond Syndrome (*SBDS*) gene, which encode the SBDS protein. SBDS protein cooperates with its partner elongation factor-like GTPase 1 (EFL1) to catalyse the release of the ribosomal anti-association factor eIF6, facilitating the assembly of the functional 80S ribosome [2-4]. The IBMFS are also cancer predisposition syndromes, in particular myelodysplastic syndrome (MDS) and acute myeloid leukaemia (AML). In the general population, MDS has an incidence ranging from 2-12 cases per 100,000 people, which increases as individuals age [5]. Patients with SDS demonstrate a risk of evolution to MDS of 8.1% and 36% at 10 and 30 years, respectively [6]. A recent genomic analysis of 1514 patients with MDS who underwent a stem cell transplant showed that 4% of the young adult patients had undiagnosed compound heterozygous mutations in *SBDS*, suggesting that SDS prevalence among MDS/AML patients may be underestimated [7]. AML derives from dysregulated proliferation and accumulation of immature myeloid progenitor cells into the bone marrow and peripheral blood, which finally leads to a severe impairment of the hematopoietic system. Acute leukaemias rapidly disseminate after initial inception, escaping the anti-leukemic immunity process. Regulatory T

cells play a key role in the maintenance of immune tolerance, which acts as a regulator of the tumour immunity [8]. CD4/CD8 double negative (DN) T cells have gained prominence among T regulatory cell subsets engaged in immunosurveillance. DN T cells are mature T cells representing almost 3-5% of the total peripheral T cell population [9]. Most human and murine T cells express and rearrange the α and β chains of the T cell receptor (TCR) and are recognized as TCRαβ T cells, whereas a small part of T cells do express the ɣ and δ chains, which are mostly DN T cells [9]. Interestingly, DN T cells showed anti-leukemic activity and synergy with conventional chemotherapies both *in vitro* and in patient-derived xenograft models of AML [10,11]. In a mouse model of AML, the leukemic cells promoted T cell tolerance with suppression of anti-tumour $CD8^+$ T cells [12]. Failure of T cell-mediated anti-cancer immune response is associated with disease progression and poor outcome in MDS and AML.

IL6/JAK/STAT3 signalling axis plays a key role in leukemogenesis [13]. The genes encoding the kinase protein JAK2 have indeed often been mutated in myeloproliferative disorders, leading to constitutive hyper-activation of its downstream effector, the transcription factor STAT3 [14]. Of note, STAT3 hyper-activation has been found in tumour-infiltrating leukocytes, in which STAT3 orchestrates the crosstalk between cancer and immune cells [15]. Furthermore, it has been reported that STAT3 inhibition in the myeloid compartment remarkably induces the anti-tumour capabilities of

T cells and promotes their expansion *in vivo* [16,17]. STAT3 activation in immune cells is indeed associated with suppression of anti-tumour immunity. STAT3 excessive activation may be triggered by elevated levels of IL6 present in the serum or released within the tumour microenvironment [14]. IL6 may act in an autocrine or paracrine manner. IL6 binds to its IL6 receptor (IL-6R), localized onto the plasma membrane (membrane bound (mb)IL-6R), which is physically associated with the gp130 protein. This process is recognized as classical IL6 signalling and leads to gp130 homodimerization, resulting in the activation of the IL6 receptor complex [18]. In addition, IL6 binds to the small extracellular secretory soluble IL6 receptor (sIL-6R), which is generated by alternative splicing of IL-6R gene or by metalloproteinase-dependent cleavage of mbIL-6R. The sIL-6R mediates JAK-STAT3 activation in gp130 positive cells, which do not express mbIL-6R through a process termed IL6 trans-signalling [19]. The IL6 trans-signalling pathway has been reported in murine haematopoietic stem cells [20,21]. Elevated levels of IL6 have been found in adult bone marrow niche of patients with AML [22]. Serum IL6 levels were found to be significantly increased in paediatric patients with AML [23]. Moreover, increased IL6 serum levels are associated with poor prognosis in several types of cancer, including AML [23]. Interestingly, IL6 gene expression can be regulated by STAT3 itself, resulting in a feedforward autocrine feedback loop [14].

STAT3 has been reported as a direct substrate for the mammalian target of rapamycin (mTOR), which induces STAT3

S727 phosphorylation [24,25]. In addition, the mTOR-inhibitor rapamycin inhibits STAT3 S727 phosphorylation [24]. Moreover, we have previously shown that mTOR can promote STAT3 phosphorylation both at residue tyrosine 705 and serine 727 in SDS leukocytes [26]. Previous studies have reported that relapse of AML is associated with the gain of additional mutations in the mTOR gene, often due to the cytotoxic chemotherapy received by patients [27,28]. Inhibition of the mTOR pathway using rapamycin or other analogue molecules, including everolimus (RAD001) as anti-leukemic agent, has shown potent anti-cancer capabilities both *in vitro* and *in vivo* [29,30]. To date, no pharmacological therapy has been developed for IBMFS-related MDS or AML, and allogeneic haematopoietic stem cell transplantation remains the unique option in these cases. Unfortunately, its efficacy is limited by the morbidity and mortality associated with graft-versus-host disease.

Here, we show further analysis of the mTOR-STAT3 axis in an extended panel of lymphocytic populations including $CD4^+$, $CD8^+$, T cells, DN T cells, γδT cells, and Natural Killer cells (NK). Moreover, we have checked the expression of IL6 in different cellular and clinical SDS models, including lymphoblastoid cell lines (LCL), bone marrow mononuclear haematopoietic progenitors (BM-MNC) and mesenchymal stromal cells (BM-MSC), and plasma obtained from an enlarged cohort of 31 patients with SDS (**Table 3.1**). Our data indicate that everolimus can restore a normal level of mTOR and STAT3

activation in primary SDS lymphocytes. Importantly, mTOR-STAT3 inhibition was paralleled by a down-regulation of IL6 expression in haematopoietic SDS cells. Our results suggest the existence of a mTOR-STAT3-IL6 loop of activation in haematopoietic SDS cells, which may affect both myeloid and lymphoid compartment, thus contributing to malignant transformation over the time. Taken together, these data strengthen the hypothesis of the involvement of lymphoid lineage in SDS and suggest everolimus or new rapalogs as potential therapeutic agents in SDS patients.

## 3.3 Experimental procedures

### 3.3.1 Human Subjects

Human samples were obtained and analysed in accordance with the declaration of Helsinki, after written consent. All protocols were approved by the Ethics Committee of San Gerardo Hospital (Monza, Italy), approval No. 504 4/9/2012, Azienda Ospedaliera Universitaria Integrata (Verona, Italy), approval No. 658 CESC, and Azienda Ospedaliero Universitaria Ospedali Riuniti (Ancona, Italy), approval No. CERM 2018-82.

### 3.3.2 Plasma isolation

Bone marrow and peripheral blood specimens were collected into EDTA-containing tubes from patients. Specimens were collected during a bone marrow harvest from healthy donors serving as donors for a related HLA-matched transplant, as permitted by the local hospital ethics committee and after informed consent was obtained. Peripheral blood and bone marrow plasma samples were prepared by centrifugation for 10 min at 600xg at 4°C. To obtain platelet-poor plasma fractions, another centrifugation was performed for 15 min at 1800xg. Plasma specimens were then stored at -80°C until analysis.

**Table 3.1**: *Clinical data and genetics of patients with SDS recruited in this study*

| UPN | Gender | Age | Genotype | PMN (cell/mm³) | Phenotype | Cytogenetics |
|---|---|---|---|---|---|---|
| 1 | M | 27 | 258+2T>C/183-184TA>CT | 1460 | PI, FTT, recurrent infection , bone malformation, HbF>2%, thrombocytopenia, | 46,XY, i(7)(q10) |
| 13 | M | 19 | 258+2T>C/183-184TA>CT+258+2T>C | 1130 | PI, FTT, recurrent infection , bone malformation, thrombocytopenia, anemia, cognitive impairment | 46,XY, del(20)q |
| 26 | M | 16 | 258+2T>C/183-184TA>CT | 58 | PI,FTT, bone malformation, thrombocytopenia | 46,XY |
| 35 | F | 15 | 258+2T>C/183-184TA>CT | 970 | PI, FTT, thrombocytopenia, anemia | 46,XX |
| 37 | F | 10 | 258+2T>C/183-184TA>CT | 1280 | PI, FTT, recurrent infection | 46,XX, i(7)(q10) |
| 47 | M | 12 | 258+2T>C/183-184TA>CT | 550 | PI, FTT, recurrent infections, bone malformation, thrombocytopenia | 46,XX |
| 52 | M | 10 | 258+2T>C/183-184TA>CT+258+2T>C | 1070 | PI, FTT, bone malformation | 46,XY |
| 56 | F | 15 | 258+2T>C/183-184TA>CT | 1840 | PI, FTT, recurrent infections, bone malformation, HbF>2%, thrombocytopenia | 46,XX |
| 57 | F | 40 | 258+2T>C/G63C | 500 | PI,FTT, bone malformation, HbF>2%, thrombocytopenia, cognitive impairment | 46,XX |
| 58 | M | 12 | 258+2T>C/183-184TA>CT | 390 | PI, FTT, recurrent infections, bone malformation, HbF>2%, thrombocytopenia, anemia | 46,XY |
| 63 | M | 15 | 258+2T>C/183-184TA>CT+258+2T>C | 536 | PI, recurrent infections, bone malformation, HbF>2%, thrombocytopenia | 46,XY |
| 65 | M | 19 | 258+2T>C/258+2T>C | 1390 | PI, FTT, recurrent infection , bone malformation, thrombocytopenia, cognitive impairment | 46,XY, del(20)q |
| 66 | M | 23 | 258+2T>C/183-184TA>CT | 1340 | PI, bone malformation, thrombocytopenia, cognitive impairment | 46,XY |
| 67 | M | 8 | 258+2T>C/183-184TA>CT | 500 | PS, FTT, bone malformation, HbF>2% | 46,XY |
| 68 | M | 22 | 258+2T>C/183-184TA>CT+258+2T>C | 600 | PS, FTT, recurrent infections, bone malformation, thrombocytopenia, cognitive impairment | 46,XY |
| 69 | F | 8 | 258+2T>C/183-184TA>CT | 770 | PI, FTT, HbF>2%, anemia, cognitive impairment | 46,XX |
| 72 | M | 28 | 258+2T>C/183-184TA>CT | 380 | PI, recurrent infections, bone malformation, thrombocytopenia, anemia, cognitive impairment | 46,XY |
| 73 | F | 7 | 258+2T>C/183-184TA>CT | 520 | PI, FTT, HbF>2%, thrombocytopenia | 46,XX |
| 74 | M | 9 | 258+2T>C/183-184TA>CT | 1430 | PI, FTT, HbF>2%, cognitive impairment | 46,XY |
| 75 | F | 7 | 258+2T>C/183-184TA>CT | 1000 | PI, FTT, bone malformation, HbF>2%, thrombocytopenia, cognitive impairment | 46,XX |
| 80 | M | 7 | 258+2T>C/183-184TA>CT | 680 | PI, FTT, recurrent infections, bone malformation, anemia, cognitive impairment | 46,XY |
| 82 | M | 16 | 258+2T>C/183-184TA>CT | 300 | PI, FTT, , recurrent infections bone malformation, thrombocytopenia, anemia, cognitive impairment | 46,XY |
| 87 | M | 18 | 258+2T>C/183-184TA>CT | 880 | PI, FTT, recurrent infections, bone malformation, cognitive impairment | 46,XY |
| 94 | F | 19 | 258+2T>C/352A>G | 2420 | PI, HbF>2%, thrombocytopenia | 46,XX |
| 104 | M | 10 | 258+2T>C/183-184TA>CT | 500 | PI, FTT, recurrent infections, bone malformation, HbF>2%, thrombocytopenia | 46,XY |
| 106 | M | 36 | 258+2T>C/183-184TA>CT | 1210 | PI, FTT, bone malformation, anemia | 46,XY |
| 108 | M | 17 | 258+2T>C/183-184TA>CT | 970 | PS, FTT, bone malformation, anemia | 46,XY |

*Abbreviations*: UPN, unique patient number; PI, pancreas insufficiency; PS, pancreas sufficiency; FTT, failure to thrive; HbF, foetal haemoglobin.

### 3.3.3 Cell Cultures

LCLs, PBMCs, BM-MNCs, and BM-MSCs were obtained from peripheral blood or bone marrow samples from 31 patients with Shwachman-Diamond Syndrome. All patients enrolled in this study were diagnosed as affected by SDS on the basis of

clinical and genetics criteria, and they were excluded if MDS/AML were present (**Table 3.1**). None of the patients underwent granulocyte colony-stimulating factor (G-CSF, filgrastim) nor steroids therapies. PBMCs and BM-MNCs were separated by stratification on Ficoll-Paque PLUS (density 1.077 g/mL, GE Healthcare, Waukesha, WI, USA) gradient and washed twice with PBS (Euroclone, Milan, Italy). Cells were seeded in 6-wells cell culture plates at 1 x $10^6$ BM-MNCs/well in 1 mL RPMI-1640 Medium (Gibco, Waltham, MA, USA) supplemented with 10% FBS (Sigma-Aldrich, St. Louis, MO) and incubated in the presence or absence of 350 nM everolimus (Sigma-Aldrich) or 7.5 μM stattic (Selleckchem, Houston, TX, USA) at 37°C in humidified atmosphere, with 5% $CO_2$ for 24 hours. Treated cell pellets were collected by centrifugation and the supernatant isolated and stored at -80°C. BM-MSCs were isolated after seeding 1.6 x $10^5$ BM-MNCs/$cm^2$ from fresh bone marrow, in Dulbecco's Modified Eagle Medium low glucose (Gibco) supplemented with 10% of FBS, 1% L-glutamine and 1% penicillin/streptomycin. BM-MNCs were incubated at 37°C in humidified atmosphere, with 5% $CO_2$ for 24 hours. Subsequently, non-adherent cells were removed by washing with PBS and culture medium was finally replaced. BM-MSCs were seeded at 4 x $10^3$ cell/$cm^2$ and incubated at 37°C in humidified atmosphere, with 5% $CO_2$ since they reached 70-80% confluence. 1 x $10^5$ MSCs were seeded in a 6-well plate and incubated for 48 hours at 37°C in humidified atmosphere, with 5% $CO_2$. Eventually, treated cells were

collected and the supernatant isolated and stored at -80°C. To obtain LCLs, B cells were seeded at a density of 3 x $10^6$ cells in 12-well cell culture plates, incubated with 3 mL RPMI-1640 supplemented with 10% FBS, and infected for 18 hours with Epstein-Barr virus (EBV) released from marmoset blood leukocytes B95.8 virus-producer cell lines as previously described [26]. 1 x $10^6$ LCLs were seeded in 6 well-cell culture plate in RPMI-1640 supplemented with 10% FBS and incubated for 48 hours at 37°C in humidified atmosphere, with 5% $CO_2$. Eventually,1 x $10^6$ LCLs were seeded in 6 well-cell culture plate in RPMI-1640 supplemented with 10% FBS, in the presence or absence of 350 nM everolimus or 7.5 μM stattic at 37°C in humidified atmosphere, with 5% $CO_2$ for 24 hours. Treated cell pellets were collected by centrifugation and the supernatant isolated and stored at -80°C. LCLs, BM-MNCs and MSCs cultured in medium containing DMSO (Sigma, dilution 1:10,000) were used as negative control.

### 3.3.4 Flow Cytometry

Plasma was separated from peripheral blood samples derived from SDS patients or healthy subjects by centrifugation at 1500xg for 10 min. Red blood cells were lysed in 40 mL of solution containing 0.89% (w/v) $NH_4Cl$, 0.10% (w/v) $KHCO_3$ and 200 μM EDTA. Leukocytes were cultured in 6-well plates containing RPMI-1640 supplemented with 10% freshly prepared, heat-inactivated human plasma, in the presence or

absence (DMSO) of 350 nM everolimus for 1 hour. Fifty to one-hundred-100 microliter aliquots of blood cells were incubated for 15 min at room temperature with combinations of the following fluorochrome-conjugated monoclonal antibodies: CD3-APC750, CD4-PC7, CD8-ECD, CD16-Pacific Blue, CD19-Chrome-Orange, CD45-APC700, and CD56-PC5 (Beckman-Coulter, Indianapolis, IN, USA). Cells were gently centrifuged (600xg) for 10 min, washed with ice-cold PBS, fixed, and permeabilized with Intracellular Fixation and Permeabilization Buffer Set (eBioscience, San Diego, CA, USA), following the manufacturer's recommendations. Subsequently, cells were washed with flow buffer and stained with anti-pS727-STAT3-PE, anti-Y705-STAT3-PE, anti-p-S2448-mTOR-PE or isotype control-PE conjugated antibodies for 30 min. Data acquisition was performed by a 10 colour, three laser Navios flow cytometer (Beckman Coulter). Analysis of the acquired data was performed by the "Navios" or Kaluza software, version 1.3 (Beckman Coulter). In order to define different subsets of lymphocytes, gating strategy and data filtering were established as follows. Cell debris were excluded using a dot plot for morphological parameters (FS, SS). Lymphocytes were gated into the side scatter (SS low) and CD45 positive area. Within the lymphocyte compartment, $CD3^+$ events were further gated into $CD4^+$ and $CD8^+$ T cells. NK cells were instead identified as CD3/CD19 double-negative events ($CD56^+$ and/or $CD16^+$). Double-negative T cells were gated by plotting T cells ($CD3^+$) in CD4 *vs* CD8 dot plots. Since it has been reported that TCR

γδ$^{+}$T cells are recognizable by the bright expression on their membrane of the CD3 molecule [51], CD3 bright DN T cells (DNγδ) were gated by plotting CD3 bright positive area into CD4 *vs* CD8 dot plots. Flow cytometry was performed on at least 25,000 events. The total white blood cell count (WBC) was determined by Haematology Analyzer XN- 9000 (Sysmex Europe GmbH, Norderstedt, Germany).

### 3.3.5 qRT-PCR

Total RNA from LCLs and MNCs was isolated using High Pure RNA Isolation Kit (Roche, Mannheim, Germany) following the manufacturer's instructions. RNA was eluted in 50 µL of RNAse free water. Final RNA concentration was determined using NanoDrop 2000 spectrophotometer (Thermo Fisher Scientific, Foster City, CA, USA) and then stored at -80°C until use. A total amount of 500 ng of RNA was reverse transcribed to cDNA using a High Capacity cDNA Reverse Transcription Kit with random primers (Applied Biosystems by Thermo Fisher Scientific) for 120 min at 37°C and 5 min at 85°C in a final reaction volume of 20 µL. For real-time qPCR analysis, 5 µL of cDNA were used for each reaction to quantify the relative gene expression. The cDNA was then amplified for 45 PCR cycles using Platinum SYBR Green qPCR Super Mix-UDG (Invitrogen by Thermo Fisher Scientific) in a 20 µL reaction using the Rotor-Gene 6000 cycler (Qiagen, Hilden, Germany). In order to perform the PCR reaction, QuantiTect Primer Assays (Qiagen)

for IL6 (Hs_IL6_1_SG, NM_000600), STAT3 (Hs_STAT3_1_SG, NM_003150), mTOR (Hs_MTOR_1_SG, NM_004958), and GAPDH (HS_GAPDH_1_SG, NM_001256799) were purchased. Each target gene expression was normalized with GAPDH gene expression and relative quantification was calculated by the ΔCt method.

### 3.3.6 IL6 and sIL-6R Detection

Bio-Plex Pro Human IL6 Assay (Bio-Rad Laboratories, Philadelphia, PA, USA) was used to measure IL6 protein released into cell supernatants and plasma samples (sample volume 50 µL). The assays were performed using the Bio-Plex Suspension Array System, with the Bio-Rad 96-well plate reader. Data were analysed by the Bio-Plex Manager software (Bio-Rad Laboratories). The *in-vitro* quantitative determination of soluble IL6 Receptor (sIL-6R) in plasma was performed by using the Human IL-6R/CD126 ELISA Kit (Origene, Rockville, MD, USA), according to the manufacturer's instructions. Plasma samples were assayed after 1:200 dilution.

### 3.3.7 Western blot

A total of 30 µg of cell extract was denatured for 5 min at 95°C in 4x Laemmli Sample Buffer, (277.8 mM Tris-HCl, pH 6.8, 44.4% glycerol, 4.4% LDS, 0.02% bromophenol blue) (Bio-Rad Laboratoires) supplemented with 355 mM 2-mercaptoethanol. The samples were loaded on 7.5%

polyacrylamide SDS-PAGE gel in Tris-glycine Buffer (25 mM Tris, 192 mM glycine, and 0.1% SDS) using tag protein ladder (Spectra Multicolor Broad Range Protein Ladder, Thermo Scientific, Waltham, MA, USA) to determine molecular weight. The electrotransfer was performed into nitrocellulose membrane (iBlot Gel Transfer Stacks Nitrocellulose, Thermo Fisher) at 20V using iBlot Dry Blotting System (Invitrogen, Waltham, MA, USA) for 10 min. The membranes were blocked in BSA 5% for 90 min at room temperature and washed with TBS (5 mM Tris-HCl pH 7.6, 150 mM NaCl) supplemented with 0.05% tween-20 (TBS/T) for 15 min. Subsequently, membranes were probed with primary anti-human STAT3 rabbit polyclonal antibody (SAB2104912 Sigma-Aldrich, Missouri, USA, dilution 1:500) in primary antibody dilution buffer (TBS/T with 5% BSA) and incubated overnight at 4°C. After washes, membranes were incubated with mouse anti-rabbit IgG- Horseradish Peroxidase-Coupled secondary antibody (Sigma-Aldrich, dilution 1:2000) diluted TBS/T for 90 min at room temperature. Immunocomplexes were visualized using chemiluminescence (ECL PlusWestern Blotting Substrate, Pierce, Thermo Scientific), incubating ECL for 5 min at room temperature. Band intensity was calculated by scanning video densitometry using the ChemiDoc imaging system (UVP, LCC, Upland, CA, USA). Blots were re-probed with monoclonal β-Actin-Peroxidase clone AC-15 antibody (Sigma-Aldrich, dilution1:5000) in TBS/T for 90 min.

### 3.3.8 Gene silencing

Both *mTOR* and *STAT3* genes were knocked-down by siRNA. The lipid-based agent for reverse transfection, siPORT NeoFX (Thermo Fisher), was used according to the manufacturer's instructions. LCLs derived from healthy donors and SDS patients were transiently transfected with 2 different specific siRNA sequences designed against mTOR and STAT3 genes or with a scrambled sequence as control. The siRNA molecules were complexed with cationic liposomes, siPORT Neo-FX (Thermo Fisher). Briefly, siPORT Neo-FX (1 µL/well) was complexed with siRNA or Scrambled oligos (40 nM each) in 250 µL RPMI-1640 medium supplemented with 0.5% FBS. 1 × $10^5$ LCLs were incubated in 24-wells plates for 48 hours at 37°C. Knock-down of *mTOR* and *STAT3* gene expression was determined by Real Time qRT-PCR.

### 3.3.9 Apoptosis assay

Dead Cell Apoptosis kit with Annexin V FITC and PI for flow cytometry (Invitrogen, Carlsbad, CA, USA) was used following manufacturer's protocol. Briefly, LCLs derived from SDS patients and healthy donors were incubated in the presence or absence (DMSO) of 350 nM everolimus or 7.5 µM stattic for 24 h in RPMI-1640 medium supplemented with 10% FBS (Biosera, Kansas City, MO, USA). Five µL of FITC-conjugated Annexin V were added to 100 µL of the cell suspension and incubated for 15 min at RT. Cells were then

resuspended in 200 µL and 5 µL of propidium iodide were added to cells. Fluorescence signals were acquired using FACS Canto II (BD Biosciences, Franklin Lakes, NJ, USA) analyzer. A tube of unstained cells was run as internal control. Positive events for either Annexin V only (early apoptosis) or Annexin V and PI double-positive (late apoptosis) or positive for PI only (necrosis) were considered.

### 3.3.10 Statistical analysis

Normal distribution was tested in each experiment using the Shapiro-Wilk test. Based on that evaluation, independent group determination was tested using Mann-Whitney test, while Student's t-test was used in case of paired data. A p-value $< 0.05$ was considered statistically significant. The statistical software SigmaPlot (Systat Software Inc., San Jose, CA, USA) was used.

## 3.4 Results

### 3.4.1 mTOR-STAT3 pathway is hyper-activated also in SDS lymphocyte subsets and everolimus can reduce this process *in vitro*

The JAK/STAT3 pathway regulates T cell cytotoxic gene expression, proliferation, and survival. STAT3 inhibition in the myeloid compartment displays a remarkable induction of the T cell anti-tumour capabilities and promotes their expansion *in vivo* [16,17]. Thus, STAT3 activation in immune cells is associated with suppression of anti-tumour immunity. The protein kinase mTOR acts as an activator of the STAT3 pathway [24,25;31]. Accordingly, we recently reported that mTOR can activate STAT3 pathway in B cells, neutrophils and monocytes from SDS patients [26]. To assess the activation of mTOR-STAT3 pathway in SDS lymphoid compartment, we determined the phosphorylation of mTOR (S2448) and STAT3 (Y705 and S727) in $CD4^+$ and $CD8^+$ T cells, DN T cells, γδT cells, and NK cells isolated from peripheral blood from seven patients with SDS. In SDS patients, all cell subsets except NK displayed significantly elevated levels of phospho-mTOR (**Figure 3.1**) and -STAT3 (**Figure 3.2**) compared to age-matched healthy donors. Then, we tested the effect of the clinically-approved rapamycin analogues, everolimus (RAD001) on mTOR, and STAT3 phosphorylation in SDS patient-derived T cell subsets. Results show that everolimus restores normal levels of phosphorylation of mTOR (**Figure 3.1**) and STAT3

(**Figure 3.2**), confirming the existence of an mTOR-STAT3 axis activation in the lymphoid compartment of SDS patients. To determine whether up-regulation *STAT3* gene expression eventually exists in SDS cells along with hyper-phosphorylation, we measured and correlated *STAT3* transcript expression with protein levels in LCLs and primary PBMCs isolated from several SDS patients with different genotypes, compared to age-matched healthy controls. Our studies showed that STAT3 expression is elevated in lymphocytes obtained from SDS patients compared to control subjects (**Figures 3.3 and 3.4**; **Supplementary Figures 3.1 and 3.2**).

**a**

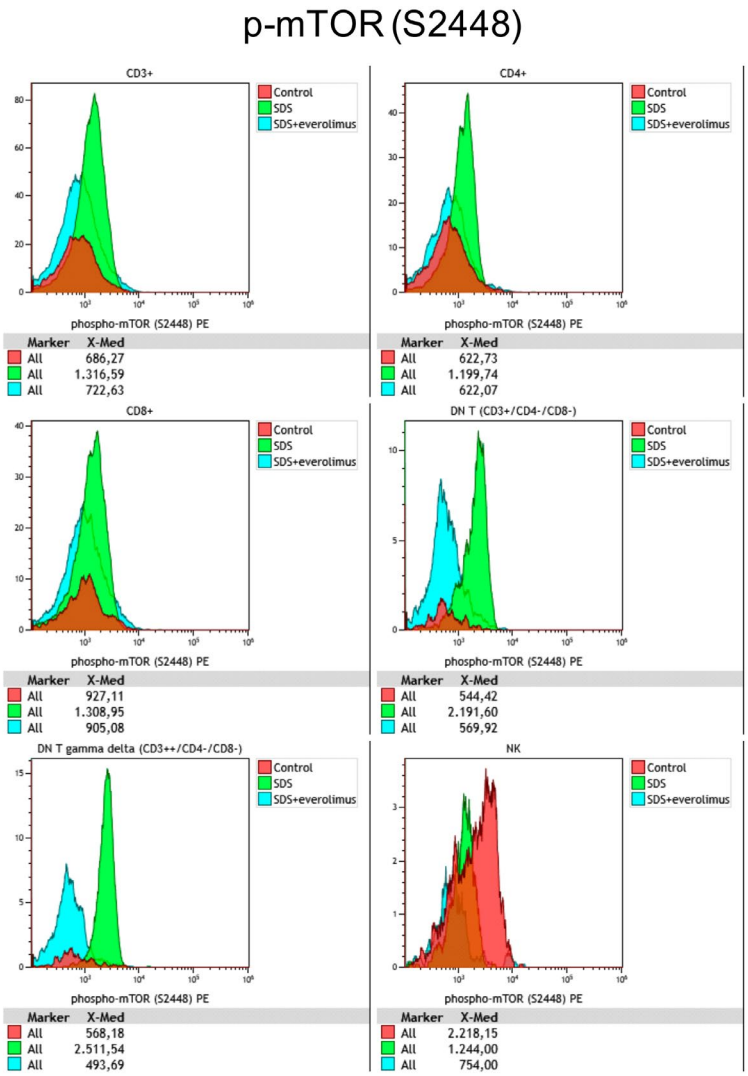
p-mTOR (S2448)
CD3+
Control
SDS
SDS+everolimus
phospho-mTOR (S2448) PE
Marker X-Med
All 686,27
All 1.316,59
All 722,63
CD4+
Control
SDS
SDS+everolimus
phospho-mTOR (S2448) PE
Marker X-Med
All 622,73
All 1.199,74
All 622,07
CD8+
Control
SDS
SDS+everolimus
phospho-mTOR (S2448) PE
Marker X-Med
All 927,11
All 1.308,95
All 905,08
DN T (CD3+/CD4-/CD8-)
Control
SDS
SDS+everolimus
phospho-mTOR (S2448) PE
Marker X-Med
All 544,42
All 2.191,60
All 569,92
DN T gamma delta (CD3++/CD4-/CD8-)
Control
SDS
SDS+everolimus
phospho-mTOR (S2448) PE
Marker X-Med
All 568,18
All 2.511,54
All 493,69
NK
Control
SDS
SDS+everolimus
phospho-mTOR (S2448) PE
Marker X-Med
All 2.218,15
All 1.244,00
All 754,00

*Figure 3.1 a*

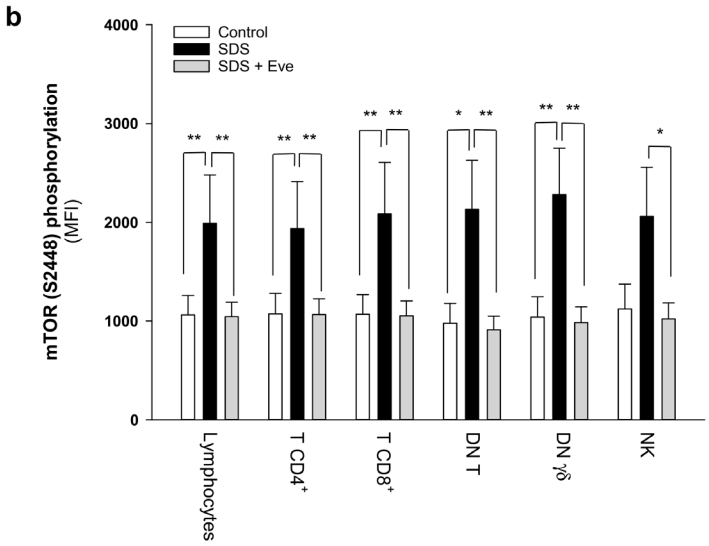


**Figure 3.1**: *Phospho-flow analysis of mTOR S2448 in a panel of primary lymphocyte subsets*

(**a**) Representative experiments conducted on peripheral blood samples obtained from patients with SDS. Red histograms represent age-matched healthy control cells; green histograms represent SDS lymphocytes; blue histograms represent SDS lymphocytes upon everolimus (350 nM) treatment. (**b**) Data are mean ± SEM of seven experiments conducted on SDS lymphocytes obtained from seven SDS patients (UPN37, UPN58, UPN69, UPN73, UPN87, UPN106, UPN108). Statistics: normal distribution was tested by the Shapiro-Wilk test. Subsequently, the Mann-Whitney Rank Sum Test was calculated. * $p < 0.05$; ** $p < 0.01$.

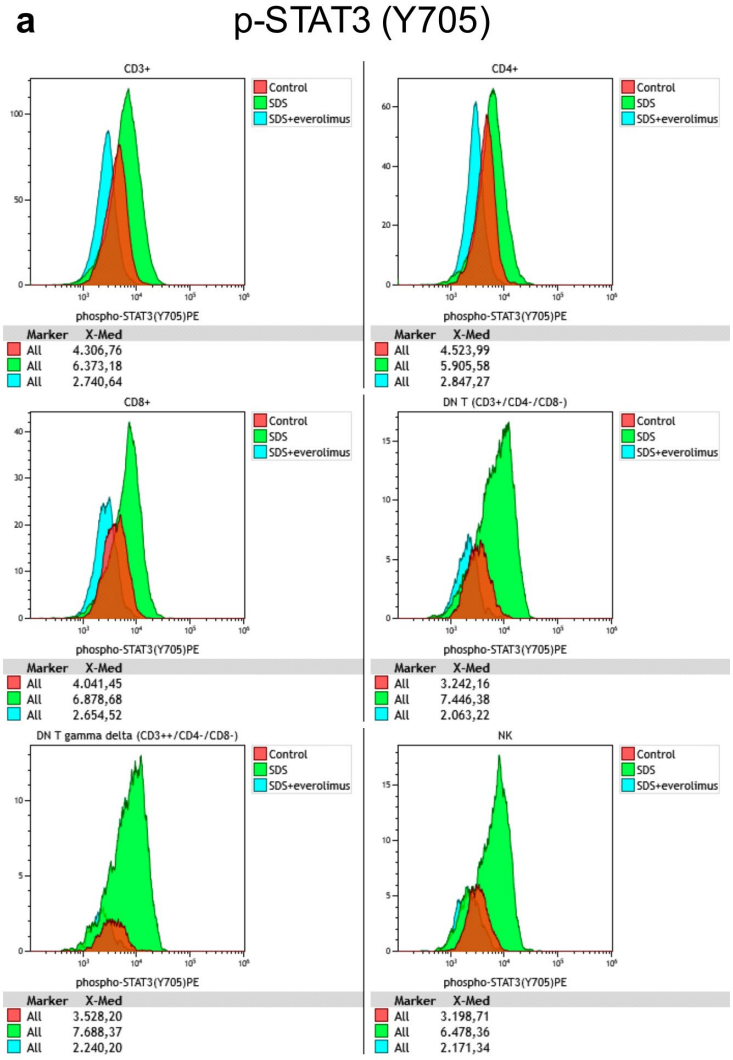
a
p-STAT3 (Y705)
CD3+
Control
SDS
SDS+everolimus
phospho-STAT3(Y705)PE
Marker X-Med
All 4.306,76
All 6.373,18
All 2.740,64
CD4+
Control
SDS
SDS+everolimus
phospho-STAT3(Y705)PE
Marker X-Med
All 4.523,99
All 5.905,58
All 2.847,27
CD8+
Control
SDS
SDS+everolimus
phospho-STAT3(Y705)PE
Marker X-Med
All 4.041,45
All 6.878,68
All 2.654,52
DN T (CD3+/CD4-/CD8-)
Control
SDS
SDS+everolimus
phospho-STAT3(Y705)PE
Marker X-Med
All 3.242,16
All 7.446,38
All 2.063,22
DN T gamma delta (CD3++/CD4-/CD8-)
Control
SDS
SDS+everolimus
phospho-STAT3(Y705)PE
Marker X-Med
All 3.528,20
All 7.688,37
All 2.240,20
NK
Control
SDS
SDS+everolimus
phospho-STAT3(Y705)PE
Marker X-Med
All 3.198,71
All 6.478,36
All 2.171,34

*Figure 3.2 a*

**b** p-STAT3 (S727)

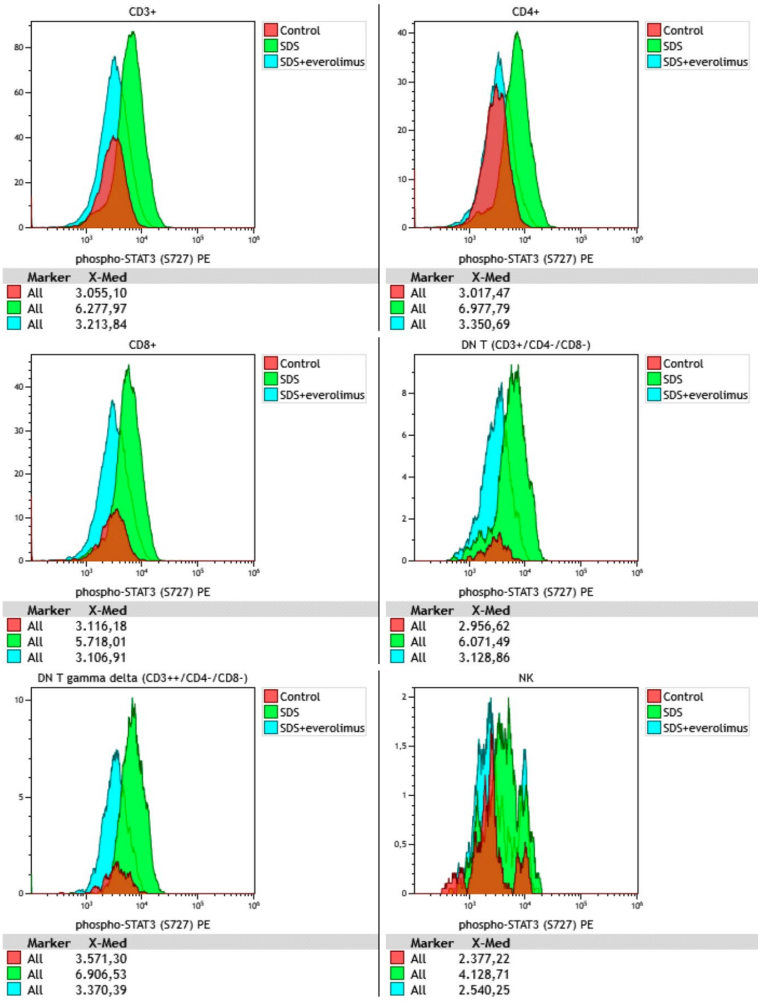


*Figure 3.2 b*

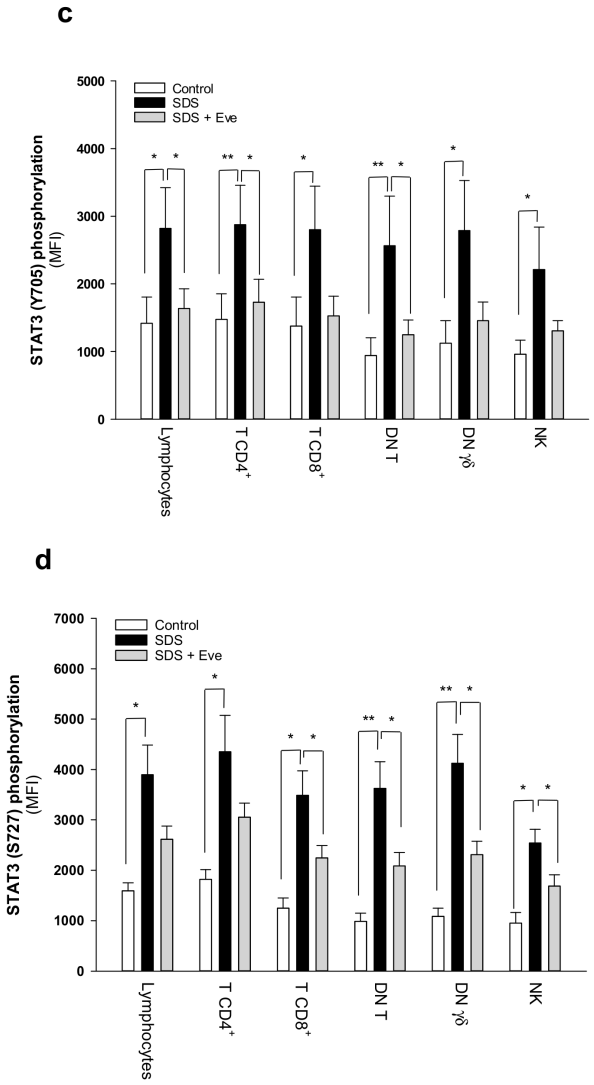


**Figure 3.2**: *Phospho-flow analysis of STAT3 in a panel of primary lymphocyte subsets*

(**a**) Representative analysis of phospho-STAT3 Y705 in lymphocyte subsets. (**b**) Representative analysis of phospho-STAT3 S727 in lymphocyte subsets. Red histograms represent age-matched healthy control cells; green histograms represent SDS patient-derived lymphocytes; blue histograms represent SDS lymphocytes upon everolimus (350 nM) treatment. Data are mean ± SEM of seven experiments conducted on SDS patient-derived lymphocytes obtained from seven SDS patients (UPN37, UPN58, UPN69, UPN73, UPN87, UPN106, UPN108). Statistical Student's t test for paired data has

been calculated. * $p < 0.05$; ** $p < 0.01$. (**c**) STAT3 (Y705) Median Fluorescence Intensity as measured by phospho-flow assays. (**d**) STAT3 (S727) Median Fluorescence Intensity as measured by phospho-flow assays. Data are mean ± SEM of seven experiments conducted on SDS lymphocytes obtained from seven SDS patients (UPN37, UPN58, UPN69, UPN73, UPN87, UPN106, UPN108). Statistics: Normal distribution was tested by the Shapiro-Wilk test. Subsequently, the Mann-Whitney Rank Sum Test was calculated. * $p < 0.05$; ** $p < 0.01$.

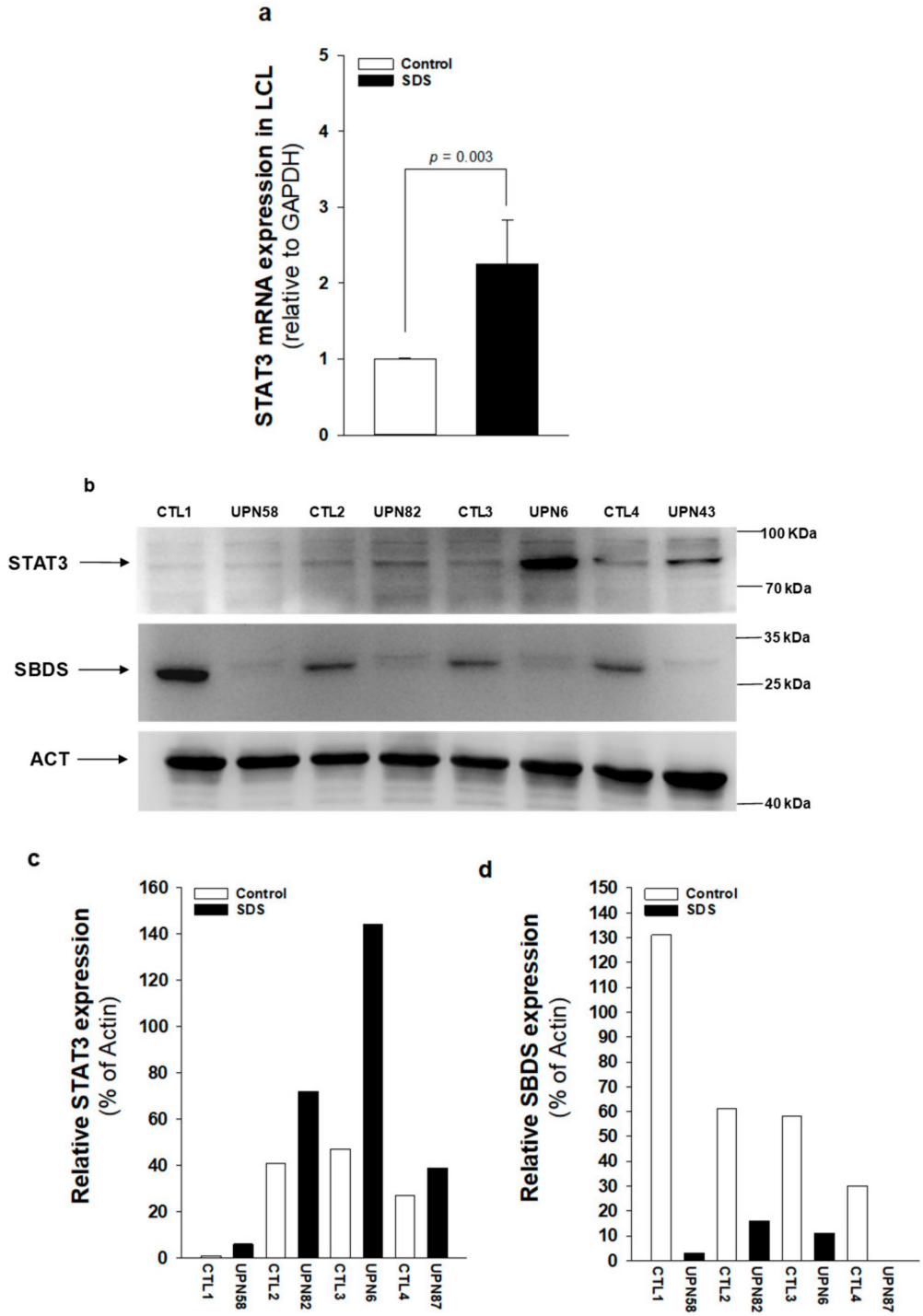
a
STAT3 mRNA expression in LCL
(relative to GAPDH)
Control
SDS
p = 0.003
0
1
2
3
4
5
b
CTL1
UPN58
CTL2
UPN82
CTL3
UPN6
CTL4
UPN43
STAT3
SBDS
ACT
100 KDa
70 kDa
35 kDa
25 kDa
40 kDa
c
Relative STAT3 expression
(% of Actin)
Control
SDS
0
20
40
60
80
100
120
140
160
CTL1
UPN58
CTL2
UPN82
CTL3
UPN6
CTL4
UPN87
d
Relative SBDS expression
(% of Actin)
Control
SDS
0
10
20
30
40
50
60
70
80
90
100
110
120
130
140
150
CTL1
UPN58
CTL2
UPN82
CTL3
UPN6
CTL4
UPN87

**Figure 3.3**: *STAT3 transcript and protein expression is up-regulated in SDS patient-derived LCLs*

(**a**) *STAT3* mRNA expression in LCLs isolated from UPN6, UPN43, UPN58, UPN82 (black bar), and from age-matched controls (white bar), measured by qRT-PCR. Data are mean ± SEM of four experiments performed in duplicate. (**b**) STAT3 protein level was measured in LCLs (UPN6, UPN43, UPN58, UPN82) by Western blot analysis. (**c**, **d**) Densitometric analysis of Western blots showed in panel **b**. Statistics: Normal distribution was tested by the Shapiro-Wilk test. Subsequently, the Mann-Whitney Rank Sum Test was calculated and reported within histograms.

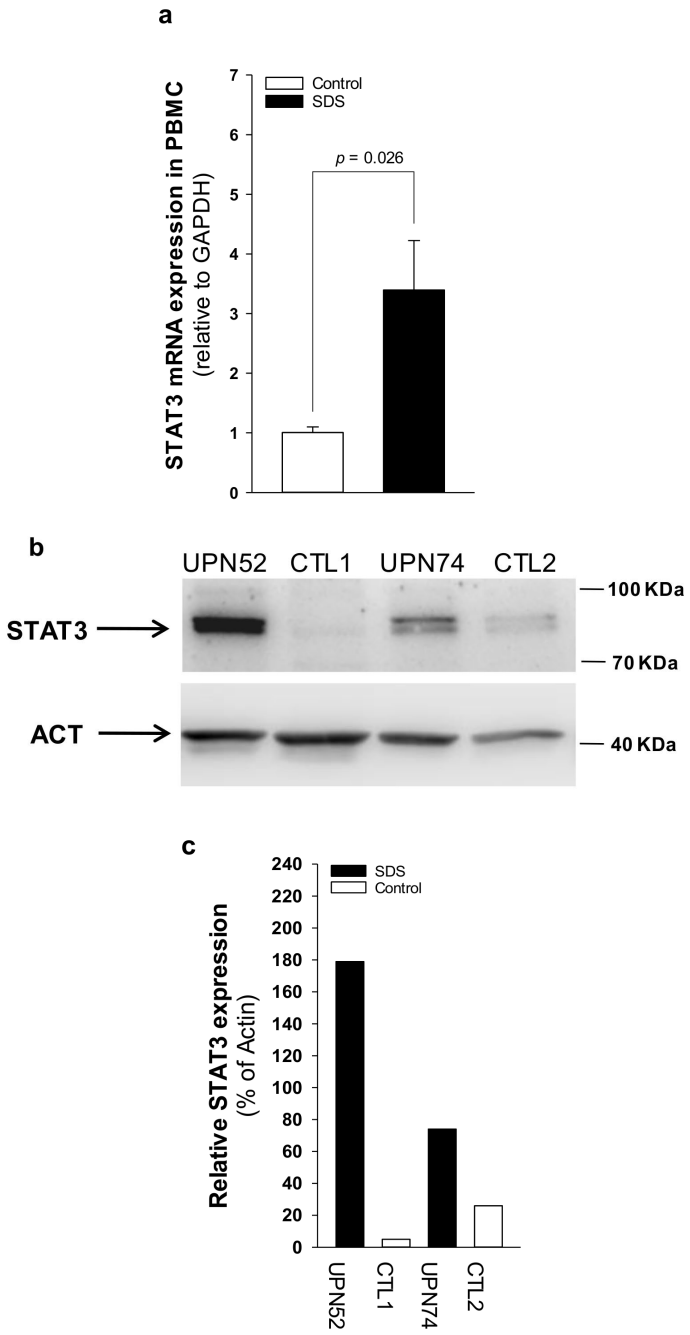


**Figure 3.4**: *STAT3 transcript and protein expression is up-regulated in SDS patient-derived primary PBMCs*

(**a**) *STAT3* mRNA expression in primary PBMCs isolated from UPN26, UPN69, UPN73, UPN87, UPN94, UPN106, and UPN108

(black bar), and from age-matched controls (white bar), measured by qRT-PCR. Data are mean ± SEM of seven experiments. (**b**) STAT3 protein level was measured in PBMC (UPN52 and UPN74) by Western blot analysis. (**c**) Densitometric analysis of Western blots showed in panel **b**. Statistics: Normal distribution was tested by the Shapiro-Wilk test. Subsequently, the Mann-Whitney Rank Sum Test was calculated and reported within histograms.

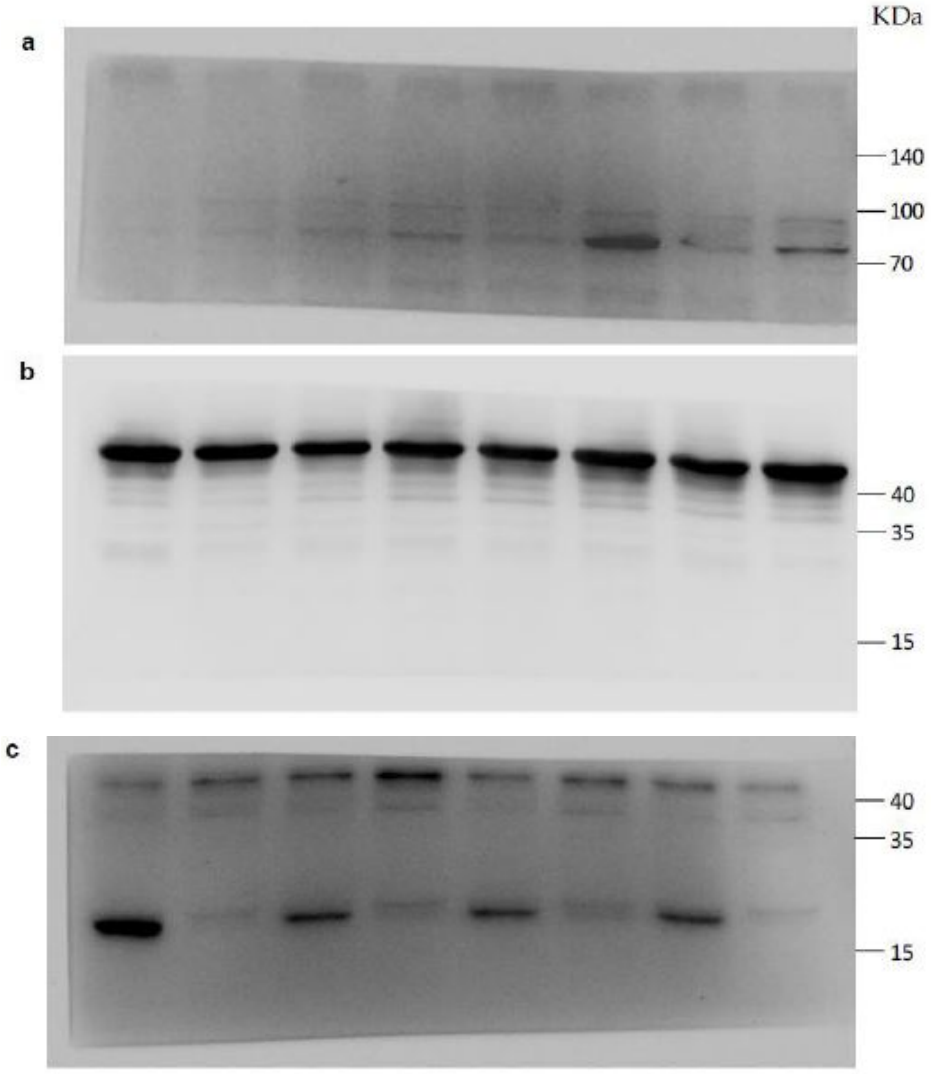


**Supplementary Figure 3.1**. Whole blots showing all the bands with all molecular weight markers on the Western blot reported in **Figure 3.3 b**. (**a**) Upper portion of nitrocellulose membrane (STAT3 88 KDa). (**b**, **c**) Lower portion of nitrocellulose membrane (Actin 42 KDa and SBDS 28.6 KDa, respectively). The membrane was cut at ~50 KDa before primary antibody staining in order to minimize the antibody loads.

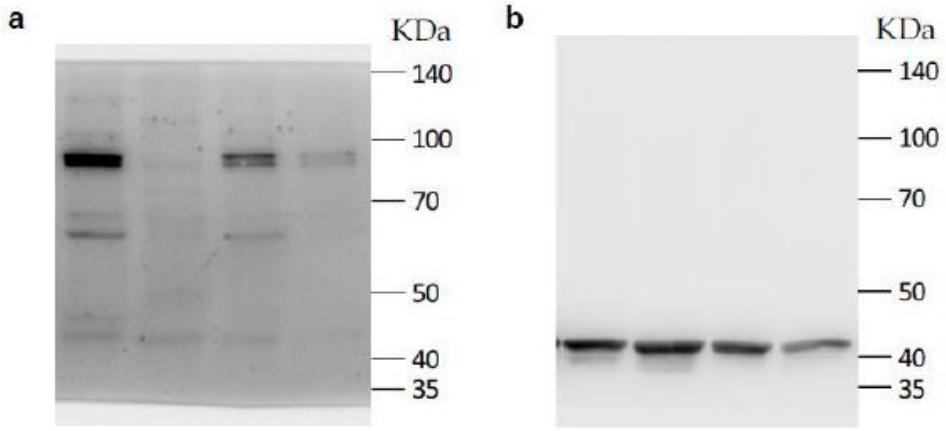


**Supplementary Figure 3.2**. Whole blots showing all the bands with all molecular weight markers on the Western blot reported in **Figure 3.4 b**. (**a**) STAT3 88 KDa; (**b**) Actin 42 KDa.

### 3.4.2 IL6 expression is up-regulated in SDS

Plasma levels of IL6 are generally close to the detection limit (1 pg/mL) in healthy individuals but significantly increase during the inflammatory process and cancers [32]. IL6 is a major activator of JAK-STAT3 signalling, and IL6 transcript expression is up-regulated by STAT3 activation, generating an autocrine/paracrine loop of activation [14]. Since mTOR-STAT3 axis is up-regulated in SDS patient-derived myeloid cells [26], we sought to find out whether hyper-activation of this pathway is associated with IL6 over-expression in non-myeloid SDS cell models. Both LCLs and BM-MSCs obtained from patients with SDS displayed significantly up-regulated IL6 release into cell culture supernatants compared with age-matched healthy controls (**Figure 3.5 a and 3.5 b**). In particular, IL6 levels were significantly elevated in primary SDS BM-MSCs, which released ~8 ng/mL in 2 x $10^5$ cells in our experimental conditions (**Figure 3.5 b**). Plasma samples obtained from the peripheral blood collected from an expanded cohort of 21 patients with SDS showed significantly increased levels of IL6 (mean 3.66 ± 4.58) compared to aged-matched controls (mean 1.19 ± 1.89), consistent with *in vitro* results (**Figure 3.5 c**). Since SDS BM-MSCs showed an impressive up-regulation of IL6 expression, we sought to find out whether IL6 were further concentrated in plasma derived from the bone marrow of patients. IL6 levels in bone marrow plasma were even more elevated (mean 4.75 ± 3.82) than those found in peripheral blood (mean 3.04 ± 2.05) obtained in parallel, from the same patients (**Figure 3.5 d**).

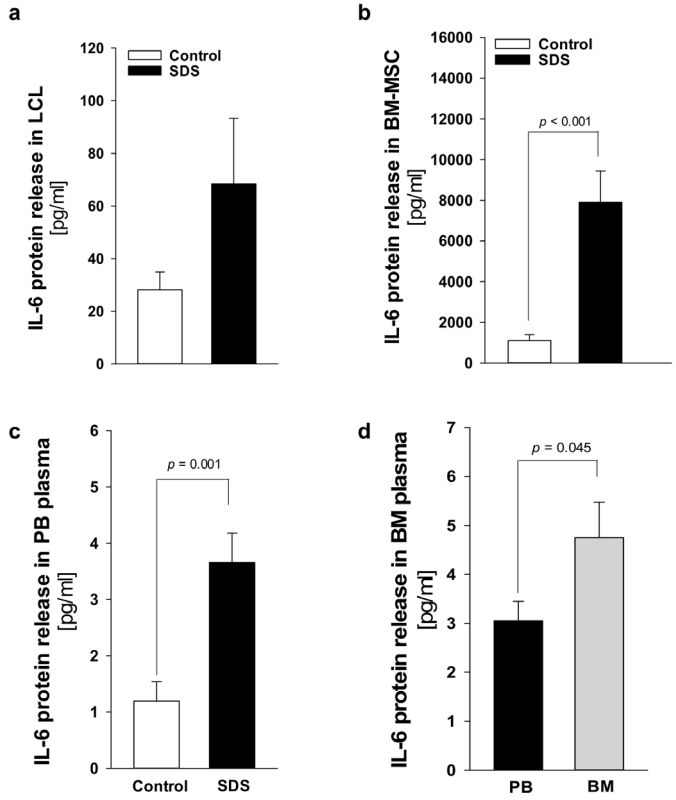


**Figure 3.5**: *IL6 release is elevated in SDS specimens compared to age-matched donor controls*

(**a**) Measurement of IL6 released in supernatants collected from 1 x $10^6$ LCLs after 48h. Data are mean ± SEM of 10 experiments conducted on LCLs obtained from UPN24, UPN26, UPN58, UPN68, UPN75, and UPN106. (**b**) IL6 released in supernatants collected from 2 x $10^5$ primary BM-MSCs after 48 h. (**c**) IL6 concentration in peripheral blood (PB) plasma samples obtained from 21 patients with SDS (UPN1, 13, 26, 37, 47, 52, 56, 57, 58, 63, 65, 66, 69, 72, 73, 74, 87, 94, 104, 106, 108) compared with age-matched plasma controls. (**d**) IL6 concentration in bone marrow (BM) plasma samples obtained from eight patients with SDS (UPN 47, 56, 65, 74, 87, 94, 106, 108) compared to PB plasma samples obtained from the same patients. Normal distribution was tested by the Shapiro-Wilk test. The Mann-Whitney Rank Sum Test was calculated and reported within histograms.

### 3.4.3 Patients with SDS show reduced levels of soluble IL6 receptor

IL6 signalling cascade occurs by classical activation through mbIL-6R or trans-signalling via the soluble sIL-6R [19]. The latter mechanism allows cells that do not express mbIL-6R, but do express gp130, to be responsive to IL6. Undifferentiated MSCs lack the expression of IL6 receptor although they normally express gp130 [33]. Thus, trans-signalling should be required to activate these cells upon IL6 stimulation. Nevertheless, BM-MSCs can constitutively release large quantities of IL6 [34]. In this work, we quantified sIL-6R in plasma samples obtained from 21 patients with SDS. In healthy individuals, plasma levels of sIL-6R range between 50-70 ng/mL [35]. Of note, we found that the soluble receptor release is reduced in SDS patients (44.3 ± 15.4 pg/μL) compared to age-matched healthy donors (71.6 ± 14.7 pg/μL) (**Figure 3.6 a**). To verify whether the bone marrow compartment, which showed increased levels of IL6, exhibits also higher levels of sIL-6R, we compared sIL-6R expression in peripheral blood plasma with the expression found in bone marrow plasma obtained in parallel from the same patients. However, peripheral blood and bone marrow plasma showed comparable levels of sIL-6R expression (**Figure 3.6 b**).

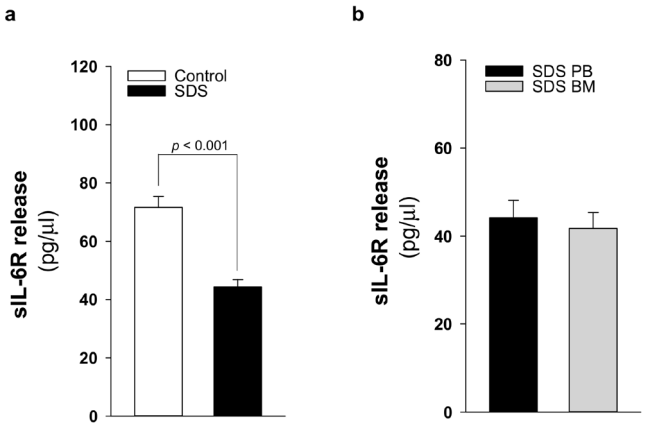


**Figure 3.6**: *sIL6-R release is reduced in patients with SDS*

(**a**) sIL-6R protein release was quantified by ELISA in PB plasma samples obtained from 21 patients with SDS (UPN 1, 13, 26, 37, 47, 52, 56, 57, 58, 63, 65, 66, 69, 72, 73, 74, 87, 94, 104, 106, 108) compared with age-matched plasma controls. (**b**) sIL-6R concentration in BM plasma samples obtained from eight patients with SDS (UPN 47, 56, 65, 74, 87, 94, 106, 108) compared with PB plasma samples obtained from the same patients. Normal distribution was tested by the Shapiro-Wilk test. The Mann-Whitney Rank Sum Test was calculated and reported within histograms.

### 3.4.4 Elevated IL6 gene expression in haematopoietic cells is primarily driven by mTOR-STAT3 pathway in SDS

Fifty to eighty percent of patients with AML present a constitutive activation of the mTOR pathway, showing significantly shorter disease-free and overall survival rates compared with patients without constitutive activation [36,37]. In the last decade, the development of new rapamycin (sirolimus) analogues showing improved pharmacokinetic profile, such as the clinically approved rapalog, everolimus, have given rise to great interest for anti-cancer therapy [29]. We previously reported that rapamycin-dependent mTOR inhibition leads to normal levels of phosphorylation of STAT3 in SDS cells [26]. Here, we show that everolimus (350 nM) and STAT3 inhibitor stattic (7.5 μM) significantly reduce IL6 mRNA expression in LCLs and in primary BM-MNCs obtained from patients with SDS (**Figure 3.7 a, c**). Decreased IL6 mRNA expression is paralleled by a reduction of IL6 release in culture supernatants upon everolimus and stattic treatments both in LCLs (-46.6% and -68%, respectively) and BM-MNCs (-34.6% and -66%, respectively) (**Figure 3.7 b, d**). In order to validate these data, we also knocked-down the expression of *mTOR* and *STAT3* in SDS cells using a short interference (si)RNA strategy. To this aim, we transfected two different siRNA sequences for each target gene and a negative control sequence (scrambled), which was previously validated [29], using siRNA-specific liposomes as a vector. We significantly knocked-down *mTOR* and *STAT3* gene expression in SDS LCLs (**Figure 3.8 a, b**).

Consistently with pharmacological inhibition, both *mTOR* and *STAT3* gene silencing lead to a strong inhibition of IL6 expression in SDS cells (**Figure 3.8 c, d**). In particular, knock-down of the *STAT3* gene resulted in a statistically significant reduction of *IL6* expression in terms of mRNA (-85%) and protein release (-51%). However, no effect of everolimus nor stattic on IL6 release was reported in BM-MSCs obtained from four SDS patients (**Figure 3.7 f**), and *IL6* mRNA transcription was surprisingly increased (2-fold increase) upon stattic treatment in these cells (**Figure 3.7 e**).

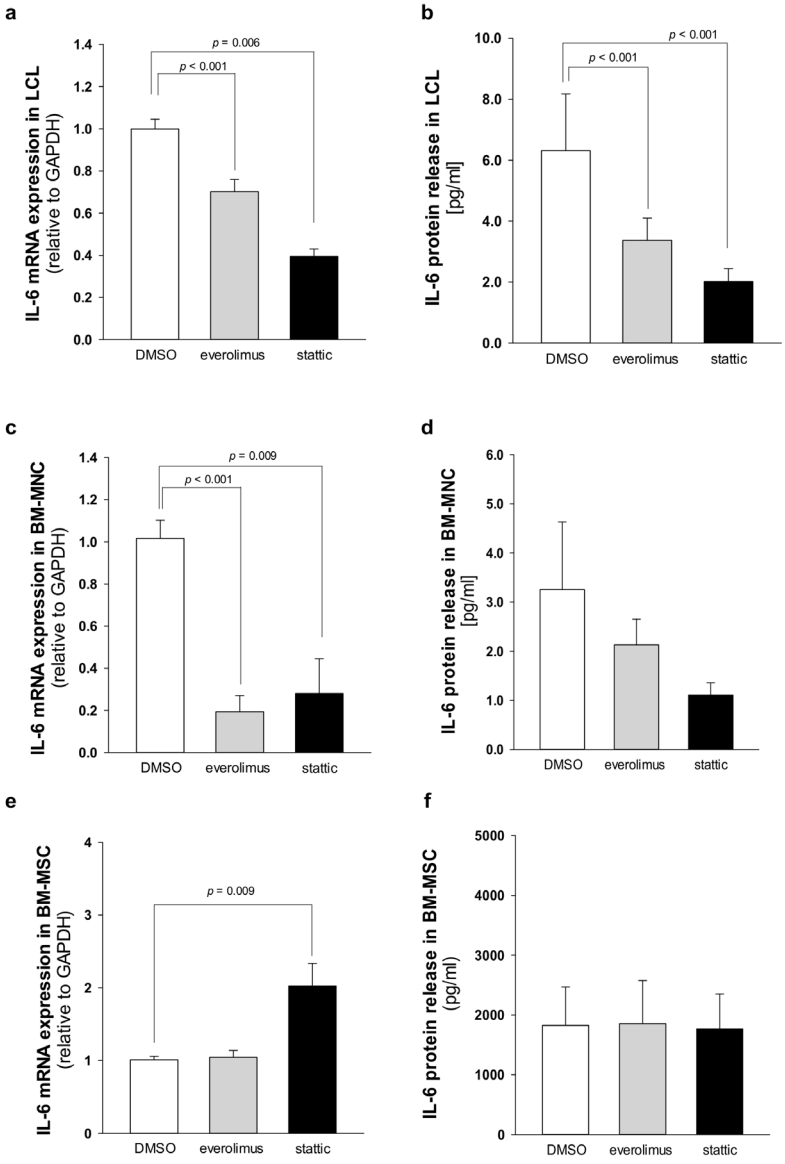


**Figure 3.7**: *Everolimus and stattic inhibit IL6 expression in SDS patient-derived haematopoietic cells*
(**a**) *IL6* transcript expression in LCLs incubated in the absence (DMSO) or in the presence of 350 nM everolimus or 7.5 µM stattic for 24 h was quantified by qRT-PCR. Data are mean ± SEM of six experiments performed in duplicate from three affected individuals (UPN58, UPN75, and UPN106). (**b**) IL6 release in supernatants collected from LCLs incubated in the absence (DMSO) or in the presence of 350 nM everolimus or 7.5 µM stattic for 24 h, as

measured by Bio-plex assay. Data are mean ± SEM of six experiments conducted as reported in panel **a**. (**c**) *IL6* mRNA expression in primary BM-MNCs incubated in the absence (DMSO) or in the presence of 350 nM everolimus or 7.5 μM stattic for 24 h was quantified by qRT-PCR. Data are mean ± SEM of four experiments performed in duplicate from four affected individuals (UPN74, UPN80, UPN94, and UPN106). (**d**) IL6 release in supernatants collected from BM-MNC as measured by Bio-plex assay. Data are mean ± SEM of four experiments conducted as reported in panel **c**. (**e**) *IL6* transcript expression in BM-MSC incubated in the absence (DMSO) or in the presence of 350 nM everolimus or 7.5 μM stattic for 24 h was quantified by qRT-PCR. Data are mean ± SEM of four experiments performed in duplicate from four affected individuals (UPN33, UPN35, UPN67 and UPN91). (**f**) IL6 release in supernatants collected from BM-MSCs (UPN33, UPN35, UPN67 and UPN91) as measured by Bio-plex assay. Data are mean ± SEM of four experiments conducted as reported in panel **e**. Statistics: Normal distribution was tested by the Shapiro-Wilk test, and the Student's t test for paired data has been calculated and reported within histograms, accordingly.

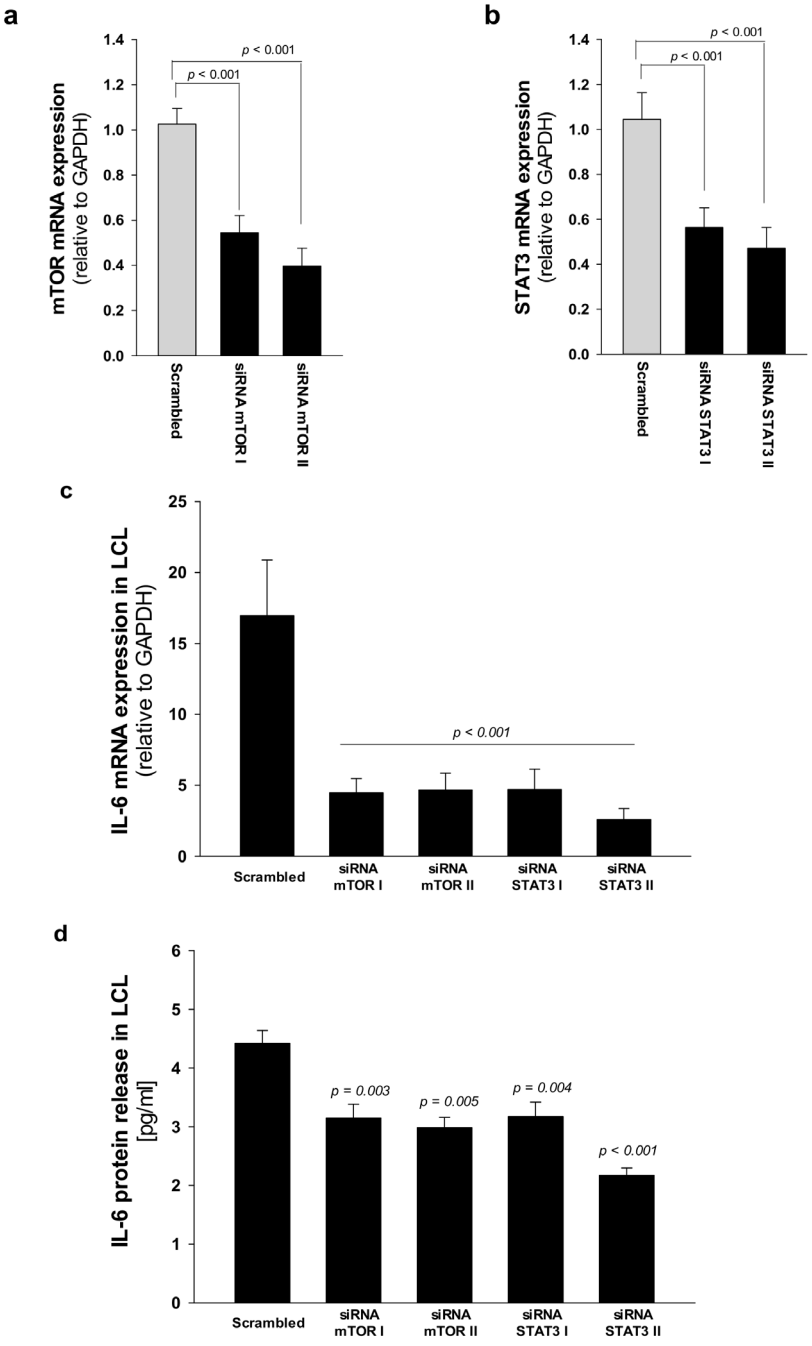


**Figure 3.8**: *STAT3 and mTOR gene silencing inhibit IL6 expression in LCLs from SDS patients*

(**a**) Reduced expression of *mTOR* mRNA after siRNA-mediated gene silencing. LCLs obtained from UPN58, UPN75 and UPN106 were cultured with two different siRNA sequences against target genes, or scrambled sequence (negative control for 48 h). Data are mean ± SEM of four experiments performed in duplicate. (**b**) Reduced expression of *STAT3* mRNA after siRNA-mediated gene silencing in LCLs, as performed in panel **a**. Data are mean ± SEM of four experiments performed in duplicate. (**c**) *IL6* mRNA expression in LCLs treated as indicated in panels **a** and **b**. (**d**) IL6 release was measured by Bio-plex assay in supernatants obtained from LCLs treated as indicated in **a**. Statistics: Normal distribution was tested by the Shapiro-Wilk test. Subsequently, the Mann-Whitney Rank Sum Test was calculated and reported within histograms.

## 3.5 Discussion

Although it has been widely reported that SDS mainly involves the neutrophil lineage, a number of patients suffer from anaemia, thrombocytopenia or pancytopenia (**Table 3.1**). Because the bone marrow is often hypocellular, lymphoid and stromal cells may contribute to reduced blood cell formation and myelodysplasia. We recently described a severe deficit of T cells, in particular of DN T subpopulation in SDS patients [38]. Here, we show that T cell subpopulations isolated from SDS patients display also hyper-activation of mTOR-STAT3 pathway. In addition, STAT3 transcript and protein expression are markedly increased in PBMCs and LCLs obtained from SDS patients, confirming the involvement of the STAT3 pathway in lymphoid lineages. Given the key role of STAT3 in reducing T regulatory cell accumulation [39], our results could partially explain the reduced number of DN T cells observed in SDS patients [38]. Furthermore, STAT3 activation in lymphocytes is associated with T cell impaired functions [17] and reduced anti-tumour activity [16,40]. Accordingly, impaired functions of T cells have been previously described in SDS [41]. Thus, STAT3 pathway up-regulation could lead to harmful consequences both on myeloid differentiation in the bone marrow and on innate and adaptive immunosurveillance mechanisms in SDS.

IL6 is a major activator of STAT3, and IL6 transcript expression is itself a target of STAT3 [14]. Thus, we measured

IL6 expression both at mRNA and protein levels in several SDS cell types. We found that IL6 expression is elevated in LCLs, primary BM-MNCs and BM-MSCs, compared to age-matched healthy controls. BM-MSCs produce large amounts of IL6 even in unstimulated and undifferentiated conditions [34]. Accordingly, BM-MSCs obtained from SDS patients released huge amounts of IL6 protein into the supernatants (~8 ng/mL, from 2 x $10^5$ cells), that is an amount comparable with the dose of IL6 commonly used to stimulate *in vitro* these cells (10 ng/mL). Interestingly, that concentration of IL6 has also been reported as the driving force leading to a further increase of mTOR-STAT3 activation in SDS leukocytes [26], suggesting the existence of a feedforward autocrine/paracrine feedback loop between STAT3 and IL6 in SDS bone marrow. In order to verify this hypothesis in clinical samples, we measured peripheral blood plasma levels of IL6 in a cohort of 21 patients with SDS. We found that IL6 levels in peripheral blood plasma are elevated in SDS patients. Then, we measured IL6 released into bone marrow plasma and we found even more elevated cytokine levels. Since BM-MNCs do release very low amounts of IL6 compared to BM-MSCs, we speculate that IL6 accumulation into the bone marrow environment is mainly due to the contribution from the stromal compartment. The MSCs compartment is involved in AML development, contributing to disease initiation both in animal models and in patients [42-44]. For instance, studies on BM-MSCs obtained from patients with MDS or AML reported altered expression of several cytokines

and other soluble pro-inflammatory mediators [45]. Thus, increased IL6 levels in bone marrow of patients with SDS, together with mTOR-STAT3 axis hyper-activation in haematopoietic cells, may clarify the reason why these subjects are prone to develop AML. We previously reported that rapamycin (sirolimus) treatment reduced the phosphorylation of both mTOR (S2448) and STAT3 (Y705 and S727) in cell lines as well as in primary neutrophils, monocytes and B cells isolated from patients with SDS. Here, we show that the clinically approved rapalog, everolimus, can restore normal level of activation of both mTOR and STAT3 in SDS lymphocyte populations. Importantly, in this study we show that everolimus and a commercially available STAT3 chemical inhibitor, namely stattic, can significantly inhibit IL6 release in SDS LCLs and BM-MNCs. In the light of these findings, novel clinically approved inhibitors of mTOR and STAT3 might be helpful in reducing pro-leukemic pathways in SDS hematopoietic cells. STAT3 inhibitors are being evaluated as chemotherapeutic agents in leukaemia, due to their strong pro-apoptotic activity [13]. Although we used 7.5 μM stattic, which was a previously reported dose that can inhibit STAT3 without affecting lymphoid cell viability *in vitro* [46], we observed a stattic-dependent induction of late apoptosis in LCLs (**Supplementary Figure 3.3**). We cannot exclude the fact that the effect observed in this case may partially be due to pro-apoptotic activity. However, since everolimus reduced both STAT3 activation and *IL6* expression in SDS LCLs and BM-MNCs without inducing pro-

apoptotic processes (**Supplementary Figure 3.3**), we can assume that mTOR-STAT3 pathway inhibition might be useful in reducing the excessive cytokine release. Both everolimus and stattic did not reduce the huge release of IL6 from undifferentiated SDS BM-MSCs, which remains one of the main sources of IL6 within the bone marrow compartment. This finding suggests other regulatory pathways of IL6 gene expression exist in BM-MSCs.

IL6 can trigger JAK-STAT3 signalling activation through the direct binding to mbIL-6R or via the soluble sIL-6R (IL6 trans-signalling), as result of alternative splicing or protease cleavage of mbIL-6R [19]. In order to evaluate whether the mTOR-STAT3-IL6 loop is generated by increased IL6 trans-signalling in SDS, we measured sIL-6R levels in plasma samples obtained from 21 patients. However, results indicate that sIL-6R expression is reduced in SDS patients compared to age-matched healthy donors, thus suggesting that this loop is mainly generated via the classical IL6 signalling in haematopoietic cells. Interestingly, *ex vivo* undifferentiated BM-MSCs lack the expression of mbIL-6R, even if they normally do express the gp130 protein [33]. Besides, only a few cell types do express mbIL-6R and therefore are able to respond to IL6 generating the IL6-STAT3-IL6 loop of activation. Among these cells, major players are represented by macrophages, neutrophils, T cells, and hepatocytes. On the contrary, gp130 is generally ubiquitously expressed [47,48]. It has been suggested that the lack of mbIL-6R is a regulatory mechanism of BM-

MSCs that inhibits the IL6-dependent chondrogenic/osteogenic differentiation, thus maintaining the stemness [33]. During osteogenic differentiation, the expression of *IL-6R* indeed increases in BM-MSC, allowing the autocrine/paracrine activation of the IL6-STAT3 signalling pathway [49]. Thus, reduced sIL-6R levels in plasma suggest that the impaired ossification reported in SDS [50] might be partially due to decreased IL6 trans-signalling in BM-MSCs. The lack of IL6 trans-signalling might therefore also partially explain why everolimus and stattic cannot reduce *IL6* expression in BM-MSCs. Our results indicate that BM-MSCs are unable to activate the autocrine/paracrine feedforward loop of mTOR-STAT3-IL6.

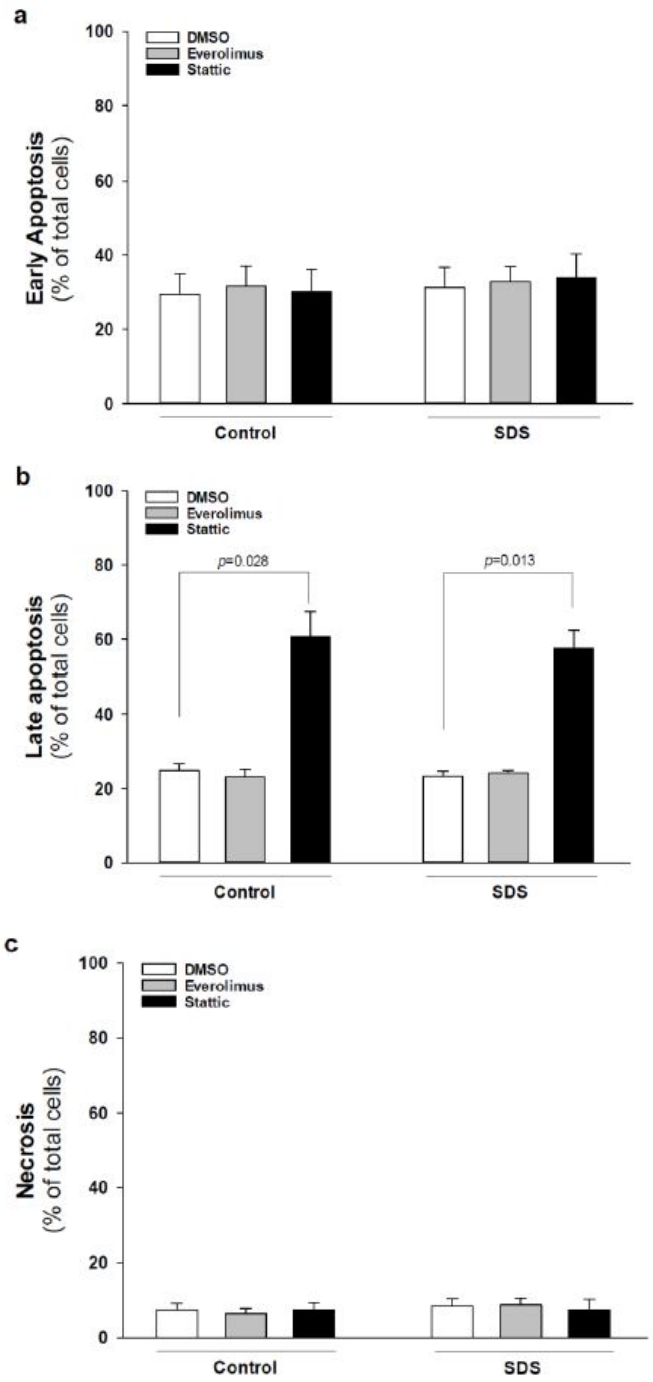


**Supplementary Figure 3.3**. Apoptosis assay in LCLs. LCLs derived from patients with SDS or healthy controls were treated with 350 nM everolimus (grey bars) or 7.5 μM stattic (black bars) for 24 h.

Apoptotic rate was detected by Dead Cell Apoptosis kit with Annexin V FITC and PI for flow cytometry. (**a**) Early apoptotic cells (Annexin-V positive, PI negative events). (**b**) Late apoptotic cells (Annexin V-positive, PI positive events). (**c**) Necrotic cells (Annexin V-negative, PI positive events). Data are mean ± SEM of 3 experiments performed in duplicate. Statistics: normal distribution was tested by the Shapiro-Wilk test. Subsequently, Mann-Whitney Rank Sum Test was calculated and reported within histograms.

# REFERENCES


[1] Dror Y., et al. Draft consensus guidelines for diagnosis and treatment of Shwachman-Diamond syndrome. Ann N Y Acad Sci. 2011 Dec;1242:40-55.
[2] Kargas V., et al. Mechanism of completion of peptidyltransferase centre assembly in eukaryotes. Elife. 2019 May;8:e44904.
[3] Weis F., et al. Mechanism of eif6 release from the nascent 60s ribosomal subunit. Nat Struct Mol Biol. 2015 Nov; 22(11):914-19.
[4] Finch A.J., et al. Uncoupling of gtp hydrolysis from eif6 release on the ribosome causes Shwachman-Diamond Syndrome. Genes Dev. 2011 May;25(9):917-29.
[5] Corey S.J., et al. Myelodysplastic syndromes: The complexity of stem-cell diseases. Nat Rev Cancer. 2007 Feb;7(2):118-29.
[6] Donadieu J., et al. Analysis of risk factors for myelodysplasias, leukemias and death from infection among patients with congenital neutropenia. Experience of the french severe chronic neutropenia study group. Haematologica. 2005 Jan;90(1):45-53.
[7] Lindsley R.C., et al. Prognostic mutations in myelodysplastic syndrome after stem-cell transplantation. N Engl J Med. 2017 Feb;376(6):536-47.
[8] Curran E.K., et al. Mechanisms of immune tolerance in leukemia and lymphoma. Trends Immunol. 2017 Jul;38(7):513-25.
[9] D'Acquisto F., Crompton T. Cd3+cd4-cd8- (double negative) t cells: Saviours or villains of the immune response? Biochem Pharmacol. 2011 Aug;82(4):333-40.
[10] Chen B., et al. Targeting chemotherapy-resistant leukemia by combining dnt cellular therapy with conventional chemotherapy. J Exp Clin Cancer Res. 2018 Apr;37(1):88.
[11] Lee J., et al. Allogeneic human double negative t cells as a novel immunotherapy for acute myeloid leukemia and its underlying mechanisms. Clin Cancer Res. 2018 Jan; 24(2):370-82.
[12] Zhang L., et al. Cd40 ligation reverses t cell tolerance in acute myeloid leukemia. J Clin Investig. 2013 May;123(5):1999-2010.
[13] O'Shea J.J., et al. Jaks and stats in immunity, immunodeficiency, and cancer. N Engl J Med. 2013 Jan;368(2):161-70.
[14] Johnson D.E., et al. Targeting the il-6/jak/stat3 signalling axis in cancer. Nat Rev Clin Oncol. 2018 Apr;15(4):234-48.

[15] Yu H., et al. Crosstalk between cancer and immune cells: Role of stat3 in the tumour microenvironment. Nat Rev Immunol. 2007 Jan;7(1):41-51.
[16] Herrmann A., et al. Targeting Stat3 in the myeloid compartment drastically improves the in vivo antitumor functions of adoptively transferred t cells. Cancer Res. 2010 Oct;70(19):7455-64.
[17] Kujawski M., et al. Targeting STAT3 in adoptively transferred t cells promotes their in vivo expansion and antitumor effects. Cancer Res. 2010 Dec;70(23):9599-610.
[18] Kumari N., et al. Role of interleukin-6 in cancer progression and therapeutic resistance. Tumour Biol. 2016 Sep;37(9):11553-72.
[19] Chalaris A., et al. The soluble interleukin 6 receptor: Generation and role in inflammation and cancer. Eur J Cell Biol. 2011 Jun-Jul;90(6-7):484-94.
[20] Audet J., et al. Distinct role of gp130 activation in promoting self-renewal divisions by mitogenically stimulated murine hematopoietic stem cells. Proc Natl Acad Sci USA. 2001 Feb;98(4):1757-62.
[21] Walker F., et al. IL6/sIL6R complex contributes to emergency granulopoietic responses in g-csf- and gm-csf-deficient mice. Blood. 2008 Apr;111(8):3978-85.
[22] Han Y., et al. Th17 cells and interleukin-17 increase with poor prognosis in patients with acute myeloid leukemia. Cancer Sci. 2014 Aug;105(8):933-42.
[23] Sanchez-Correa B., et al. Cytokine profiles in acute myeloid leukemia patients at diagnosis: Survival is inversely correlated with IL-6 and directly correlated with IL-10 levels. Cytokine. 2013 Mar;61(3):885-91.
[24] Yokogami K., et al. Serine phosphorylation and maximal activation of STAT3 during CNTF signaling is mediated by the rapamycin target mTOR. Curr Biol. 2000 Jan;10(1):47–50.
[25] Dodd K.M., et al. mTORC1 drives HIF-1α and VEGF-A signalling via multiple mechanisms involving 4E-BP1, S6K1 and STAT3. Oncogene. 2015 Apr;34(17):2239-50.
[26] Bezzerri V., et al. New insights into the Shwachman-Diamond Syndrome-related haematological disorder: Hyper-activation of mTOR and STAT3 in leukocytes. Sci Rep. 2016 Sep;6:33165.
[27] Chapuis N., et al. Perspectives on inhibiting mTOR as a future treatment strategy for hematological malignancies. Leukemia. 2010 Oct;24(10):1686-99.
[28] Hoshii T., et al. Pleiotropic roles of mTOR complexes in haemato-lymphopoiesis and leukemogenesis. J Biochem. 2014 Aug;156(2):73-83.
[29] Porta C., et al. Targeting PI3K/Akt/mTOR signaling in cancer. Front Oncol. 2014 Apr;4:64.

[30] Witzig T.E., et al. The mTORC1 inhibitor everolimus has antitumor activity in vitro and produces tumor responses in patients with relapsed t-cell lymphoma. Blood. 2015 Jul;126(3):328-35.
[31] Cai Y., et al. Differential roles of the mTOR-STAT3 signaling in dermal γδ T cell effector function in skin inflammation. Cell Rep. 2019 Jun;27(10):3034-48.
[32] Rose-John S. IL-6 trans-signaling via the soluble IL-6 receptor: Importance for the pro-inflammatory activities of IL-6. Int J Biol Sci. 2012;8(9):1237-47.
[33] Erices A., et al. Gp130 activation by soluble interleukin-6 receptor/interleukin-6 enhances osteoblastic differentiation of human bone marrow-derived mesenchymal stem cells. Exp Cell Res. 2002 Oct;280(1):24-32.
[34] Pricola K.L., et al. Interleukin-6 maintains bone marrow-derived mesenchymal stem cell stemness by an ERK1/2-dependent mechanism. J Cell Biochem. 2009 Oct;108(3):577-88.
[35] Calabrese L.H., Rose-John S. IL-6 biology: Implications for clinical targeting in rheumatic disease. Nat Rev Rheumatol. 2014 Dec;10(12):720-27.
[36] Altman J.K., et al. Targeting mTOR for the treatment of AML. New agents and new directions. Oncotarget. 2011 Jun;2(6):510-17.
[37] Dinner S., Platanias L.C. Targeting the mTOR pathway in leukemia. J Cell Biochem. 2016 Aug;117(8):1745-52.
[38] Bezzerri V., et al. Peripheral blood immunophenotyping in a large cohort of patients with Shwachman-Diamond Syndrome. Pediatr Blood Cancer. 2019 May;66(5):e27597.
[39] Durant L., et al. Diverse targets of the transcription factor STAT3 contribute to T cell pathogenicity and homeostasis. Immunity. 2010 May;32(5):605-15.
[40] Hossain D.M., et al. Leukemia cell-targeted STAT3 silencing and TLR9 triggering generate systemic antitumor immunity. Blood. 2014 Jan;123(1):15-25.
[41] Dror Y., et al. Immune function in patients with Shwachman-Diamond Syndrome. Br J Haematol. 2001 Sep;114(3):712-17.
[42] Raaijmakers M.H., et al. Bone progenitor dysfunction induces myelodysplasia and secondary leukaemia. Nature. 2010 Apr;464(7290):852-57.
[43] Santamaría C., et al. Impaired expression of DICER, DROSHA, SBDS and some microRNAs in mesenchymal stromal cells from myelodysplastic syndrome patients. Haematologica. 2012 Aug;97(8):1218-24.
[44] Geyh S., et al. Insufficient stromal support in MDS results from molecular and functional deficits of mesenchymal stromal cells. Leukemia. 2013 Sep;27(9):1841-51.

[45] Schroeder T., et al. Mesenchymal stromal cells in myeloid malignancies. Blood Res. 2016 Dec;51(4):225-32.
[46] Severin F., et al. In chronic lymphocytic leukemia the JAK2/STAT3 pathway is constitutively activated and its inhibition leads to CLL cell death unaffected by the protective bone marrow microenvironment. Cancers. 2019 Dec;11(12):1939.
[47] Oberg H.H., et al. Differential expression of CD126 and CD130 mediates different STAT-3 phosphorylation in CD4+CD25- and CD25high regulatory T cells. Int Immunol. 2006 Apr;18(4):555-63.
[48] Scheller J., Rose-John S. Interleukin-6 and its receptor: From bench to bedside. Med Microbiol Immunol. 2006 Dec; 195(4):173-83.
[49] Kondo M., et al. Contribution of the interleukin-6/STAT-3 signaling pathway to chondrogenic differentiation of human mesenchymal stem cells. Arthritis Rheumatol. 2015 May;67(5):1250-60.
[50] Bezzerri V., Cipolli M. Shwachman-Diamond Syndrome: Molecular mechanisms and current perspectives. Mol Diagn Ther. 2018 Apr;23(2):281-90.
[51] Lambert C., Genin C. CD3 bright lymphocyte population reveal gammadelta t cells. Cytom B Clin Cytom. 2004 Sep;61(1):45-53.
[52] Zhang H., et al. STAT3 controls myeloid progenitor growth during emergency granulopoiesis. Blood. 2010 Oct;116(14):2462-71.

# Chapter 4

## Summary, conclusion and future directions

Shwachman-Diamond Syndrome (SDS) is a multiple organ impairment disorder mainly characterized by bone marrow (BM) dysfunctions and exocrine pancreatic insufficiency. SDS patients present also severe haematologic abnormalities, with neutropenia as the most common deficiency. Of note, SDS patients have an increased risk for myelodysplastic syndrome (MDS) and malignant transformation to acute myeloid leukaemia (AML) [1,2].

In the first part of this work, we focused our attention on the altered *in vitro* angiogenic capability of SDS-mesenchymal stromal cells (MSCs). Angiogenesis is not only involved in the pathogenesis of solid tumours but also in haematological malignancies [3]. Mesenchymal stromal cells can potentiate angiogenesis via direct cell differentiation, cell-cell interaction, and autocrine or paracrine effects [4-6]. During the last years, using both *in vitro* and *in vivo* models, our research group demonstrated that these cells display a marked impairment in their angiogenic potential [7]. Here, we firstly confirm that SDS-MSCs obtained from a cohort of 10 patients show altered angiogenic capability under specific angiogenic stimulation. Next, we demonstrate that the defective SDS *in vitro* tube formation is associated with alterations in TGFβ1/VEGFA signalling. Indeed, the increased P53 protein levels of SDS-MSCs under angiogenic *stimuli* could modulate VEGFα mRNA, whereas the lack of TGFβ1 could influence the expression of both endoglin (*CD105*) and platelet endothelial cell adhesion molecule (*PECAM-1* or *CD31*), thus impacting on the

angiogenic properties of SDS-MSCs. Interestingly, by providing the exogenous administration of TGFβ1 or VEGFA, we demonstrate that only MSCs from severely neutropenic patients can recovery their capillary-like ability after both treatments. Of note, our preliminary results also show that the exogenous addition of VEGFA protein leads to the normalization of P53 protein levels only in MSCs derived from severely neutropenic patient able to recreate a well-defined tubular structure after treatment. Collectively, these findings seem to sustain the hypothesis that, under angiogenic stimulation, the inhibition of TGFβ1 and VEGFA signalling is responsible of the altered *in vitro* angiogenic capability of SDS-MSCs. Moreover, it seems that defective SDS-MSCs angiogenic properties could be related to the degree of neutropenia. For the future, we will better characterise the down-stream transcriptional factors of TGFβ1/VEGFA axis, focusing our attention on the differences previously found between MSCs derived from neutropenic and severely neutropenic SDS patients. Moreover, we will deeply analyse the molecular correlation between STAT3 and P53 in dictating the altered angiogenic capability of SDS-MSCs. Finally, we will evaluate the bone marrow biopsy specimens of SDS patients to assess whether microvessel density could be associated with bone marrow neutrophil counts. The identification of a possible link between aberrant angiogenesis and haematological abnormalities in SDS patients will be a crucial step for the better comprehension of the disease pathogenesis. Furthermore, the study of potentially targetable

molecular pathways able to modify SDS angiogenesis could provide a rationale for designing new highly personalised strategies for the treatment and cure of this rare bone marrow failure syndrome.

The second part of our study was focused on the analysis of the molecular mechanisms and signalling pathways responsible of SDS neutropenia, and eventual evolution to MDS or AML [8]. Signal transducer and activator of transcription 3 (STAT3) is a key regulator of several cellular processes including neutrophil granulogenesis, leukaemia, and lymphoma malignant transformation [9]. Firstly described as an interleukin-6 (IL6)-activated transcription factor [10], nowadays STAT3 is also recognised as a direct substrate of the mammalian target of rapamycin (mTOR) [11,12]. Recently, it has been demonstrated that both mTOR and STAT3 pathways are constitutively up-regulated in primary leukocytes and lymphoblastoid cell lines derived from SDS patients [13]. Here, we further analyse the hyper-activation of mTOR-STAT3 signalling pathway in specific lymphocytic populations of SDS patients [8]. Our data also reveal elevated IL6 levels in different SDS-derived cell culture supernatants and plasma samples. Interestingly, the clinical pharmacological approved rapalog restores normal levels of both mTOR and STAT3 activation in SDS lymphocyte populations, and significantly inhibits IL6 release in cell culture supernatants. Elevated IL6 levels have been found in adult BM niche of AML patients [14]. Moreover, it has also been demonstrated that increased IL6 levels correlate

with poor prognosis in paediatric patients with AML [15]. Therefore, our findings, strengthening the hypothesis of the existence of an mTOR-STAT3-IL6 activation loop in haematopoietic SDS cells which may affect both myeloid and lymphoid compartment, may clarify the reason why SDS patients are prone to develop AML [8]. However, further studies are needed to clarify the putative role of IL6 in driving SDS pathophysiology as well as to identify its correlation with specific clinical/subclinical or biochemical markers of the disease.

The discovery of new altered molecular pathways underlying SDS pathology could lead to the identification of new therapeutic targets for the correction of SDS-related haematological defects and for the prevention of leukemic evolution.

# REFERENCES

[1] Nelson A.S., Myers K.C. Diagnosis, Treatment, and Molecular Pathology of Shwachman-Diamond Syndrome. Hematol Oncol Clin North Am. 2018 Aug;32(4):687-700.
[2] Nelson A., Myers K. Shwachman-Diamond Syndrome. 2008 Jul 17 [Updated 2018 Oct 18]. In: Adam M.P., et al., editors. GeneReviews® [Internet]. Seattle (WA): University of Washington, Seattle; 1993-2020.
[3] Moehler T., et al. Antiangiogenic therapy in hematologic malignancies. Curr Pharm Des. 2003;10(11):1221-34.
[4] Lee M.W., et al. Mesenchymal stem cells in suppression or progression of hematologic malignancy: current status and challenges. Leukemia. 2019 Mar;33(3):597-611.
[5] Caplan A.I., Dennis J.E. Mesenchymal stem cells as trophic mediators. J Cell Biochem. 2006 Aug;98(5):1076-84.
[6] Xia X., et al. Growth Hormone-Releasing Hormone and Its Analogues: Significance for MSCs-Mediated Angiogenesis. Stem Cells Int. 2016;8737589.
[7] Bardelli D., et al. Mesenchymal stromal cells from Shwachman-Diamond syndrome patients fail to recreate a bone marrow niche in vivo and exhibit impaired angiogenesis. Br J Haematol. 2018 Jul;182(1):114-24.
[8] Vella A., et al. mTOR and STAT3 Pathway Hyper-Activation is Associated with elevated Interleukin-6 Levels in Patients with Shwachman-Diamond Syndrome: Further Evidence of Lymphoid Lineage Impairment. Cancers (Basel). 2020 Mar 5;12(3):597.
[9] O'Shea J.J., et al. Jaks and stats in immunity, immunodeficiency, and cancer. N Engl J Med. 2013 Jan;368(2):161-70.
[10] Zhong Z., et al. Stat3: a STAT family member activated by tyrosine phosphorylation in response to epidermal growth factor and interleukin-6. Science. 1994 Apr 1;264(5155):95-8.
[11] Yokogami K., et al. Serine phosphorylation and maximal activation of STAT3 during CNTF signaling is mediated by the rapamycin target mTOR. Curr Biol. 2000 Jan;10(1):47–50.
[12] Dodd K.M., et al. mTORC1 drives HIF-1α and VEGF-A signalling via multiple mechanisms involving 4E-BP1, S6K1 and STAT3. Oncogene. 2015 Apr;34(17):2239-50.

[13] Bezzerri V., et al. New insights into the Shwachman-Diamond Syndrome-related haematological disorder: hyper-activation of mTOR and STAT3 in leukocytes. Sci Rep. 2016 Sep 23;6:33165.
[14] Han Y., et al. Th17 cells and interleukin-17 increase with poor prognosis in patients with acute myeloid leukemia. Cancer Sci. 2014 Aug;105(8):933-42.
[15] Sanchez-Correa B., et al. Cytokine profiles in acute myeloid leukemia patients at diagnosis: Survival is inversely correlated with IL-6 and directly correlated with IL-10 levels. Cytokine. 2013 Mar;61(3):885-91.

# Other publications

MONOCYTE-MACROPHAGE POLARIZATION AND RECRUITMENT PATHWAYS IN THE TUMOR MICROENVIRONMENT OF B-ALL. Dander E., Fallati A., Gulic T., Pagni F., Gaspari S., Silvestri D., Cricrì G., ***Bedini Gloria***, Portale F., Buracchi C., Brizzolara L., Maglia O., Mantovani A., Garlanda C., Valsecchi M.G., Locatelli F., Biondi A., Bottazzi B., Allavena P. and D'Amico G. Accepted for publication in British Journal of Haematology.

VASCULAR REMODELING IN MOYAMOYA ANGIOPATHY: FROM PERIPHERAL BLOOD MONONUCLEAR CELLS TO ENDOTHELIAL CELLS. Tinelli F., Nava S., Arioli F., ***Bedini Gloria***, Scelzo E., Lisini D., Faragò G., Gioppo A., Ciceri E.F., Acerbi F., Ferroli P., Vetrano I.G., Esposito S., Saletti V., Pantaleoni P., Zibordi F., Nardocci N., Zedde M.L., Pezzini A., Di Lazzaro V., Capone F., Dell'Acqua M.L., Vajkoczy P., Tournier-Lasserve E., Parati E.A., Bersano A., Gatti L. Int J Mol Sci. 2020 Aug 11;21(16):5763.

GEN-O-MA PROJECT: AN ITALIAN NETWORK STUDYING CLINICAL COURSE AND PATHOGENIC PATHWAYS OF MOYAMOYA DISEASE-STUDY PROTOCOL AND PRELIMINARY RESULTS. Bersano A., ***Bedini Gloria***, Nava S., Acerbi F., Sebastiano D.R., Binelli S., Franceschetti S., Faragò G., Grisoli M., Gioppo A., Ferroli P., Bruzzone M.G., Riva D., Ciceri E., Pantaleoni C., Saletti V., Esposito S., Nardocci N., Zibordi F., Caputi L., Marzoli S.B., Zedde M.L., Pavanello M., Raso A., Capra V., Pantoni L., Sarti C., Pezzini A, Caria F, Dell' Acqua ML, Zini A, Baracchini C, Farina F, Sanguigni S, De Lodovici M.L., Bono G., Capone F., Di Lazzaro V., Lanfranconi S., Toscano M., Di Piero V., Sacco S., Carolei A., Toni D., Paciaroni M., Caso V., Perrone P., Calloni M.V., Romani A., Cenzato M., Fratianni A., Ciusani E., Prontera P., Lasserve E.T., Blecharz K., Vajkoczy P., Parati E.A.; GEN-O-MA study group. Neurol Sci. 2019 Jan 3.

MICRODUPLICATION OF 15q13.3 AND MICRODELETION OF 18q21.32 IN A PATIENT WITH MOYAMOYA SYNDROME. Sciacca

F.L., Rizzo A., ***Bedini Gloria***, Capone F., Di Lazzaro V., Nava S., Acerbi F., Rossi Sebastiano D., Binelli S., Faragò G., Gioppo A., Grisoli M., Bruzzone M.G., Ferroli P., Pantaleoni C., Caputi L., Vela Gomez J., Parati E.A. and Bersano A. Int. J. Mol. Sci. 2018, 19 (11), 3675. Correction: Int J Mol Sci. 2019 Dec 18;21(1).

ADIPOSE TISSUE-DERIVED MESENCHYMAL STROMAL CELLS FOR CLINICAL APPLICATION: AN EFFICIENT ISOLATION APPROACH. Lisini D., Nava S., Pogliani S., Avanzini M.A., Lenta E., ***Bedini Gloria***, Mantelli M., Pecciarini L., Croce S., Boncoraglio G., Maccario R., Parati E.A., Frigerio S. Curr Res Transl Med. 2019 Feb; 67 (1), 20-7.

THE ROLE OF CLINICAL AND NEUROIMAGING FEATURES IN THE DIAGNOSIS OF CADASIL. Bersano A., ***Bedini Gloria***, Markus H.S., Vitali P., Colli-Tibaldi E., Taroni F., Gellera C., Baratta S., Mosca L., Carrera P., Ferrari M., Cereda C., Grieco G., Lanfranconi S., Mazucchelli F., Zarcone D., De Lodovici M.L., Bono G., Boncoraglio G.B., Parati E.A., Calloni M.V., Perrone P., Bordo B.M., Motto C., Agostoni E., Pezzini A., Padovani A., Micieli G., Cavallini A., Molini G., Sasanelli F., Sessa M., Comi G., Checcarelli N., Carmerlingo M., Corato M., Marcheselli S., Fusi L., Grampa G., Uccellini D., Beretta S., Ferrarese C., Incorvaia B., Tadeo C.S., Adobbati L., Silani V., Faragò G., Trobia N., Grond-Ginsbach C., Candelise L.; Lombardia GENS-group. J Neurol. 2018 Oct 11.

TAKOTSUBO SYNDROME: CLINICAL FEATURES, PATHOGENESIS, TREATMENT, AND RELATIONSHIP WITH CEREBROVASCULAR DISEASES. Ranieri M., Finsterer G., ***Bedini Gloria***, Parati E.A., Bersano A. Current Neurology and Neuroscience Reports. 2018 Mar 22;18(5):20.

MESENCHYMAL STEM CELL THERAPY IN INTRACEREBRAL HAEMORRHAGIC STROKE. ***Bedini Gloria***, Bersano A., Zanier E.R., Pischiutta F., Parati E.A. Curr Med Chem. 2018;25(19):2176-97.